APPLICATIONS OF THE INTEGRAL METHOD TO STEADY STATE LAMINAR MIXED CONVECTION HEAT TRANSFER

By

DONALD HENRY ASIRE

Bachelor of Science
Illinois Institute of Technology
Chicago, Illinois
1947

Master of Science
Air Force Institute of Technology
Wright-Patterson Air Force Base, Ohio
1958

Submitted to the faculty of the Graduate School of
the Oklahoma State University
in partial fulfillment of the requirements
for the degree of
DOCTOR OF PHILOSOPHY
May, 1965

APPLICATIONS OF THE INTEGRAL METHOD

TO STEADY STATE LAMINAR

MIXED CONVECTION

HEAT TRANSFER

Thesis Approved:

Gerald D. Parker
Thesis Adviser

O. R. Haworth

Ladislaus J. Fila

Paul E. Torg

J. H. Boggs
Dean of the Graduate School

PREFACE

It is the purpose of this study to find a general and widely applicable method of solution of the laminar mixed convection heat transfer problem. Mixed convection refers to those flow and heat transfer situations which are neither clearly forced convection nor free or natural convection.

The application of the integral method to mixed convection heat transfer was originally suggested by Dr. J. D. Parker. I am also indebted to him for his encouragement and suggestions during the course of this work and for his insight into the almost daily problems which arose. I wish to thank Dr. D. Grosvenor of the Oklahoma State University Computer Center for making available the considerable amount of computer time that has been used. Thanks are also extended to my wife, Ardyce, for her heroic typing of the drafts and final copy.

TABLE OF CONTENTS

LIST OF FIGURES

NOMENCLATURE

Symbols are listed in the order of their appearance in the text.

x, y	= coordinate distances
Gr_x	= Grashof number, $\frac{\lvert g \rvert \cdot \beta \cdot \lvert (T_w - T_\infty) \rvert x^3}{\nu^2}$
g	= acceleration due to gravity
β	= volumetric coefficient of expansion
T	= fluid temperature as a function of x and y
T_w	= wall temperature
T_∞	= free stream temperature
ν, μ	= fluid viscosity, $\nu = \frac{\mu}{\rho}$
U_∞	= free stream velocity
U	= longitudinal free stream velocity as a function of x just outside of the boundary layer
u, v	= velocities within the boundary layer
ρ, ρ_∞	= local fluid density and free stream density
P	= fluid pressure
g_x	= x component of acceleration due to gravity
R	= universal gas constant
k	= fluid thermal conductivity
C_P	= fluid specific heat at constant pressure
θ	= $\frac{T - T_\infty}{T_w - T_\infty}$
Re_x	= Reynolds number, $\frac{Ux}{\nu}$
u_1	= $\frac{u}{U_\infty}$

v_1 = $\frac{\nu}{U_\infty}\sqrt{Re_x}$

y_1 = $\frac{y}{x}\sqrt{Re_x}$

L = characteristic length

U_1 = U/U_∞

Z = $Gr_x/Re_x^2 = \frac{|g|\cdot\beta\cdot|(T_w-T_\infty)|\,x}{U^2}$

v_2 = $v_1\sqrt{\frac{Re_x^2}{Gr_x}}$

y_2 = $y_1\sqrt{\frac{Gr_x}{Re_x^2}}$

α = thermal diffusivity, $\frac{k}{\rho g C_p}$

Pr = Prandtl number, $\frac{\nu}{\alpha}$ or $\frac{\mu g C_p}{k}$

$h(\eta_T)$ = temperature profile function

$f(\eta)$ = velocity profile function

δ_2 = dimensionless velocity boundary layer thickness

δ_{T2} = dimensionless thermal boundary layer thickness

δ_1 = $\frac{\delta}{x}\sqrt{Re_x}$

δ_2 = $\delta_1\sqrt{Z}$

δ_{T_1} = $\frac{\delta_T}{x}\sqrt{Re_x}$

δ_{T_2} = $\delta_{T_1}\sqrt{Z}$

Δ, Δ_o = $\frac{\delta_T}{\delta} = \frac{\delta_{T_1}}{\delta_1} = \frac{\delta_{T_2}}{\delta_2}$, boundary layer thickness ratio, or Δ at Z = 0

η = $\frac{y}{\delta} = \frac{y_1}{\delta_1} = \frac{y_2}{\delta_2}$

η_T = $\frac{y}{\delta_T} = \frac{y_1}{\delta_{T_1}} = \frac{y_2}{\delta_{T_2}}$

v = temperature factor, $\theta\big]_{\eta_T=1} = (1-\nu)$

w = velocity factor, $u_1\big]_{\eta=1} = w$

a, b, c,... = velocity profile coefficients

A, B, C,... = temperature profile coefficients

n = order of derivatives of u_1 or θ at the boundary layer edge

j = $\left(\pm 1 + \frac{1}{U_1}\frac{dU_1}{dZ}\right)$

H_1, H_2, H_3 = polynomials in Δ, $\Xi = 0$

q = heat transferred per unit time

h = heat transfer coefficient

Nu_x = Nusselt number, hx/k

τ_w = fluid shear stress at the wall

C_f = wall friction factor, $\frac{2\tau_w}{\rho U^2}$

γ = constant in $(T_w - T_\infty) = \gamma x$

J = $(T_w - T_\infty)$

q'' = heat transferred per unit time per unit area or heat flux

Q = $\frac{q''}{k}\left(\frac{\nu\, U_\infty}{|g| \cdot \beta}\right)^{1/2}$

K = $\frac{\nu_w}{\nu_\infty}$, ratio of viscosity at the wall to free stream viscosity

CHAPTER I

INTRODUCTION

The purpose of this thesis is to present a reasonably complete analysis of mixed convection heat transfer associated with the external flow of a fluid over a vertical or nearly vertical surface. Mixed convection implies that both free and forced convection effects are present. This study is restricted to the laminar flow of an incompressible fluid, incompressible in the sense that density varies only with temperature and only in the buoyancy body force term of the applicable differential equation.

Fluids with Prandtl numbers from 0.01 to 1000, a range which includes liquid metals, gases, and viscous oils, are investigated. Flow situations are those for a flat plate and a wedge in an infinite medium. The effects of variable properties and different boundary conditions at the wall are analyzed.

The mixed convection problem is a challenging one since it involves the interaction in the boundary layer equations of the Reynolds, Grashof, and Prandtl numbers, surface geometry and surface thermal boundary conditions, and the orientation of a body force. The buoyancy force, which is opposite in direction to the fluid body force and which is characterized by the Grashof number, is always present in forced convection. The determination of the buoyancy effect on forced convection and the conditions existing when that effect becomes important are two objec-

tives of this study. Another is to explore further the popular integral method: to see if it can be improved so as to work more effectively on this type of problem, to determine its degree of accuracy, and to find out how practical the integral method is for different mixed convection geometries and boundary conditions. The fourth object of the study is the exploration of the velocity distributions of different Prandtl number fluids in the boundary layer when free and forced convection are competing.

Let us consider an example of a mixed convection problem which might arise during the designing of a nuclear power reactor. Suppose that for some reason the reactor was to be shut down after a long run. Afterheat removal is necessary, and the designer must be able to calculate the cooling fluid flow rate that would be required to do this. However, to cover possible emergency situations, he would also want to know the minimum flow rate that could be used and at what point free convection effects alone were reliable.

The integral method for solving partial differential equations of the boundary-layer type is employed throughout this thesis. By this method one or more partial differential equations can be reduced to ordinary differential equations, which in turn can be more readily integrated. The integral method yields an approximate solution since the original partial differential equations are not solved at every point in the field as they should be for exactness. The solution instead depends on the choice of boundary conditions at the wall and at the edge of the thermal and velocity boundary layers and on the choice of the analytical expressions for temperature and velocity profiles across the boundary layers.

Mixed convection has been studied by several authors. A. Acrivos (1958) used the integral method to investigate combined forced and free convection on a vertical flat plate for fluids with Prandtl numbers of 0.73, 10, and 100. J. R. Kliegel (1959) improved upon the work of Acrivos and also verified his own theory by experiments with air flowing over a vertical heated plate. The present thesis further extends the work of these two investigators and generally uses the same approach to a solution through the integral method but with significant modifications. Sparrow, Eichhorn, and Gregg (1959) arrived at an exact solution for the mixed convection flow of a gas over a vertically oriented wedge surface although similarity requirements restricted their results to special cases of wedge angle and wall temperature distribution. Their results are used to check the accuracy of the integral method employed in this study.

Rosen and Hanratty (1961) reported on mixed convection flow in a vertical tube and also used a variation of the integral method. Gill and Del Casal (1962) and Mori (1961) have studied the effects of natural convection, or buoyancy effects, in forced convection flow over a horizontal plate. Mori made use of the integral method. Eckert and Diaguila (1954) have shown the regime of Grashof and Reynolds numbers for flow in a vertical tube over which mixed-convection effects are important. Sparrow and Gregg (1959) have done the same thing for a vertical flat plate. A good summary of mixed convection work up to 1961 was given by Gebhart (1961) on pages 273 to 279 of his book.

H. C. Agrawal (1962) used a variational method to solve the mixed convection flow of a fluid in a vertical rectangular duct at two Rayleigh numbers. Finally, Brindley (1963) used Meksyn's approximate

technique to solve the mixed convection problem for a wedge and extended Sparrow, Eichhorn, and Gregg's (1959) solution to Pr = 7 as well. However, Brindley's method is restricted to those situations in which a similarity transformation can be made.

CHAPTER II

THE INTEGRAL METHOD APPLIED TO MIXED CONVECTION

Convection heat transfer can be described as forced convection, mixed convection, or free or natural convection. In forced convection, either the free stream velocity of the fluid is so large or the temperature difference between the wall and the fluid, the distance along the wall, and the volumetric coefficient of expansion of the fluid are all so small that free convection buoyancy effects can be neglected. Conversely, in free convection the temperature difference, body length, and expansion coefficient are controlling, and any one of the three can become large enough to override the effect of at least a small free stream velocity and cause the flow situation to be essentially a free convection one. This combination of circumstances is well described by the value of the ratio of two dimensionless parameters, the Grashof number,

$$Gr_x = \frac{|g| \cdot \beta \cdot |(T_w - T_\infty)| \quad x^3}{\nu^2} \quad ,$$

and the Reynolds number squared,

$$Re_x^2 = \left(\frac{Ux}{\nu}\right)^2 \quad .$$

Their ratio, which occurs as a coefficient in the buoyancy force term in one non-dimensional version of the boundary layer equation, (Appendix B), is: $\frac{Gr_x}{Re_x^2} = \frac{|g| \cdot \beta \cdot |(T_w - T_\infty)| \; x}{U^2}$.

For small values of Gr_x/Re_x^2, the flow situation is forced convection since inertia forces dominate. For large values of Gr_x/Re_x^2, the quantities in the numerator have become important, the buoyancy force term is large, and the flow is free convection. Mixed convection occurs for intermediate values of Gr_x/Re_x^2, between about 0.1 and 15.0, as will be shown.

Forced and free convection problems have been solved in the past by the integral method. This method was first used in boundary layer problem solutions by K. Pohlhausen. The method is especially useful when no exact or similarity solutions can be found for the governing partial differential equations. With the availability of digital electronic computers the integral method is most useful, for example, in reducing a two-dimensional velocity and temperature field problem to a one-dimensional problem involving two ordinary differential equations which the electronic computer can easily handle.

The Governing Equations

The steady-state, two-dimensional boundary layer equation derived from the Navier-Stokes equations by boundary layer assumptions is

$$\rho\left(u\frac{\partial u}{\partial x} + v\frac{\partial u}{\partial y}\right) = -\rho g_x - \frac{dP}{dx} + \mu\frac{\partial^2 u}{\partial y^2} .$$

This single equation with its body force term, $-\rho g_x$, implies that there is no force term of significance in the y-direction and that $\frac{dP}{dy} = 0$. The orientation of U_∞, g, u, v, and the immersed body's surface are shown in Figure 1.

If the above equation is evaluated at the edge of the boundary layer, the result is

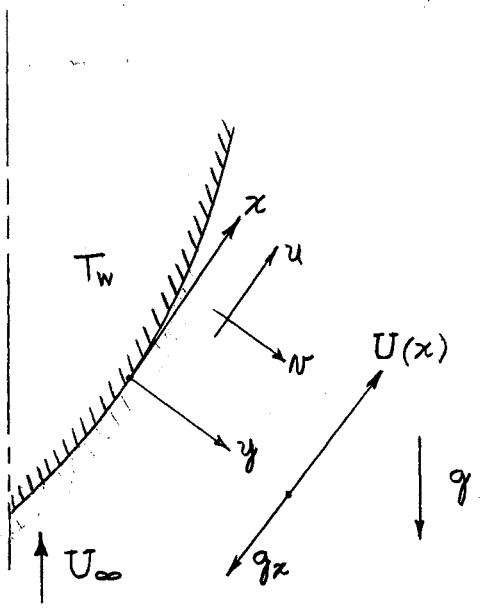

Fig. 1. Orientation of Immersed Body

$$\rho_\infty U\frac{dU}{dx} = -\rho_\infty g_x - \frac{dP}{dx} \quad ,$$

or

$$\frac{dP}{dx} = -\rho_\infty g_x - \rho_\infty U\frac{dU}{dx} \quad .$$

Then upon substitution for $\frac{dP}{dx}$ in the boundary layer equation,

$$\rho\left(u\frac{\partial u}{\partial x} + v\frac{\partial u}{\partial y}\right) = \rho_\infty U\frac{dU}{dx} + g_x(\rho_\infty - \rho) + \mu\frac{\partial^2 u}{\partial y^2} \quad .$$

For constant β , where β is the volumetric coefficient of expansion,

$$\frac{\rho_\infty}{\rho} = 1 + \beta(T - T_\infty) \quad .$$

Therefore,

$$g_x(\rho_\infty - \rho) = g_x\rho\left(\frac{\rho_\infty}{\rho} - 1\right) = g_x\rho\beta(T - T_\infty) \quad .$$

With the assumption that $\frac{\rho_\infty}{\rho} \cong 1$ and is therefore not significant as a coefficient of $U\frac{dU}{dx}$, the boundary layer equation becomes

$$u\frac{\partial u}{\partial x} + v\frac{\partial u}{\partial y} = g_x\beta(T - T_\infty) + U\frac{dU}{dx} + \nu\frac{\partial^2 u}{\partial y^2} \quad .$$

The buoyancy term, $g_x \beta(T-T_\infty)$, is necessary for free convective action.

For a perfect gas, at any x,

$$\frac{\rho_\infty}{\rho(y)} = \frac{T(y)}{T_\infty}$$

since $p=p_\infty$ at any given x, and $p=\rho RT$. Therefore,

$$g_x(\rho_\infty-\rho) = g_x\rho\left(\frac{T}{T_\infty}-1\right) = g_x\rho\cdot\frac{1}{T_\infty}(T-T_\infty)$$

which implies that for a perfect gas, $\beta = \frac{1}{T_\infty}$, and not $\frac{1}{T}$.

The constant property mixed convection problem is described completely by the boundary layer equation with its buoyancy term, by the thermal boundary layer equation, by the continuity equation, and by boundary conditions, one of which specifies that $U_\infty \neq 0$. The three equations involved, the boundary layer equations, are:

$$u\frac{\partial u}{\partial x} + v\frac{\partial u}{\partial y} = g_x\beta(T-T_\infty) + U\frac{dU}{dx} + \nu\frac{\partial^2 u}{\partial y^2}$$

$$u\frac{\partial T}{\partial x} + v\frac{\partial T}{\partial y} = \frac{k}{\rho C_p}\frac{\partial^2 T}{\partial y^2}$$

$$\frac{\partial u}{\partial x} + \frac{\partial v}{\partial y} = 0$$

The problem is to solve these equations simultaneously for the three unknowns, u, v, and T, in terms of the space coordinates, x and y. This is essentially what the integral method does, but it solves the equations in an indirect manner.

Appendix B details the two consecutive transformations of these equations to their final non-dimensional form in terms of u_1, v_2, θ, Z, y_2, and the Prandtl number, Pr. After the first transformation, it is

seen (Appendix B) that the buoyancy term is $\pm(Gr_x/Re_x^2)\theta$, as mentioned earlier. The signs preceding the term are necessary since Gr_x/Re_x^2 is always positive. The plus sign refers to the normal aiding flow case of a fluid being heated in upflow or cooled in downflow. The minus sign refers to the opposing flow case, a fluid being heated in downflow or cooled in upflow.

The results of the transformations in Appendix B are the non-dimensionalized boundary layer equations in the new variables which will be used hence in this thesis. They apply to steady-state, constant-property, non-dissipating flow.

$$u_1 \frac{\partial u_1}{\partial z} + v_2 \frac{\partial u_1}{\partial y_2} = \pm U_1^2 \theta + U_1 \frac{dU_1}{dz} + U_1 \frac{\partial^2 u_1}{\partial y_2^2} \tag{1}$$

$$u_1 \frac{\partial \theta}{\partial z} + v_2 \frac{\partial \theta}{\partial y_2} = \frac{U_1}{Pr} \frac{\partial^2 \theta}{\partial y_2^2} \tag{2}$$

$$\frac{\partial u_1}{\partial z} + \frac{\partial v_2}{\partial y_2} = 0 \tag{3}$$

In these equations the new independent and dependent variables are defined as:

$$z = \frac{Gr_x}{Re_x^2}$$

$$y_2 = \frac{y}{x} \sqrt{Re_x} \sqrt{\frac{Gr_x}{Re_x^2}}$$

$$u_1 = \frac{u}{U_\infty}$$

and

$$v_2 = \frac{v}{U_\infty} \sqrt{Re_x} \sqrt{\frac{Re_x^2}{Gr_x}}$$

The dimensionless temperature is

$$\theta = \frac{T - T_\infty}{T_w - T_\infty} \quad ,$$

and the dimensionless velocity just outside of the velocity boundary layer is $U_1 = \frac{U}{U_\infty}$.

Appendix C details the usual steps employed to convert equations (1), (2), and (3) to their differential-integral forms, the momentum integral and the energy integral equations. In their more general forms for a velocity distribution U_1 about a body they are (Appendix C):

$$\frac{d}{dz}\left[U_1^2 \delta_2 \int_0^1 f(1-f)\,d\eta\right] + U_1 \frac{dU_1}{dz} \cdot \delta_2 \int_0^1 (1-f)\,d\eta = \mp U_1^2 \delta_{T_2} \int_0^1 h\,d\eta_T + U_1 \left(\frac{\partial u_1}{\partial y_2}\right)_w \tag{4}$$

$$\frac{d}{dz}\left[\int_0^\infty u_1 \theta\, dy_2\right] = -\frac{U_1}{P_r}\left(\frac{\partial \theta}{\partial y_2}\right)_w \tag{5}$$

The four definite integrals and the two partial derivatives in equations (4) and (5) can be evaluated and the resulting two simultaneous ordinary differential equations in δ_2 and δ_{T_2} with Z as their independent variable can be solved numerically if u_1 and θ are known as functions of y_2 and Z. Since u_1 and θ are functions of y_2 and Z, the procedure at this point in an integral method solution is to let u_1 and θ be represented by some type of series in y_2 with the coefficients of the individual terms in the series as yet undetermined functions of Z. These coefficients will actually be expressed in terms of δ_2 and δ_{T_2}, which are themselves functions of Z; δ_2 and δ_{T_2} are, of course, in-

dependent of y_2.

It is also convenient to use η and η_T to replace y_2 in the series representations of u_1 and θ. Since $\eta = \frac{y_2}{\delta_2}$ and $\eta_T = \frac{y_2}{\delta_{T_2}}$, the integrations that are required in equations (4) and (5) can be performed to an upper limit of one instead of to upper limits of δ_2 and δ_{T_2}. The introduction of η and η_T also makes it much easier to apply boundary conditions at the edges of the boundary layers to u_1 and θ since now $\eta = 1$ or $\eta_T = 1$ instead of $y_2 = \delta_2$ or $y_2 = \delta_{T_2}$. The final results are naturally the same whether η and η_T or y_2 are selected to form the series for u_1 and θ.

The introduction of the two parameters δ_2 and δ_{T_2}, the velocity and thermal boundary layer thicknesses, makes possible the evaluation of the improper integrals that occur in the integral equations (4) and (5). For example,

$$\int_0^\infty u_1 (U_1 - u_1)\, dy_2$$

becomes the readily integrable

$$\delta_2 U_1^2 \int_0^1 f(1-f)\, d\eta .$$

In this example, δ_2 represents the y_2 distance at which the integrand $u_1(U_1-u_1)$ becomes zero and stays zero, and the integral therefore is bounded. Similarly, δ_{T_2} represents the y_2 distance at which the integrand in $\int_0^\infty \theta\, dy_2$ becomes zero and the integral bounded. Since the parameters δ_2 and δ_{T_2} arise in this way, they can be physically meaningful dependent variables.

However, it is at this point that the integral method displays some of its weaknesses. In actuality u_1 approaches U_1 and θ approaches zero asymptotically; that is, $\frac{\partial^n u_1}{\partial y_2^n}$ and $\frac{\partial^n \theta}{\partial y_2^n}$, $n = 1, 2, 3, \ldots$, are all zero as y_2 approaches infinity. But in the integral method it

is the practice to say that $u_1 = U_1$ at $y_2 = \delta_2$, and $\theta = 0$ at $y_2 = \delta_{T_2}$. Further, the velocity boundary layer thickness is customarily defined, for example, by Schlichting (1960), as the point at which $u_1 = .99\ U_1$; the true thermal boundary layer thickness would have a similar definition, say $\theta = .01$ at $y_2 = \delta_{T_2}$. Also, the nature of the integral method requires that the largest value of n be some reasonably small number instead of infinity, since it has been specified that $u_1 = U_1$ and $\theta = 0$ at some finite transverse distances, δ_2 and δ_{T_2} , contrary to the definition of an asymptote.

The series representations for u_1 and θ were chosen to be polynomials in η and η_T whose coefficients a, b, c,... and A, B, C,... are functions of δ_2 and δ_{T_2} (or Z) as stated above:

$$\frac{u_1}{U_1} = f(\eta) = a\eta + b\eta^2 + c\eta^3 + \cdots$$

and

$$\theta = h(\eta_T) = 1 + A\eta_T + B\eta_T^2 + C\eta_T^3 + \cdots$$

The form of these two polynomials allows θ to equal one and u_1/U_1 to equal zero at the wall or the surface of the immersed body. The evaluation of the coefficients and the degree of the polynomials will depend directly on the other boundary conditions that can be applied at the wall and at the edges of the defined boundary layers. If a sufficient number of boundary conditions could be found and a corresponding pair of high degree polynomials employed for u_1/U_1 and θ, the resulting final solutions for u_1, v_2, and θ as functions of Z and y_2 would closely approach the exact solutions of equations (1), (2), and (3). Anything less, of course, is responsible for the necessarily approximate nature of this type of solution.

Selection of Boundary Conditions

It was decided to use both similar and equal numbers of boundary conditions on u_1 and θ, so that in the limiting case of $Z = 0$, which would imply pure forced convection, for a Prandtl number of one and for a flat plate with constant wall temperature, the velocity boundary layer thickness, δ_z , would equal the thermal boundary layer thickness, δ_{T_z}. This equality is dictated by the similarity of the velocity and thermal boundary layer equations under these special conditions where the buoyancy force term is small enough to be ignored:

$$u_1 \frac{\partial u_1}{\partial z} + v_z \frac{\partial u_1}{\partial y_z} = \frac{\partial^2 u_1}{\partial y_z^2}$$

$$u_1 \frac{\partial \theta}{\partial z} + v_z \frac{\partial \theta}{\partial y_z} = \frac{\partial^2 \theta}{\partial y_z^2}$$

These two equations obviously would have a common solution.

At the edges of the boundary layers, at $\eta_T = 1$ and $\eta = 1$,

$$\theta = 0$$

and

$$u_1 = U_1$$

There are also available a finite number of "asymptotic" boundary conditions at $\eta = 1$ and $\eta_T = 1$:

$$\left.\frac{\partial u_1}{\partial y_z}\right]_{\eta=1} = \left.\frac{\partial^2 u_1}{\partial y_z^2}\right]_{\eta=1} = \left.\frac{\partial^3 u_1}{\partial y_z^3}\right]_{\eta=1} = \cdots = 0$$

$$\left.\frac{\partial \theta}{\partial y_z}\right]_{\eta_T=1} = \left.\frac{\partial^2 \theta}{\partial y_z^2}\right]_{\eta_T=1} = \left.\frac{\partial^3 \theta}{\partial y_z^3}\right]_{\eta_T=1} = \cdots = 0$$

It was decided to employ these boundary conditions up to the third partial derivative although the use of only the first and also only the

first and second derivatives was evaluated at the same time. If the final forms for θ are plotted against η_T it is seen, Fig. 2, that the use of three derivatives gives a better simulation of the shape of an exact solution temperature profile curve than either the use of one or two derivatives. The same would be true for the velocity profile.

If equations (1) and (2) are evaluated at the wall, where u_1 and v_1 are zero,

$$\left.\frac{\partial^2 u_1}{\partial y_2^2}\right]_w = -\left(\pm U_1 + \frac{dU_1}{dz}\right)$$

and

$$\left.\frac{\partial^2 \theta}{\partial y_2^2}\right]_w = 0 .$$

Further, if equations (1) and (2) are each differentiated with respect to y_2,

$$u_1\frac{\partial^2 u_1}{\partial y_2 \partial z} + \frac{\partial u_1}{\partial y_2}\cdot\frac{\partial u_1}{\partial z} + v_2\frac{\partial^2 u_1}{\partial y_2^2} + \frac{\partial v_2}{\partial y_2}\cdot\frac{\partial u_1}{\partial y_2} = \pm U_1^2\frac{\partial^2\theta}{\partial y_2^2} + U_1\frac{\partial^3 u_1}{\partial y_2^3} ,$$

and

$$u_1\frac{\partial^2\theta}{\partial y_2\partial z} + \frac{\partial u_1}{\partial y_2}\frac{\partial\theta}{\partial z} + v_2\frac{\partial^2\theta}{\partial y_2^2} + \frac{\partial v_2}{\partial y_2}\frac{\partial\theta}{\partial y_2} = \frac{U_1}{Pr}\frac{\partial^3\theta}{\partial y_2^3} .$$

Since $\frac{\partial u_1}{\partial z} = -\frac{\partial v_2}{\partial y_2}$ from the continuity equation, at the wall:

$$\left.\frac{\partial^3 u_1}{\partial y_2^3}\right]_w = \mp U_1\left.\frac{\partial\theta}{\partial y_2}\right]_w$$

and

$$\left.\frac{U_1}{Pr}\frac{\partial^3\theta}{\partial y_2^3}\right]_w = \left.\frac{\partial u_1}{\partial y_2}\right]_w\cdot\left.\frac{\partial\theta}{\partial z}\right]_w .$$

Subsequent differentiations of equations (1) and (2) with respect to y_2 would introduce partial derivatives of the coefficients with re-

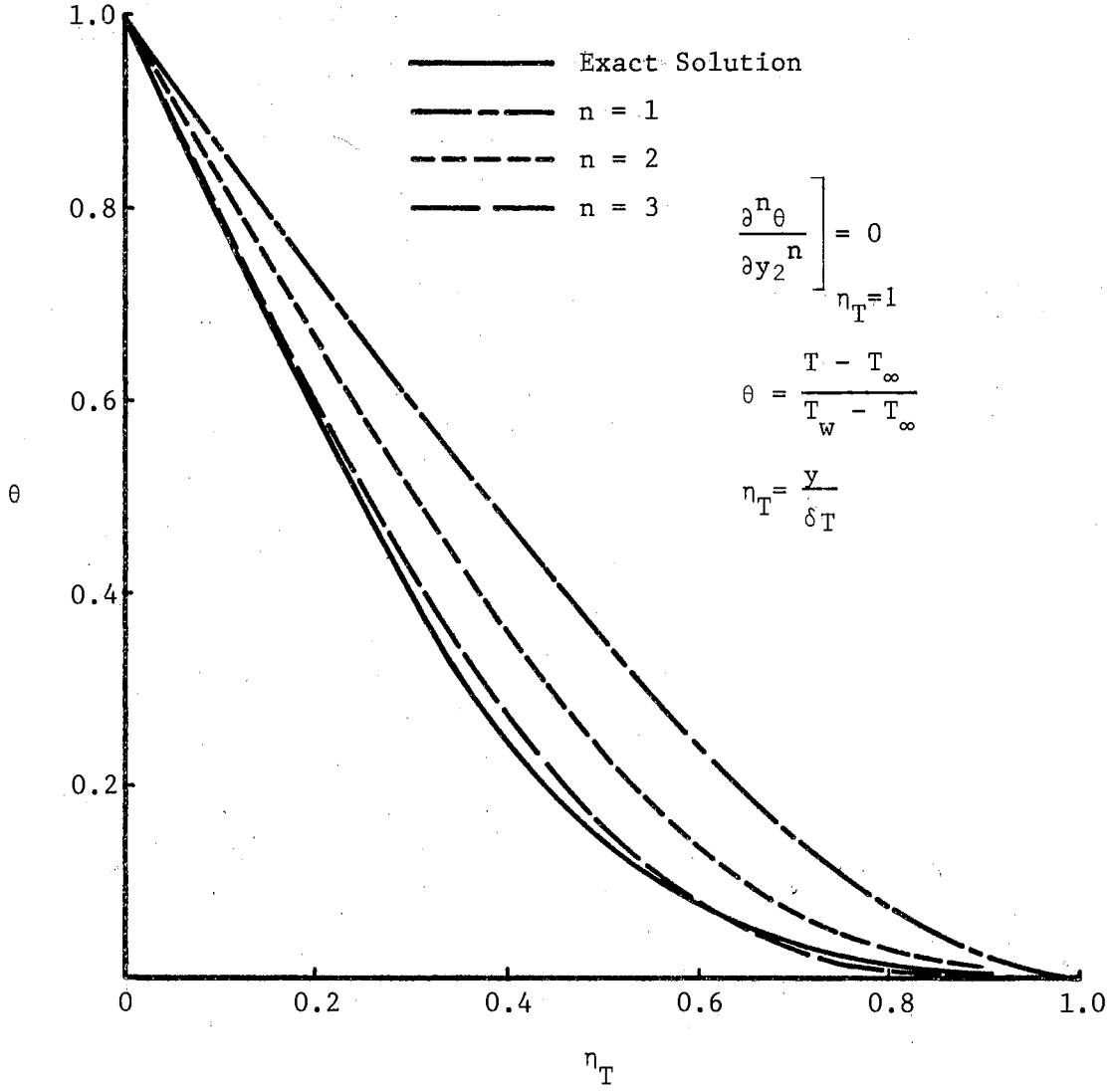

Figure 2. Comparison of Temperature Profiles From a Wedge Flow Exact Solution, z = 0, Sparrow, et al (1959) and From the Approximate Solution With One, Two, and Three Asymptotic Boundary Conditions.

spect to Z. This would greatly complicate the determination of the coefficients of the polynomials representing u_1/U_1 and θ. Therefore, this procedure was not utilized beyond one differentiation. For example, the next differentiation of equation (1) gives

$$\left.\frac{\partial^4 u_1}{\partial y_2^4}\right]_w = \left.\frac{1}{U_1}\frac{\partial u_1}{\partial y_2}\right]_w \cdot \left.\frac{\partial^2 u_1}{\partial y_2 \partial z}\right]_w ,$$

which involves terms in a and $\frac{\partial a}{\partial z}$, where a is the first coefficient in $f(\eta)$.

The six boundary conditions on u_1 then are:

$$\left.u_1\right]_{\eta=1} = U_1 , \tag{6}$$

$$\left.\frac{\partial u_1}{\partial y_2}\right]_{\eta=1} = \left.\frac{\partial^2 u_1}{\partial y_2^2}\right]_{\eta=1} = \left.\frac{\partial^3 u_1}{\partial y_2^3}\right]_{\eta=1} = 0 , \tag{7}$$

$$\left.\frac{\partial^2 u_1}{\partial y_2^2}\right]_w = -\left[\pm U_1 + \frac{dU_1}{dz}\right] , \tag{8}$$

and

$$\left.\frac{\partial^3 u_1}{\partial y_2^3}\right]_w = \mp U_1 \left.\frac{\partial \theta}{\partial y_2}\right]_w , \tag{9}$$

and the six boundary conditions on θ, if a constant wall temperature is assumed, are:

$$\left.\theta\right]_{\eta_T=1} = 0 \tag{10}$$

$$\left.\frac{\partial \theta}{\partial y_2}\right]_{\eta_T=1} = \left.\frac{\partial^2 \theta}{\partial y_2^2}\right]_{\eta_T=1} = \left.\frac{\partial^3 \theta}{\partial y_2^3}\right]_{\eta_T=1} = 0 \quad , \tag{11}$$

$$\left.\frac{\partial^2 \theta}{\partial y_2^2}\right]_{w} = 0 \quad , \tag{12}$$

and

$$\left.\frac{\partial^3 \theta}{\partial y_2^3}\right]_{w} = 0 \quad . \tag{13}$$

The twelve boundary conditions selected will allow the polynomials chosen for u_1/U_1 and θ to be determined in terms of δ_2 , δ_{T_2} , η , and η_T although they are only approximations to the true velocity and temperature profiles. Nevertheless, when these approximations are inserted into the momentum and energy integral equations, (4) and (5), the final solutions for u_1, v_2, and θ will satisfy the condition of continuity and the conservation of energy and momentum. The results, therefore, can be misleading and must be carefully weighed against known exact solutions and other criteria.

Evaluation of Coefficients

The polynomials that represent u_1/U_1 and θ are now written as:

$$\frac{u_1}{U_1} = f(\eta) = a\eta + b\eta^2 + c\eta^3 + d\eta^4 + e\eta^5 + f\eta^6 \tag{14}$$

and

$$\theta = h(\eta_T) = 1 + A\eta_T + B\eta_T^2 + C\eta_T^3 + D\eta_T^4 + E\eta_T^5 + F\eta_T^6 \tag{15}$$

since a total of twelve boundary conditions are available.

The six derivatives of equations (14) and (15) with respect to y_2 that are required by the boundary conditions are

$$\frac{\partial u_1}{\partial y_2} = \frac{U_1}{\delta_2}\frac{\partial\left(\frac{u_1}{U_1}\right)}{\partial \eta} = \frac{U_1}{\delta_2}\left(a + 2b\eta + 3c\eta^2 + 4d\eta^3 + 5e\eta^4 + 6f\eta^5\right),$$

$$\frac{\partial^2 u_1}{\partial y_2^2} = \frac{U_1}{\delta_2^2}\left(2b + 6c\eta + 12d\eta^2 + 20e\eta^3 + 30f\eta^4\right),$$

$$\frac{\partial^3 u_1}{\partial y_2^3} = \frac{U_1}{\delta_2^3}\left(6c + 24d\eta + 60e\eta^2 + 120f\eta^3\right),$$

$$\frac{\partial \theta}{\partial y_2} = \frac{1}{\delta_{T_2}}\frac{\partial \theta}{\partial \eta_T} = \frac{1}{\delta_{T_2}}\left(A + 2B\eta_T + 3C\eta_T^2 + 4D\eta_T^3 + 5E\eta_T^4 + 6F\eta_T^5\right),$$

$$\frac{\partial^2 \theta}{\partial y_2^2} = \frac{1}{\delta_{T_2}^2}\left(2B + 6C\eta_T + 12D\eta_T^2 + 20E\eta_T^3 + 30F\eta_T^4\right),$$

and

$$\frac{\partial^3 \theta}{\partial y_2^3} = \frac{1}{\delta_T^3}\left(6C + 24D\eta_T + 60E\eta_T^2 + 120F\eta_T^3\right).$$

First, looking at the temperature profile coefficients, from equation (10),

$$A + B + C + D + E + F = -1 ,$$

from equation (11),

$$A + 2B + 3C + 4D + 5E + 6F = 0 ,$$

$$B + 3C + 6D + 10E + 15F = 0 ,$$

$$C + 4D + 10E + 20F = 0 ,$$

and from equations (12) and (13),

$$B = 0$$

$$C = 0$$

The four linear coefficient equations are solved simultaneously to give:

$$A = -2$$
$$D = 5$$
$$E = -6$$
$$F = 2$$

so that

$$\theta = 1 - 2\eta_T + 5\eta_T^4 - 6\eta_T^5 + 2\eta_T^6. \tag{16}$$

The coefficients of θ are constants and not functions of Z. The approximate integral method predicts that all temperature profiles for any fluid are similar in mixed convection for a constant wall temperature. Heat transfer at the wall, however, is proportional to $\left.\frac{\partial\theta}{\partial y_2}\right]_w$ and since

$$\left.\frac{\partial\theta}{\partial y_2}\right]_w = \frac{1}{\delta_{T_2}}\left.\frac{\partial\theta}{\partial\eta}\right]_w = -\frac{2}{\delta_{T_2}},$$

heat transfer is inversely proportional to the thermal boundary layer thickness.

Equation (9) is applied as a boundary condition on u_1 after the expression for θ has been determined.

The coefficients of the polynomial expressing u_1/U_1 can now be determined. From equation (6),

$$a + b + c + d + e + f = 1$$

and from equation (7),

$$a + 2b + 3c + 4d + 5e + 6f = 0$$
$$b + 3c + 6d + 10e + 15f = 0$$
$$c + 4d + 10e + 20f = 0$$

If these four equations are solved for b and c,

$$a + d + e + f = 1 - b - c$$

$$a + 4d + 5e + 6f = -2b - 3c$$

$$6d + 10e + 15f = -b - 3c$$

$$4d + 10e + 20f = -c$$

From equation (8),

$$\frac{U_1}{\delta_2^2}(2b) = -\left[\pm U_1 + \frac{dU_1}{dz}\right]$$

or

$$b = -\frac{\delta_2^2}{2}\left[\pm 1 + \frac{1}{U_1}\frac{dU_1}{dz}\right]$$

From equation (9),

$$\frac{U_1}{\delta_2^3}(6c) = -U_1\left(-\frac{2}{\delta_{T_2}}\right)$$

or

$$c = \pm\frac{1}{3}\frac{\delta_2^3}{\delta_{T_2}} = \pm\frac{1}{3}\frac{\delta_2^2}{\Delta} \quad , \text{ where } \Delta = \frac{\delta_{T_2}}{\delta_2} .$$

The introduction of $\Delta = \frac{\delta_{T_2}}{\delta_2}$ affords a convenient variable, the ratio of the thermal boundary layer to the velocity boundary layer thickness, which will replace δ_{T_2} . It is also more convenient to use δ_2^2 instead of δ_2 as the other dependent vaiable. The two dependent variables then that will be solved for in equations (4) and (5) are, therefore,

$$\delta_2^2 = \frac{\delta^2}{x^2}\left(\frac{Gr_x}{Re_x^2}\right)\left(Re_x\right) = \frac{\delta^2}{x^2}\cdot Z\cdot Re_x \quad ,$$

and

$$\Delta = \frac{\delta_{T_2}}{\delta_2} = \frac{\delta_T}{\delta} = \frac{\eta}{\eta_T} .$$

Δ and δ_2^2 can subsequently be used to find the velocity and temperature at any point within the boundary layer and to find the local Nusselt number and local shear stress at the wall.

The coefficients of the velocity profile polynomial can now be written as:

$$
\begin{aligned}
a &= 2 + \tfrac{1}{5}\delta_2^2 j \mp \tfrac{1}{30}\frac{\delta_2^2}{\Delta} \\
b &= -\tfrac{1}{2}\delta_2^2 j \\
c &= \pm\tfrac{1}{3}\frac{\delta_2^2}{\Delta} \\
d &= -5 + \delta_2^2 j \mp \tfrac{2}{3}\frac{\delta_2^2}{\Delta} \\
e &= 6 - \delta_2^2 j \pm \tfrac{1}{2}\frac{\delta_2^2}{\Delta} \\
f &= -2 + \tfrac{3}{10}\delta_2^2 j \mp \tfrac{2}{15}\frac{\delta_2^2}{\Delta}
\end{aligned}
\qquad (17)
$$

where $$j = \left(\pm 1 + \frac{1}{U_1}\frac{dU_1}{dz}\right).$$

For a flat plate, j = +1 for aiding flow (upflow with heating or downflow with cooling) and j = -1 for opposing flow.

Reduction of the Differential-Integral Equations to First-Order Differential Equations in $\frac{d\delta_2^2}{dz}$ and $\frac{d\Delta}{dz}$

The individual terms in the momentum integral equation, (4), can be solved in terms of the velocity and temperature profile coefficients, a, b, c,... and A, D, E, and F, as follows:

$$\delta_2 \int_0^1 f(1-f)\,d\eta$$

$$= \delta_2 \Big\{ a\Big[\tfrac{1}{2} - \tfrac{a}{3} - \tfrac{b}{4} - \tfrac{c}{5} - \tfrac{d}{6} - \tfrac{e}{7} - \tfrac{f}{8}\Big]$$
$$+ b\Big[\tfrac{1}{3} - \tfrac{a}{4} - \tfrac{b}{5} - \tfrac{c}{6} - \tfrac{d}{7} - \tfrac{e}{8} - \tfrac{f}{9}\Big]$$
$$+ c\Big[\tfrac{1}{4} - \tfrac{a}{5} - \tfrac{b}{6} - \tfrac{c}{7} - \tfrac{d}{8} - \tfrac{e}{9} - \tfrac{f}{10}\Big] \qquad (18)$$
$$+ d\Big[\tfrac{1}{5} - \tfrac{a}{6} - \tfrac{b}{7} - \tfrac{c}{8} - \tfrac{d}{9} - \tfrac{e}{10} - \tfrac{f}{11}\Big]$$
$$+ e\Big[\tfrac{1}{6} - \tfrac{a}{7} - \tfrac{b}{8} - \tfrac{c}{9} - \tfrac{d}{10} - \tfrac{e}{11} - \tfrac{f}{12}\Big]$$
$$+ f\Big[\tfrac{1}{7} - \tfrac{a}{8} - \tfrac{b}{9} - \tfrac{c}{10} - \tfrac{d}{11} - \tfrac{e}{12} - \tfrac{f}{13}\Big]\Big\} .$$

$$\delta_2 \int_0^1 (1-f)\,d\eta = \Big(1 - \frac{a}{2} - \frac{b}{3} - \frac{c}{4} - \frac{d}{5} - \frac{e}{6} - \frac{f}{7}\Big)\delta_2 . \qquad (19)$$

$$\delta_2 \Delta \int_0^1 h\,d\eta_T = \Big(1 + \frac{A}{2} + \frac{D}{5} + \frac{E}{6} + \frac{F}{7}\Big)\delta_2 \Delta . \qquad (20)$$

$$\left(\frac{\partial u_1}{\partial y_2}\right)_w = \frac{a U_1}{\delta_2} . \qquad (21)$$

Similarly for the energy integral equation, (5):

$$\left(\frac{\partial \theta}{\partial y_2}\right)_w = \frac{A}{\delta_{T_2}} . \qquad (22)$$

For $\delta_{T_2} < \delta_2$ or $\Delta < 1$, which implies $P_r > 1$, the integral in equation (5) takes the form

$$\int_0^\infty u_1 \theta\,dy_2 = U_1\,\delta_2 \Delta \int_0^1 \frac{u_1}{U_1}\,\theta\,d\eta_T$$

$$= \delta_2 U_1 \left[a\Delta^2\left(\frac{1}{2}+\frac{A}{3}+\frac{D}{6}+\frac{E}{7}+\frac{F}{8}\right) + b\Delta^3\left(\frac{1}{3}+\frac{A}{4}+\frac{D}{7}+\frac{E}{8}+\frac{F}{9}\right) + c\Delta^4\left(\frac{1}{4}+\frac{A}{5}+\frac{D}{8}+\frac{E}{9}+\frac{F}{10}\right) + d\Delta^5\left(\frac{1}{5}+\frac{A}{6}+\frac{D}{9}+\frac{E}{10}+\frac{F}{11}\right) + e\Delta^6\left(\frac{1}{6}+\frac{A}{7}+\frac{D}{10}+\frac{E}{11}+\frac{F}{12}\right) + f\Delta^7\left(\frac{1}{7}+\frac{A}{8}+\frac{D}{11}+\frac{E}{12}+\frac{F}{13}\right)\right], \quad \Delta < 1. \tag{23}$$

In other words, this integration need only be performed out to the edge of the thermal boundary layer, for from there on θ is zero.

If $\delta_{T_2} > \delta_2$ or $\Delta > 1$, $P_r < 1$, the above integration is performed in two parts,

$$\int_0^\infty u_1 \theta \, dy_2 = U_1 \int_0^{\delta_{T_2}} f \cdot h \cdot dy_2 = U_1 \left[\int_0^{\delta_2} f \cdot h \, dy_2 + \int_{\delta_2}^{\delta_{T_2}} h \, dy_2 \right],$$

since f = 1 when $y_2 > \delta_2$. Here, $f = f(\eta)$ and $h = h(\eta_T)$.

The first integral in the brackets is

$$\int_0^{\delta_2} f \cdot h \, dy_2 = \delta_2 \int_0^1 f \cdot h \, d\eta$$

$$= \delta_2 \int_0^1 \left(a\eta + b\eta^2 + c\eta^3 + d\eta^4 + e\eta^5 + f\eta^6\right)\left(1 + A\frac{\eta}{\Delta} + D\frac{\eta^4}{\Delta^4} + E\frac{\eta^5}{\Delta^5} + F\frac{\eta^6}{\Delta^6}\right) d\eta$$

$$= \delta_2 \int_0^1 \Big\{ \left(a\eta + b\eta^2 + c\eta^3 + d\eta^4 + e\eta^5 + f\eta^6\right) + \left(a\eta^2 + b\eta^3 + c\eta^4 + d\eta^5 + e\eta^6 + f\eta^7\right)\frac{A}{\Delta} + \left(a\eta^5 + b\eta^6 + c\eta^7 + d\eta^8 + e\eta^9 + f\eta^{10}\right)\frac{D}{\Delta^4} + \left(a\eta^6 + b\eta^7 + c\eta^8 + d\eta^9 + e\eta^{10} + f\eta^{11}\right)\frac{E}{\Delta^5} + \left(a\eta^7 + b\eta^8 + c\eta^9 + d\eta^{10} + e\eta^{11} + f\eta^{12}\right)\frac{F}{\Delta^6} \Big\} d\eta$$

$$\delta_2 \left\{ \left(\frac{a}{2} + \frac{b}{3} + \frac{c}{4} + \frac{d}{5} + \frac{e}{6} + \frac{f}{7} \right) \right.$$
$$+ \left(\frac{a}{3} + \frac{b}{4} + \frac{c}{5} + \frac{d}{6} + \frac{e}{7} + \frac{f}{8} \right) \frac{A}{\Delta}$$
$$+ \left(\frac{a}{6} + \frac{b}{7} + \frac{c}{8} + \frac{d}{9} + \frac{e}{10} + \frac{f}{11} \right) \frac{D}{\Delta^4}$$
$$+ \left(\frac{a}{7} + \frac{b}{8} + \frac{c}{9} + \frac{d}{10} + \frac{e}{11} + \frac{f}{12} \right) \frac{E}{\Delta^5} \qquad (24)$$
$$\left. + \left(\frac{a}{8} + \frac{b}{9} + \frac{c}{10} + \frac{d}{11} + \frac{e}{12} + \frac{f}{13} \right) \frac{F}{\Delta^6} \right\}, \quad \Delta > 1 .$$

The second integral for the case of $\Delta > 1$ is

$$\int_{\delta_2}^{\delta_{T_2}} h\, dy_2 = \int_{\delta_2}^{\delta_{T_2}} \left(1 + A \frac{y_2}{\delta_{T_2}} + D \frac{y_2^4}{\delta_{T_2}^4} + E \frac{y_2^5}{\delta_{T_2}^5} + F \frac{y_2^6}{\delta_{T_2}^6} \right) dy_2$$
$$= \left(y_2 + \frac{A}{2} \frac{y_2^2}{\delta_{T_2}} + \frac{D}{5} \frac{y_2^5}{\delta_{T_2}^4} + \frac{E}{6} \frac{y_2^6}{\delta_{T_2}^5} + \frac{F}{7} \frac{y_2^7}{\delta_{T_2}^6} \right) \Bigg]_{\delta_2}^{\delta_{T_2}} \qquad (25)$$
$$= \delta_2 \left[\Delta \left(1 + \frac{A}{2} + \frac{D}{5} + \frac{E}{6} + \frac{F}{7} \right) - 1 - \frac{A}{2\Delta} - \frac{D}{5\Delta^4} \right.$$
$$\left. - \frac{E}{6\Delta^5} - \frac{F}{7\Delta^6} \right], \quad \Delta > 1$$

Equations (18) to (25) are expanded forms, for the more general case, of the individual terms in the momentum and energy integral equations, (4) and (5). They apply to mixed convection flow of a fluid over an immersed body, with its major axes vertical, a constant wall temperature, and constant fluid properties.

Equations (18) to (25) are next substituted into the integral equations, (4) and (5). The result will be two simultaneous first-order differential equations in $\frac{d\delta_2^2}{dz}$, $\frac{d\Delta}{dz}$, δ_2^2, Δ, and Z which can be solved explicitly for

$$\frac{d\delta_2^2}{dZ} = f_1(\delta_2^2, \Delta, Z)$$

and

$$\frac{d\Delta}{dZ} = f_2(\delta_2^2, \Delta, Z) \tag{26}$$

for a given Prandtl number.

In turn, if starting or initial conditions can be determined, these two equations can be solved numerically for δ_2^2 and Δ. δ_2^2 and Δ are finally used to find velocity and temperature profiles, Nusselt number, and wall shear stress at any Z.

CHAPTER III

MIXED CONVECTION FLOW OVER A VERTICAL FLAT PLATE

For a vertical flat plate, the integral equations, (4) and (5), simplify considerably since $dU_1/dZ = 0$ and $U_1 = U/U = 1$. They become

$$\frac{d}{dz}\left[\delta_2 \int_0^1 f(1-f)\,d\eta\right] = \mp \delta_2 \Delta \int_0^1 h\, d\eta_T + \left(\frac{\partial u_1}{\partial y_2}\right)_w \tag{27}$$

and

$$\frac{d}{dz}\left[\int_0^\infty u_1 \theta\, dy_2\right] = -\frac{1}{Pr}\left(\frac{\partial \theta}{\partial y_2}\right)_w . \tag{28}$$

For a flat plate with constant wall temperature, the θ profile is:

$$\theta = h(\eta_T) = 1 - 2\eta_T + 5\eta_T^4 - 6\eta_T^5 + 2\eta_T^6$$

or

$$A = -2,\ D = 5,\ E = -6,\ F = 2 .$$

This was also the expression for an arbitrary constant temperature surface.

The velocity profile is as before

$$u_1 = f(\eta) = a\eta + b\eta^2 + c\eta^3 + d\eta^4 + e\eta^5 + f\eta^6$$

but with the coefficients modified for the flat plate case ($j = \pm 1$):

$$a = 2 \pm 0.2\,\delta_2^2 \mp \frac{1}{30}\,\frac{\delta_2^2}{\Delta}$$

$$b = \mp 0.5\,\delta_2^2$$

$$c = \pm \frac{1}{3}\,\frac{\delta_2^2}{\Delta}$$

$$d = -5 \pm \delta_2^2 \mp \frac{2}{3}\frac{\delta_2^2}{\Delta}$$

$$e = 6 \mp \delta_2^2 \pm 0.5\frac{\delta_2^2}{\Delta}$$

$$f = -2 \pm 0.3\delta_2^2 \mp \frac{2}{15}\frac{\delta_2^2}{\Delta}$$

The upper signs of the pairs $\pm$ or $\mp$ refer to aiding flow.

Upon substituting these coefficients into equations (18), (20), and (21), Chapter II, combining to make up equation (27), performing the differentiation with respect to Z, and solving for $\frac{d\delta_2^2}{dz}$, the result is

$$\frac{d\delta_2^2}{dz} = \left[\frac{a_1 + b_1\frac{d\Delta}{dz}}{c_1}\right] \tag{29}$$

where

$$a_1 = \left(\mp\frac{4}{7}\delta_2^2\Delta + 4 \pm \frac{2}{5}\delta_2^2 \mp \frac{1}{15}\frac{\delta_2^2}{\Delta}\right) \tag{29a}$$

and

$$b_1 = \left(\pm 0.00082510\,09\frac{\delta_2^4}{\Delta^2} + 0.00015281017\frac{\delta_2^6}{\Delta^2} - 0.00003798\,6712\frac{\delta_2^6}{\Delta^3}\right) \tag{29b}$$

and

$$c_1 = \left(0.10933511 \mp 0.00316350\,34\,\delta_2^2 - 0.000777\,\delta_2^4 \pm 0.00123765\,14\frac{\delta_2^2}{\Delta} + 0.00038202542\frac{\delta_2^4}{\Delta} - 0.00004748\,3389\frac{\delta_2^4}{\Delta^2}\right) \tag{29c}$$

In the limit as $Z = Gr_x/Re_x^2$ goes to zero or approaches pure forced convection, δ_2^2 also approaches zero although Δ remains greater than zero. Therefore,

$$\left.\frac{d\delta_2^2}{dz}\right]_{z\to 0} = \frac{4}{0.10933511} = 36.584771 \tag{30}$$

Calculation of the numerical coefficients in equations (29b) and (29c) has been carried out to eight significant figures. No difference in computer answers was noted between doing this and leaving the constants in their common fraction form. Originally these constants were carried to only six significant figures with drastically inaccurate digital computer answers. This inaccuracy occurred because numerous additions and subtractions are performed in the final differential equations with numbers that are almost equal to one another.

In the same manner, substituting the velocity and temperature profile coefficients into equations (22) and (23) for $\Delta < 1$ and into equations (22), (24), and (25) for $\Delta > 1$, combining to compose equation (28), performing the indicated differentiation with respect to Z, and solving for $\frac{d\Delta}{dz}$, gives

$$\frac{d\Delta}{dz} = \left[\frac{a_2 + b_2 \frac{d\delta_2}{dz}^2}{c_2} \right] \tag{31}$$

where

$$a_2 = 4/\Delta P_R ,$$

$$b_2 = -\left(H_1 \pm 3\delta_2^2 H_2 \right) ,$$

and

$$c_2 = 2\delta_2^2 \frac{dH_1}{d\Delta} \pm 2\delta_2^4 \frac{dH_2}{d\Delta}$$

If $\Delta < 1$, which implies $P_R > 1$, H_1 and H_2, which are functions only of Δ, are

$$H_1 = 0.11904762\Delta^2 - 0.0202\ldots\Delta^5 + 0.012987013\Delta^6 - 0.002497502\Delta^7$$

and

$$H_2 = -0.0019841274 + 0.011904762\,\Delta^2 - 0.007142856\,7\,\Delta^3 - 0.002693602\,7\,\Delta^4 + 0.005122655\,1\,\Delta^5 - 0.002331002\,4\,\Delta^6 + 0.000374625\,36\,\Delta^7$$

For $\Delta > 1$, or $P_r < 1$, as is the case for gases and liquid metals,

$$H_1 = -0.28571429(1-\Delta^2) + 0.11904762\,\Delta^{-1} - 0.0202\ldots\Delta^{-4} + 0.01298704\,\Delta^{-5} - 0.002497502\,3\,\Delta^{-6},$$

and

$$H_2 = 0.0095238096 - 0.00833\ldots\Delta^{-1} + 0.001587301\,6\,\Delta^{-2} + 0.001443001\,4\,\Delta^{-4} - 0.001394901\,4\,\Delta^{-5} + 0.000482850\,48\,\Delta^{-6} - 0.000058275058\,\Delta^{-7}.$$

The derivatives $\frac{dH_1}{d\Delta}$ and $\frac{dH_2}{d\Delta}$ arise since $\frac{dH_{1,2}}{dZ} = \frac{dH_{1,2}}{d\Delta} \cdot \frac{d\Delta}{dZ}$.

Equations (29) and (31) are solved simultaneously for $d\Delta/dZ$ and $\frac{d\delta_2^2}{dZ}$ to give

$$\frac{d\delta_2^2}{dZ} = \frac{a_1 c_2 + a_2 b_1}{c_1 c_2 - b_1 b_2} \tag{32}$$

and

$$\frac{d\Delta}{dZ} = \frac{a_2 c_1 + a_1 b_2}{c_1 c_2 - b_1 b_2} \tag{33}$$

These two equations are solved numerically for δ_2 and Δ (Appendix A) after initial values for Δ and $\frac{d\Delta}{dZ}$ are found at Z = 0, since $\left.\frac{d\delta_2^2}{dZ}\right]_0$ has already been determined in equation (30).

In order to find Δ_0, it is noted that the denominator of equation (31) is zero at Z = 0 where $\delta_2^2 = 0$. To put equation (31) into an indeterminate 0/0 configuration so a limit can be found as Z approaches zero, the numerator is made zero by letting

$$\frac{4}{\Delta_0 P_r} - \left[H_1 \frac{d\delta_2^2}{dz} \right]_0 = 0$$

For $\Delta < 1$, $P_r > 1$, the consequence is

$$\Delta_0^8 - 5.20\Delta_0^7 + 8.0888892\Delta_0^6 - 47.666\ldots\Delta_0^3 + (43.777\ldots)/(P_r) = 0$$

and for $\Delta > 1$, $P_r < 1$,

$$\Delta_0^7 - \Delta_0^6 + (0.4166\ldots - 0.38267288/P_r)\Delta_0^5 - 0.0707\ldots\Delta_0^2 + 0.04545\ldots\Delta_0 - 0.00874125 79 = 0$$

These polynomials were solved numerically on an IBM-1620 for Δ_0. The correct root was easy to discern since the others generally were either negative or had imaginary parts. Occasionally a second real positive root would appear but it would be either much too large or much too small. A semi-log plot of Pr vs Δ_0, Fig. 3, compares this present calculation with Acrivos (1958). His values of Pr as a function of Δ_0 were obtained without considering the third derivatives of u_1 and θ at the surface and with two "asymptotic" boundary conditions on u_1 and only one on θ. The present plot shows that $\Delta_0 = 1$ at $P_r = 1$, as it should. Eckert and Drake's (1959) relations of $\Delta_0 = (1.026 P_r^{1/3})^{-1}$ for $P_r \geq 1$ and $P_r = \frac{0.3715}{\Delta_0^2 - \Delta_0 + 0.4}$ for $P_r \leq 1$ fall very close to the present curve, although both of these equations are a little off the desired value of $\Delta_0 = 1$ at Pr = 1. The use of one, or one and two, instead of three asymptotic boundary conditions at η or $\eta_T = 1$ did not change the plot discernibly. As noted earlier, Z = 0 implies pure forced convection, so Figure 3 is also the Pr vs Δ relationship for forced convection flow over a flat plate for all laminar flow Reynolds numbers when the param-

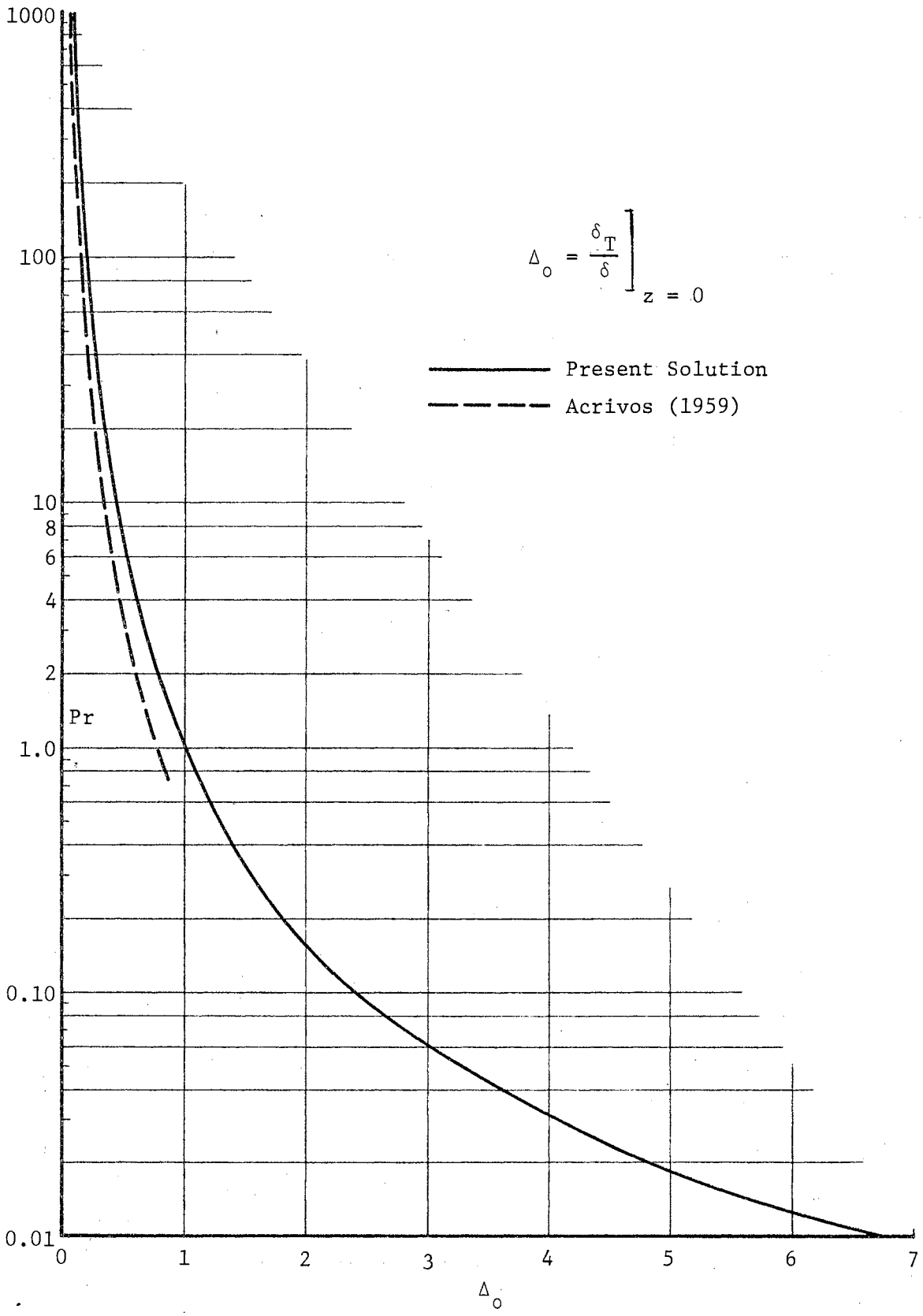

Figure 3. Pr vs Δ_o for an Isothermal Flat Plate.

eter Gr_x/Re_x^2 is negligibly small, wall temperature is constant and dissipation effects are unimportant.

$\left.\frac{d\Delta}{dZ}\right]_o$ is more tedious to find. Equation (31) is of the from 0/0 as Z approaches zero, so L'Hospital's Rule can be applied. The result is

$$\lim_{o} \frac{d\Delta}{dZ} = \left.\frac{d\Delta}{dZ}\right]_o = -\left[\frac{H_1 \frac{d^2(\delta_2^2)}{dZ^2} + 3H_2\left(\frac{d\delta_2^2}{dZ}\right)^2}{3\frac{dH_1}{d\Delta}\frac{d\delta_2^2}{dZ} + \frac{4}{\Delta^2 Pr}}\right]_o .$$

$\left.\frac{d^2(\delta_2^2)}{dZ^2}\right]_o$ is obtained by one differentiation and a simple limiting process applied to equation (29). Finally,

$$\left.\frac{d\Delta}{dZ}\right]_o = \mp \frac{36.584771\, H_2(\Delta_o) + H_1(\Delta_o)(1.5723 - 1.742\Delta_o - 0.34129\,\Delta_o^{-1})}{\left.\frac{dH_1}{d\Delta}\right]_o + \frac{0.036445038}{\Delta_o^2 Pr}}$$

This equation was solved with the previously determined Δ_o's, for Prandtl numbers of 0.01, 0.73, 10, 100, and 1000. The $\left.\frac{d\Delta}{dZ}\right]_o$ for opposing flow is of opposite sign to that for aiding flow. With Δ_o, $\left.\frac{d\Delta}{dZ}\right]_o$, and $\left.\frac{d\delta_2^2}{dZ}\right]_o$ determined, and knowing that $\left.\delta_2^2\right]_o = 0$, equations (32) and (33) can now be numerically integrated to obtain δ_2 and Δ for any Z.

Heat Transfer and Shear Stress

The local Nusselt number can be found from the following general considerations. The heat transferred per unit time from the wall to the fluid is

$$q = hA(T_w - T_\infty) = -kA\left.\frac{\partial T}{\partial y}\right]_w$$

from which

$$h = \frac{-k}{(T_w - T_\infty)}\left.\frac{\partial T}{\partial y}\right]_w = -k\left.\frac{\partial\left[\frac{T - T_\infty}{T_w - T_\infty}\right]}{\partial y}\right]_w = -k\left.\frac{\partial\theta}{\partial y}\right]_w .$$

The Nusselt number related to a distance x along the body is

$$Nu_x = \frac{hx}{k} = -x \left.\frac{\partial \theta}{\partial y}\right]_w .$$

Since $y_2 = \frac{y}{x}\sqrt{Re_x}\sqrt{\frac{Gr_x}{Re_x^2}}$,

$$-\left.\frac{\partial \theta}{\partial y_2}\right]_w = \frac{Nu_x}{\sqrt{Re_x}}\sqrt{\frac{Re_x^2}{Gr_x}} . \tag{34}$$

The shear stress at the wall is

$$\tau_w = \mu \left.\frac{\partial u}{\partial y}\right]_w = \mu \left.\frac{\partial u_1}{\partial y_2}\right]_w \frac{U_\infty}{x}\sqrt{Re_x}\sqrt{\frac{Gr_x}{Re_x^2}}$$

and therefore, the friction factor, $C_f = \frac{\tau_w}{\frac{1}{2}\rho U^2}$, is

$$C_f = \left.\frac{\partial u_1}{\partial y_2}\right]_w \frac{2\mu U_\infty}{\rho_\infty U^2 x}\sqrt{Re_x}\sqrt{\frac{Gr_x}{Re_x^2}} = \frac{2}{U_1}\left.\frac{\partial u_1}{\partial y_2}\right]_w \cdot \frac{1}{\sqrt{Re_x}}\sqrt{\frac{Gr_x}{Re_x^2}} .$$

Consequently,

$$\frac{1}{U_1}\left.\frac{\partial u_1}{\partial y_2}\right]_w = \frac{C_f}{2}\sqrt{Re_x}\sqrt{\frac{Re_x^2}{Gr_x}} \tag{35}$$

For the flat plate problem of this section,

$$\frac{Nu_x}{\sqrt{Re_x}}\sqrt{\frac{Re_x^2}{Gr_x}} = -\frac{A}{\delta_2 \Delta} = \frac{2}{\delta_2 \Delta} \tag{36}$$

and

$$\frac{C_f}{2}\sqrt{Re_x}\sqrt{\frac{Re_x^2}{Gr_x}} = \frac{a}{U_1 \delta_2} = \left(\frac{2}{\delta_2} + 0.2\,\delta_2 \mp \frac{1}{30}\frac{\delta_2}{\Delta}\right) \tag{37}$$

These two quantities, equations (36) and (37), are calculated and printed by the computer at each Z point at which δ_2 and Δ are printed out.

Since pure forced convection is represented as $Z \to 0$ and pure free convection as $Z \to \infty$, plots of $\frac{Nu_x}{\sqrt{Re_x}}\sqrt{\frac{Re_x^2}{Gr_x}}$ and $\frac{C_f}{2}\sqrt{Re_x}\sqrt{\frac{Re_x^2}{Gr_x}}$ vs Z should show asymptotic behavior to free and forced convection known

solutions at either end of the graph.

From Eckert and Drake (1959), for forced convection over a flat plate with constant wall temperature, $Pr > 0.7$,

$$Nu_x = 0.332\ Pr^{1/3}\sqrt{Re_x}$$

and for $Pr < 0.05$,

$$Nu_x = \frac{\sqrt{Re_x}\sqrt{Pr}}{1.55\sqrt{Pr} + 3.09\sqrt{0.372 - 0.15\,Pr}}$$

From the first of these two expressions,

$$\frac{Nu_x}{\sqrt{Re_x}}\sqrt{\frac{Re_x^2}{Gr_x}} = \frac{0.332\ Pr^{1/3}}{\sqrt{Z}},$$

and from the second, for $Pr = 0.01$,

$$\frac{Nu_x}{\sqrt{Re_x}}\sqrt{\frac{Re_x^2}{Gr_x}} = \frac{0.04992}{\sqrt{Z}}.$$

These are the forced convection heat transfer function asymptotes for a plot of $\frac{Nu_x}{\sqrt{Re_x}}\sqrt{\frac{Re_x^2}{Gr_x}}$ vs Z.

The free convection heat transfer function asymptotes are found from Ostrach's (1953) numerical results:

$$\frac{Nu_x}{\sqrt{Re_x}}\sqrt{\frac{Re_x^2}{Gr_x}} = \frac{-0.707\,H'(0)}{Z^{1/4}}$$

where H'(0) is Ostrach's temperature function derivative at the wall for a given Pr.

In a similar fashion, the free convection friction factor asymptotes are

$$\frac{C_f}{2}\sqrt{Re_x}\sqrt{\frac{Re_x^2}{Gr_x}} = 1.414\,F''(0)\cdot Z^{1/4}$$

where $F''(0)$ is Ostrach's stream function second derivative at the wall for a given Pr.

From Schlichting (1960), the forced convection asymptote for the wall friction factor is

$$\frac{C_f}{2}\sqrt{Re_x}\sqrt{\frac{Re_x^2}{Nu_x}} = \frac{0.332}{\sqrt{Z}}$$

which is a common asymptote for all fluids and independent of the Prandtl number. The asymptotes described above are the dashed lines in Figures 6 and 7, plots of the heat transfer function and the friction factor or wall shear stress function vs Z.

Numerical Integration

The numerical integration of the equations for $\frac{d\delta_2^2}{dZ}$ and $\frac{d\Delta}{dZ}$ as functions of δ_2^2 and Δ is explained in Appendix A. This section will describe in addition the problems encountered in these computer solutions and present some of the remedies applied to the problems.

When the flat plate differential equations for δ_2 and Δ were written with constants evaluated to only six significant figures, some integration results were questionable. For example, for Pr = 10, aiding flow, one discontinuity after another occurred in $\frac{d\Delta}{dZ}$ as Z increased from zero. For Pr = 100 and 1000, aiding flow, the Nusselt number and friction factor plots compared favorably with asymptotic criteria, but velocity profiles showed extreme forward and reverse flow peaks. However, the aiding flow case for Pr = 0.73 and the opposing flow cases for all Prandtl numbers, with the exception of Pr = 1000, were satisfactory.

Moreover, when the constants of the differential equations were more carefully evaluated to eight significant figures, it was found that Nusselt number and friction factor values were now unacceptably far off for

moderate and high Z values, with even worse velocity profiles for Pr $\geq$ 10, aiding flow. This change to greater accuracy did not affect the answers for Pr = 0.73, aiding flow, or Pr = 0.01 through 1000, opposing flow.

If δ_2 is defined alternately as the transverse distance at which $u_1 = w \cdot U_1$ and δ_{T_2} the distance at which $\theta = (1-v)$, where w and v are in the range of 0.95 to 1.05, then results which were questionable using the standard method $u_1 = U_1$ and $\theta = 0$ at $\eta = \eta_T = 1$ become more satisfactory for certain combinations of w and v. Thus, for example, for the integral $\int_0^\infty u_1(U_1-u_1)dy_2$, if w = 1.02, the integration is performed to $y_2 = \delta_2$ where $u_1 = 1.02U_1$, a fictitious upper limit to u_1. Since $\eta = \frac{y_2}{\delta_{T_2}} = 1$ at this point and $u_1 = f(\eta) \cdot U_1$, the transformed integral is still the same, $\delta_2 U_1^2 \int_0^1 f(1-f)\,d\eta$, and it is still bounded by our definition of a boundary layer thickness at which the integration terminates. The integrand, f(1-f), is now 1.02(1-1.02) = -0.0204 at the upper limit, instead of zero. This device of using w and v factors enabled computer integration to proceed to more acceptable solutions in some of the cases considered. It is believed that the w and v factors allowed a better mathematical simulation of the initial transverse integrations to infinity, required in the integral method, by modifying the velocity and temperature series representations, or profiles, in such a way as to account and compensate for the loss of the true asymptotic boundary conditions on u_1 and θ at infinity.

At this point, "numerical experimentation" was begun with the w and v factors, so that $u_1\big]_{\eta=1} = w$ instead of one, and $\theta\big]_{\eta_T=1} = (1-v)$ instead of zero. This idea originated with Hugelman (1964), who used a velocity "w factor" to settle down an otherwise intractable integral method integra-

tion for magnetohydrodynamic flow around a circular cylinder.

It was evident in aiding flow that the equations integrated correctly for small Z, or the forced convection range, but were unsatisfactory for Pr $\geq$ 10 at high Z. The final solution to this particular problem, therefore, was to phase-in the w and v factors linearly up to Z = 0.10, thus letting the w and v correction act mainly in the mixed and free convection range. The ultimate choice of w = 1.03 and v = 0.95 was made from a study of the behavior of the Nusselt and friction factor plots, for Pr = 1000, from Z = 0.01 to 1.0 with trial variations of w and v. These selected values were then used in integrating from Z = 0 to 1000 for Pr = 10, 100, and 1000. The results given in this chapter for aiding flow for Pr $\geq$ 10 were found by this method. Numerical integration was stable. Velocity profiles were more normal in appearance. Well-behaved Nusselt and friction factor plots at high and low Z asymptotes were thus the criteria for acceptable results with aiding flow after it was ascertained that no error was being introduced by rounding off constants in the differential equations.

Another difficulty, alluded to above, arose from the discontinuities in the differential equations. No discontinuities occurred for Pr >10, aiding flow; but one discontinuity did occur at Pr = 10, Z = 98.5, and another at Pr = 0.73, Z = 0.442. In both cases, $\frac{d\delta_2^2}{dz}$ and $\frac{d\Delta}{dz}$, each of the numerators and their common denominator increased or decreased without bound at that particular Z. However, δ_2 and Δ were not perturbed near these points since the discontinuities were sharply defined over a very small range of Z. Since $\left.\frac{\partial\theta}{\partial y_2}\right]_w$ and $\left.\frac{\partial u_1}{\partial y_2}\right]_w$, the Nusselt number and friction factor functions, are functions of δ_2 and Δ, they too were not perturbed in the neighborhood of the discontinui-

ties. Therefore, the integration was resumed beyond a discontinuity point by making a graphical extension of $\left.\frac{\partial \theta}{\partial y_2}\right]_w$ and $\left.\frac{\partial u_1}{\partial y_2}\right]_w$ to some new Z, which in the case of Pr = 0.73 was chosen to be Z = 0.6, for example, and then calculating values of δ_2 and Δ for new starting conditions. No physical significance was attached to the discontinuities, especially since the differential equations for δ_2 and Δ for the flat plate case are independent of Z.

The differential equations were not well behaved for Pr = 0.01, aiding flow. The liquid metal solution was acceptable up to about Z = 0.03 at which point Δ and $\frac{d\Delta}{dZ}$ begin to increase apparently without bound, an indication of a very broad discontinuity as opposed to the sharply defined ones for higher Prandtl numbers. A reverse integration from Z = 1000 was also tried where starting values of δ_2 and Δ obtained from the free convection asymptotes described earlier were used but without success. Double precision with eighteen significant figures and several numerical integration schemes, as well as a variety of w and v factors, were tried to no avail. It will be seen in Chapter IV that the equations were integrable in the case of wedge flow and Pr = 0.01.

A situation similar to the case of Pr = 0.01 in aiding flow exists for Pr = 1000, opposing flow. A broad discontinuity occurred at about Z = 0.06, and the integration could not be resumed.

Streamline Plots

Streamlines were drawn for the u_1 and v_2 velocity profiles that can be found at any Z. The v_2 profile was derived in the following way.

From the continuity equation we have

$$\frac{\partial u_1}{\partial z} = -\frac{\partial N_2}{\partial y_2} = -\frac{1}{\delta_2}\frac{\partial N_2}{\partial \eta}$$

From the equation for u_1 in terms of η,

$$\frac{\partial u_1}{\partial z} = \left(\frac{\partial a}{\partial z}\right)\eta + \left(\frac{\partial b}{\partial z}\right)\eta^2 + \left(\frac{\partial c}{\partial z}\right)\eta^3 + \left(\frac{\partial d}{\partial z}\right)\eta^4 + \left(\frac{\partial e}{\partial z}\right)\eta^5 + \left(\frac{\partial f}{\partial z}\right)\eta^6 - \frac{1}{2\delta_2^2}\frac{d\delta_2^2}{dz}\left(a\eta + 2b\eta^2 + 3c\eta^3 + 4d\eta^4 + 5e\eta^5 + 6f\eta^6\right) \equiv -\frac{1}{\delta_2}\frac{\partial N_2}{\partial \eta}.$$

Then, by partial integration with respect to η,

$$N_2 = -\delta_2\left[\left(\frac{\partial a}{\partial z}\right)\frac{\eta^2}{2} + \left(\frac{\partial b}{\partial z}\right)\frac{\eta^3}{3} + \left(\frac{\partial c}{\partial z}\right)\frac{\eta^4}{4} + \left(\frac{\partial d}{\partial z}\right)\frac{\eta^5}{5} + \left(\frac{\partial e}{\partial z}\right)\frac{\eta^6}{6} + \left(\frac{\partial f}{\partial z}\right)\frac{\eta^7}{7}\right] + \frac{1}{2\delta_2}\frac{d\delta_2^2}{dz}\left[\frac{a}{2}\eta^2 + \frac{2}{3}b\eta^3 + \frac{3}{4}c\eta^4 + \frac{4}{5}d\eta^5 + \frac{5}{6}e\eta^6 + \frac{6}{7}f\eta^7\right].$$

As a typical example of one of the coefficients in the expression for v_2 above,

$$\left(\frac{\partial a}{\partial z}\right) = \pm 0.2\frac{d\delta_2^2}{dz} \mp \frac{1}{30\Delta^2}\left(\Delta\frac{d\delta_2^2}{dz} - \delta_2^2\frac{d\Delta}{dz}\right)$$

Flat Plate Results

For comparison, the two differential equations derived from the use of just one, and of two, "asymptotic" boundary conditions, but with all the previous conditions at the wall, were solved for Pr = 0.73 and 100. With Pr = 0.73 both comparison cases, as expected, had a discontinuity at about Z = 0.4; and there were no significant changes in the values of δ_2 and Δ over the use of three "asymptotic" boundary conditions. However, with Pr = 100 integrations from Z = 0 to 1000 showed significant

differences in heat transfer, shear stress, and velocity profiles between the three cases. Figure 4 compares these results for heat transfer, with n the highest order of the asymptotic derivatives used. The n = 3 case is obviously best at the forced convection end, and this is the main reason it was used throughout. The heat transfer curves for all three cases drop below the free convection asymptote although n = 1 is superior and n = 2 is worst at high Z.

Figure 5 compares velocity profiles for n = 1, 2, and 3, Pr = 100, Z = 1000, with the profile obtained with n = 3 and w, v factors (w = 1.03, v = 0.95). The closer the heat transfer function is to the free convection asymptote, Fig. 4, the more believable the velocity profiles are, Fig. 5. For example, the n = 2 velocity profile peaks at u_1 = +1.8 and -7.1. All of the preceding differential equations had numerical constants correct to at least eight significant figures.

Figure 6 is a plot of the Nusselt number or heat transfer function, $\frac{Nu_x}{\sqrt{Re_x}}\sqrt{\frac{Re_x^2}{Gr_x}}$, versus Z for various Prandtl numbers, aiding flow, n = 3, and with w, v factors. At the point of intersection of the forced and free convection asymptotes, the local heat transfer in mixed convection is at its maximum deviation from the asymptotes. For the range of fluids between Pr = 0.73 and 1000, this maximum deviation occurs at a Z between 0.5 and 2.0. At this point local heat transfer can be about 25 percent higher than that predicted from either free or forced convection alone. Figure 6 also indicates that mixed convection effects are important for Z generally between 0.10 and 15.

Figure 7 is a plot of six times the local friction factor function which is $\frac{\tau_w}{\rho U_\infty^2}\sqrt{Re_x}\sqrt{\frac{Re_x^2}{Gr_x}}$. A multiplier of six was used to facilitate comparison with Acrivos (1958) and Kliegel (1959). Local friction be-

tween the fluid and wall at Z = 1 can be as much as 75 percent higher than either free or forced convection considerations alone would predict. The results for Pr = 10, 100, and 1000 were obtained by using w and v factors that were determined by observing the results of varying w and v for Pr = 1000 over the narrow range of Z = 0.01 to 1.0.

Figures 8 through 11 are velocity profiles for the flat plate case, Pr = 0.73 through 1000. The influence of increasing viscosity and/or decreasing thermal conductivity with increasing Prandtl number is evident. The extent of the thermal boundary layer is shown by the influence of the free convection velocity peak on the total flow. These profiles are discussed further in Chapter VI.

Figures 12 through 15 are typical streamline patterns within the boundary layer derived from u_1 and v_2 velocity components. Figure 12 for Pr = 0.73 shows the gaseous fluid being drawn into the higher velocity region near the wall from the free stream. In Figure 13 a moderately viscous liquid is shown to separate into two regions; half or more being forced out of the boundary layer region as the velocity boundary layer thickens, and the rest being pulled into the high velocity region near the wall. This behavior is also discussed further in Chapter VI.

Figures 16 and 17 are Nusselt number and friction factor plots for opposing flow over a flat plate with constant wall temperature. Heat transfer predictably decreases and falls below the forced convection asymptote as the flow is retarded by the resultant adverse buoyancy force, with the exception of Pr = 1000 where no valid answers were obtained. The separation points, indicated in Figure 17 by the rapid decrease to zero of the shear stress at the wall, are just downstream of the intersection of the forced and free convection friction factor asymp-

totes for aiding flow. Figure 18 shows the variation of the separation point with Prandtl numbers for opposing flow. The separation point for a gas, Pr = 0.73, is in fairly close agreement with an experiment by Kliegel (1959) as will be discussed in Chapter VI.

Finally, Figures 19 and 20 depict the flow field in opposing flow as the separation point is approached for a gas, Pr = 0.73, and a viscous liquid, Pr = 10. The flow is much less disturbed in the latter case.

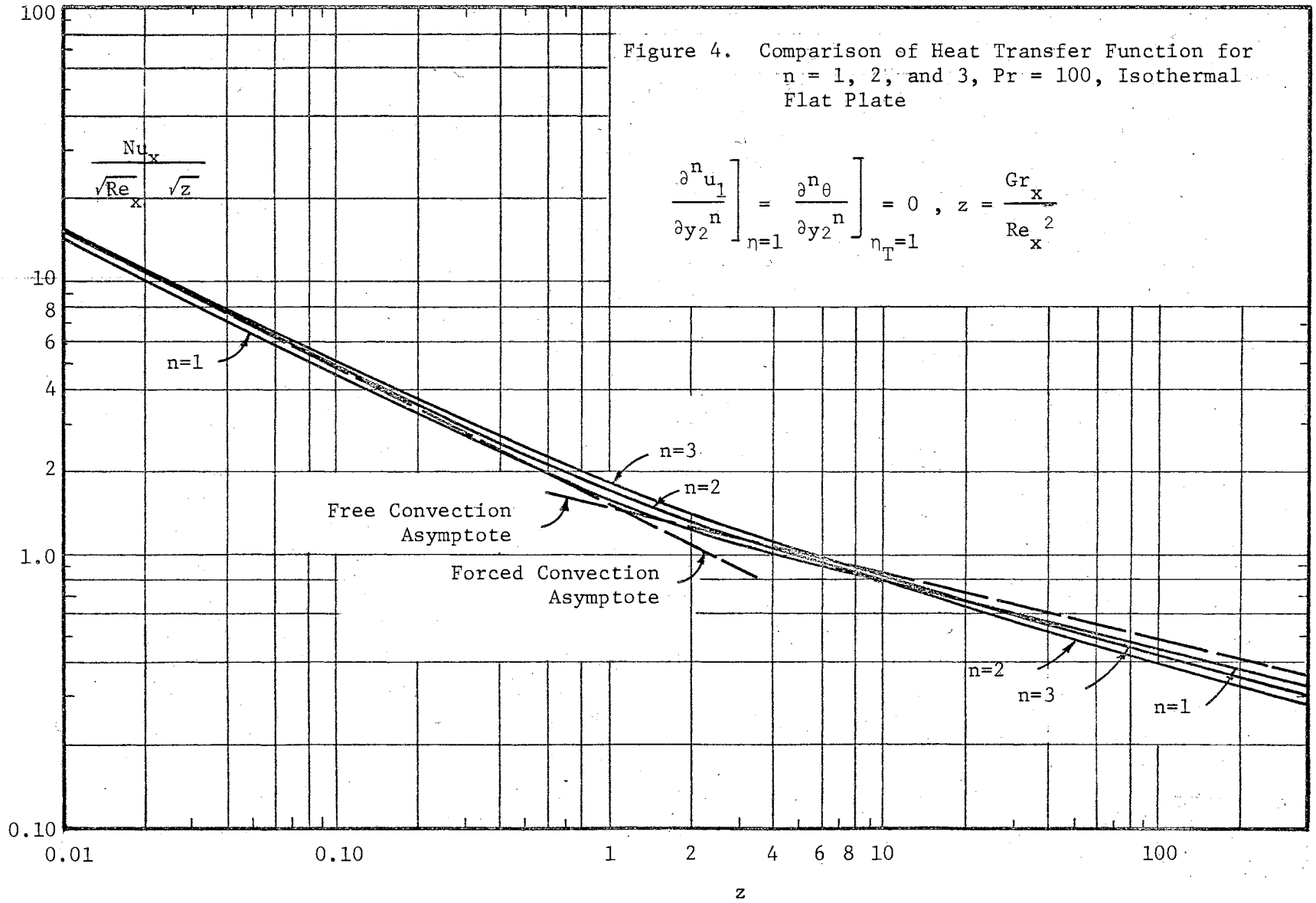

Figure 4. Comparison of Heat Transfer Function for n = 1, 2, and 3, Pr = 100, Isothermal Flat Plate

$$\left.\frac{\partial^n u_1}{\partial y_2^n}\right]_{\eta=1} = \left.\frac{\partial^n \theta}{\partial y_2^n}\right]_{\eta_T=1} = 0 \quad , \quad z = \frac{Gr_x}{Re_x^2}$$

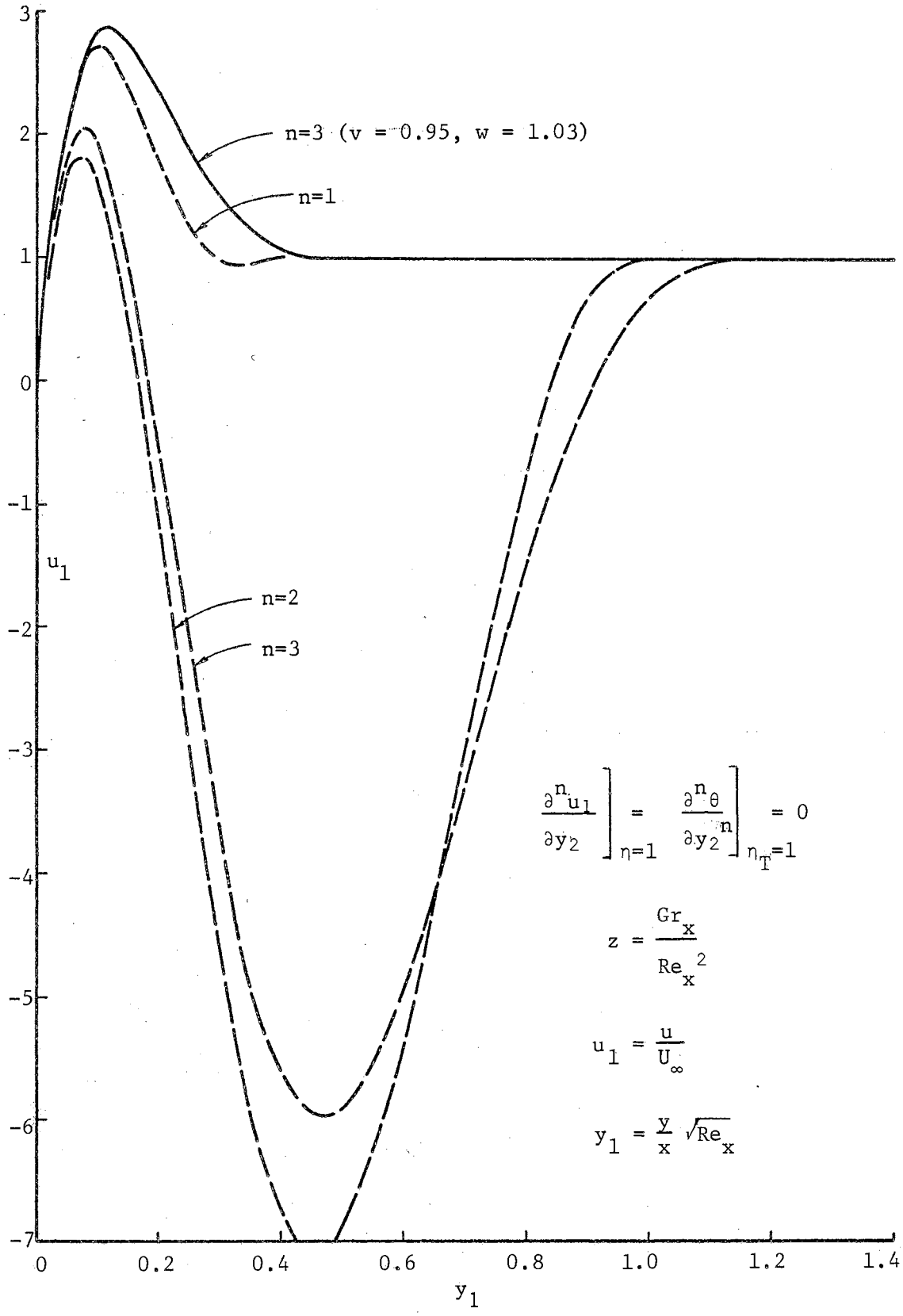

Figure 5. Comparison of Velocity Profiles, Pr = 100, z = 1000, Isothermal Flat Plate.

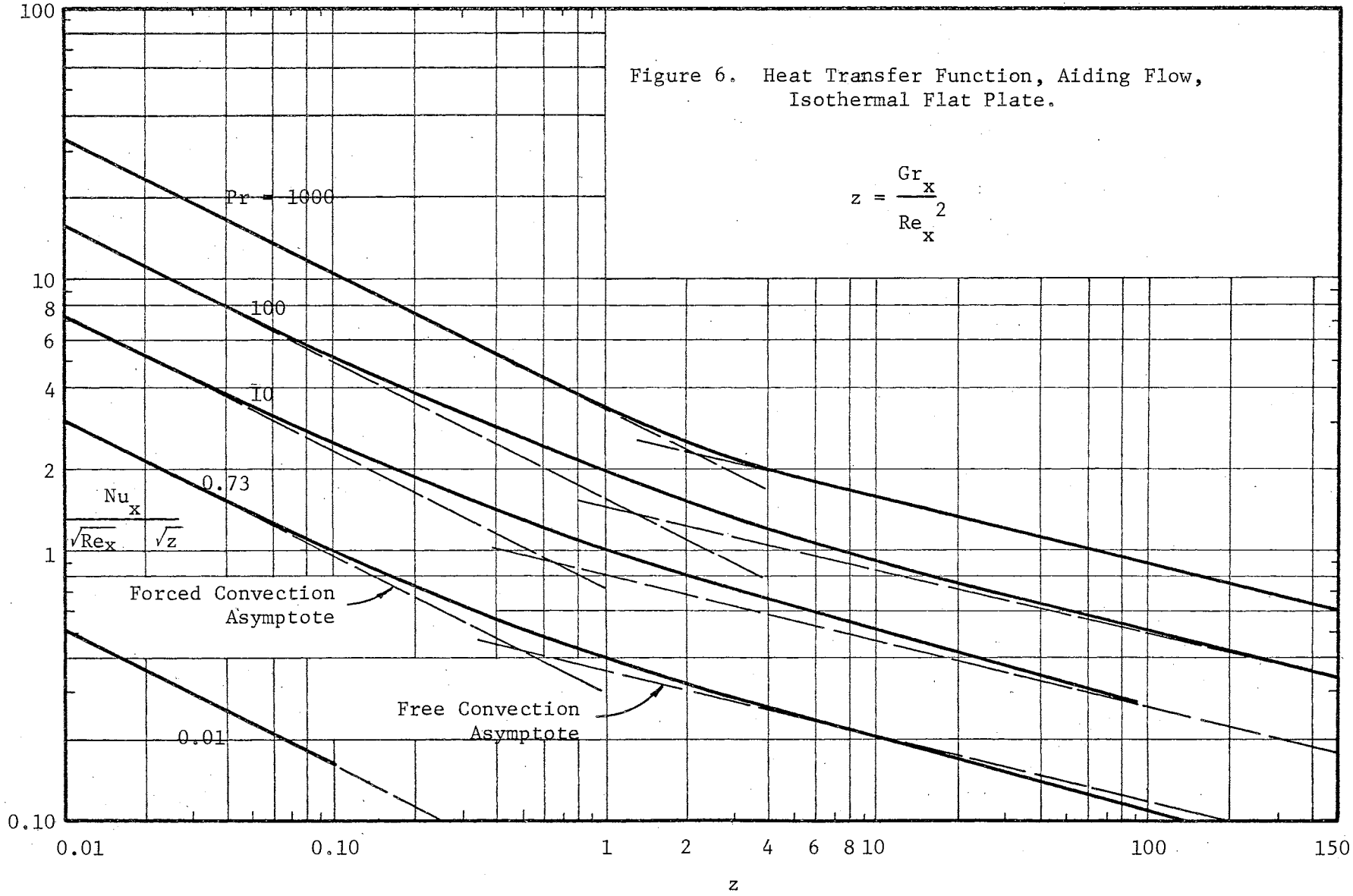

Figure 6. Heat Transfer Function, Aiding Flow, Isothermal Flat Plate.

$$z = \frac{Gr_x}{Re_x^2}$$

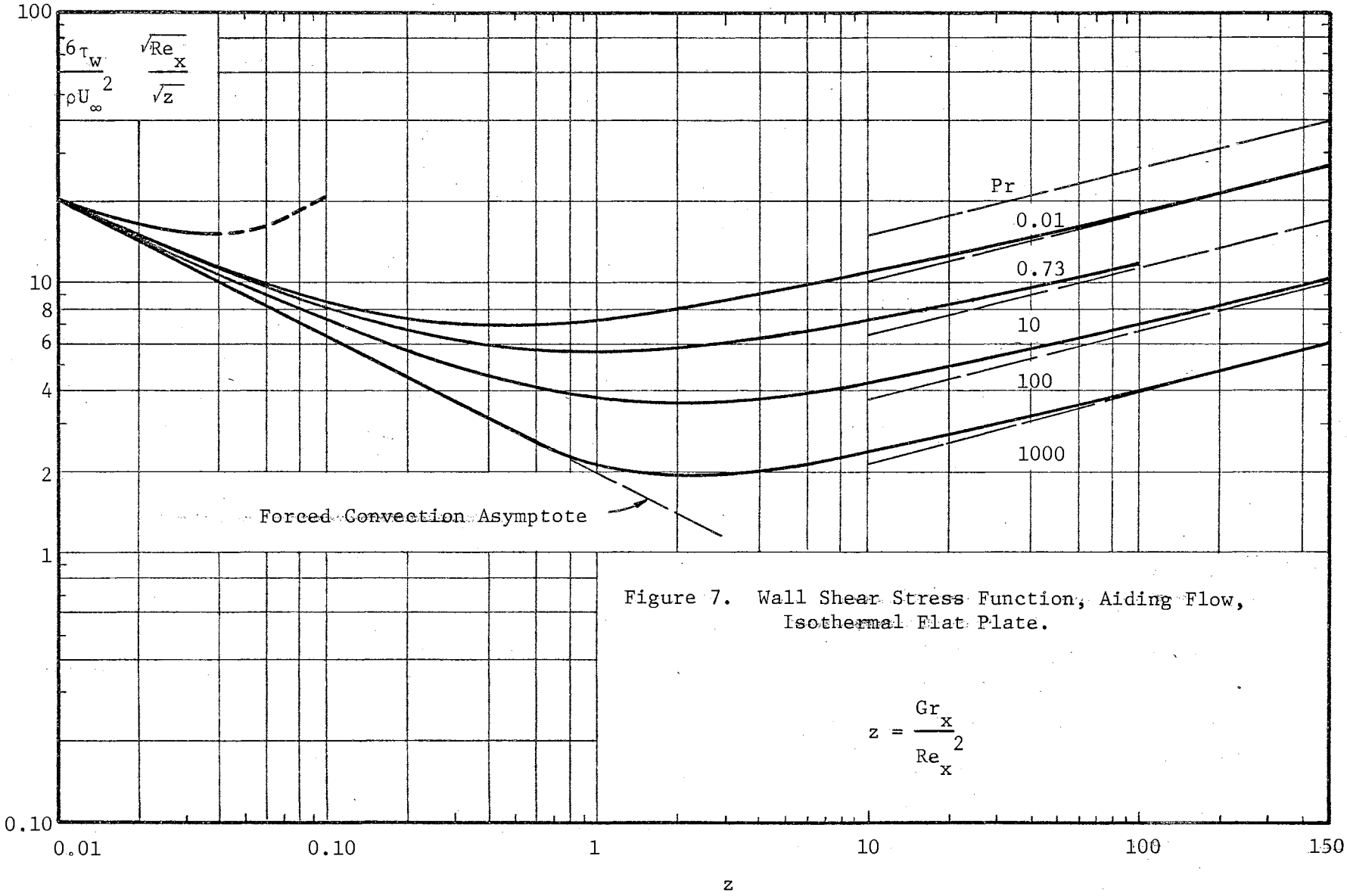

Figure 7. Wall Shear Stress Function, Aiding Flow, Isothermal Flat Plate.

$$z = \frac{Gr_x}{Re_x^2}$$

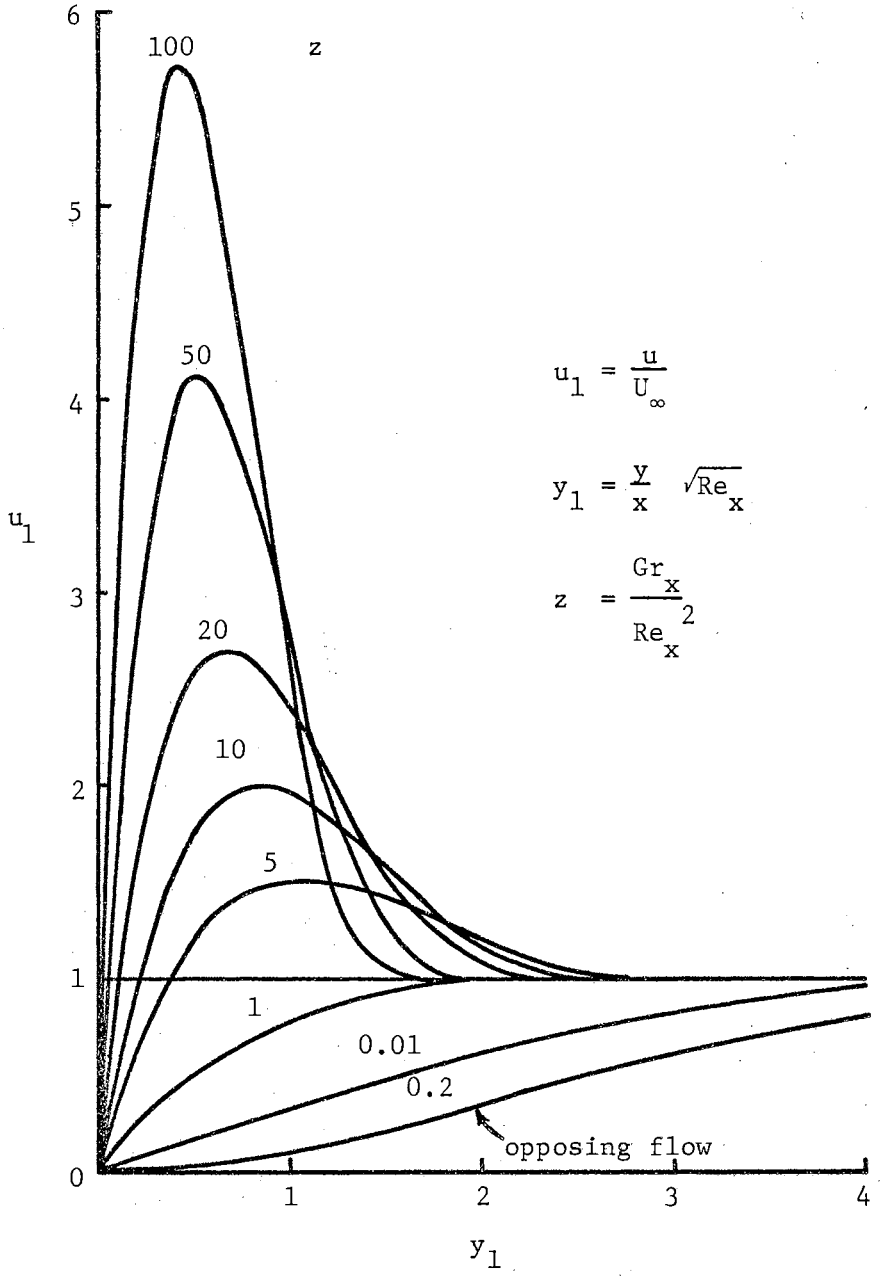

Figure 8. Velocity Profiles, Isothermal Flat Plate, Pr = 0.73, n = 3.

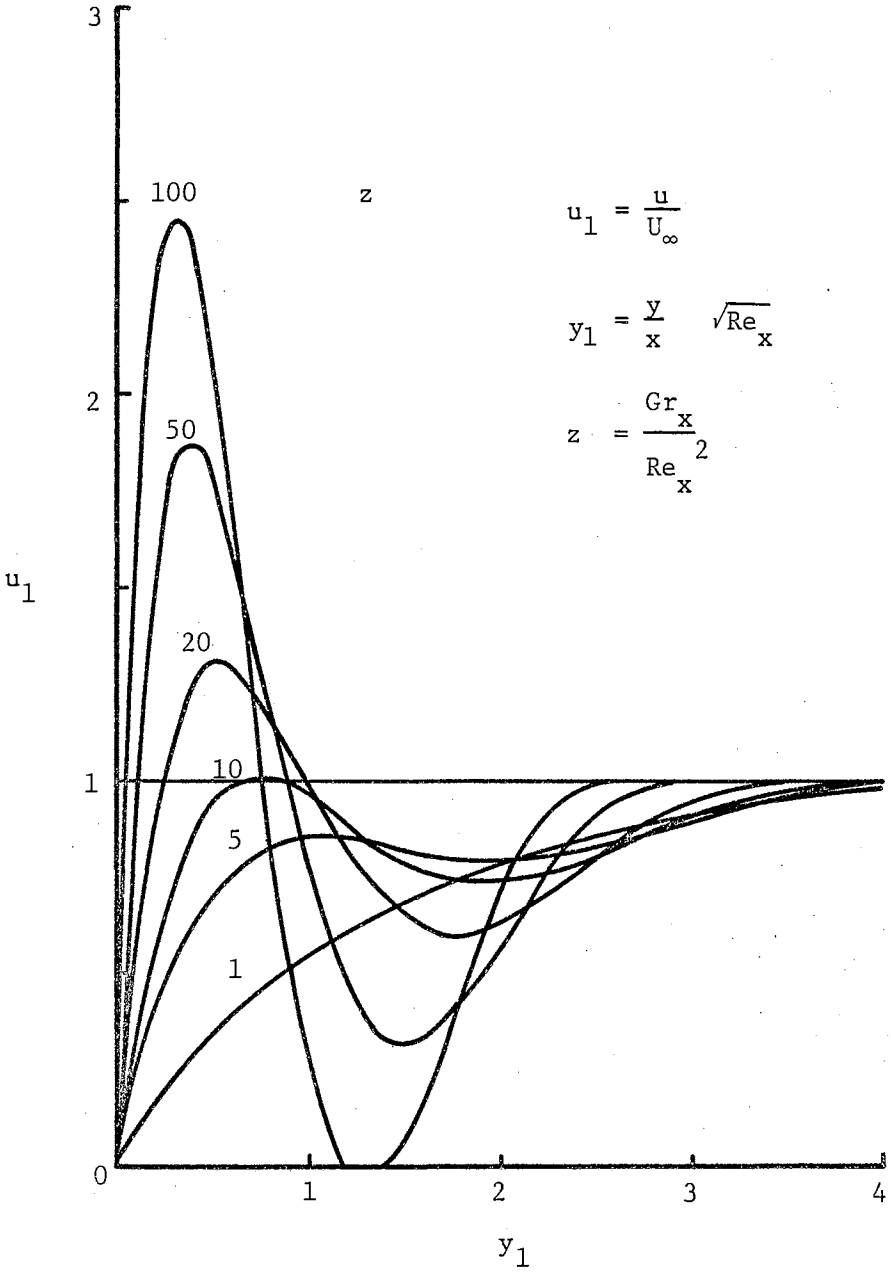

Figure 9. Velocity Profiles, Isothermal Flat Plate, Pr = 10.

n = 3, v = 0.95, w = 1.03

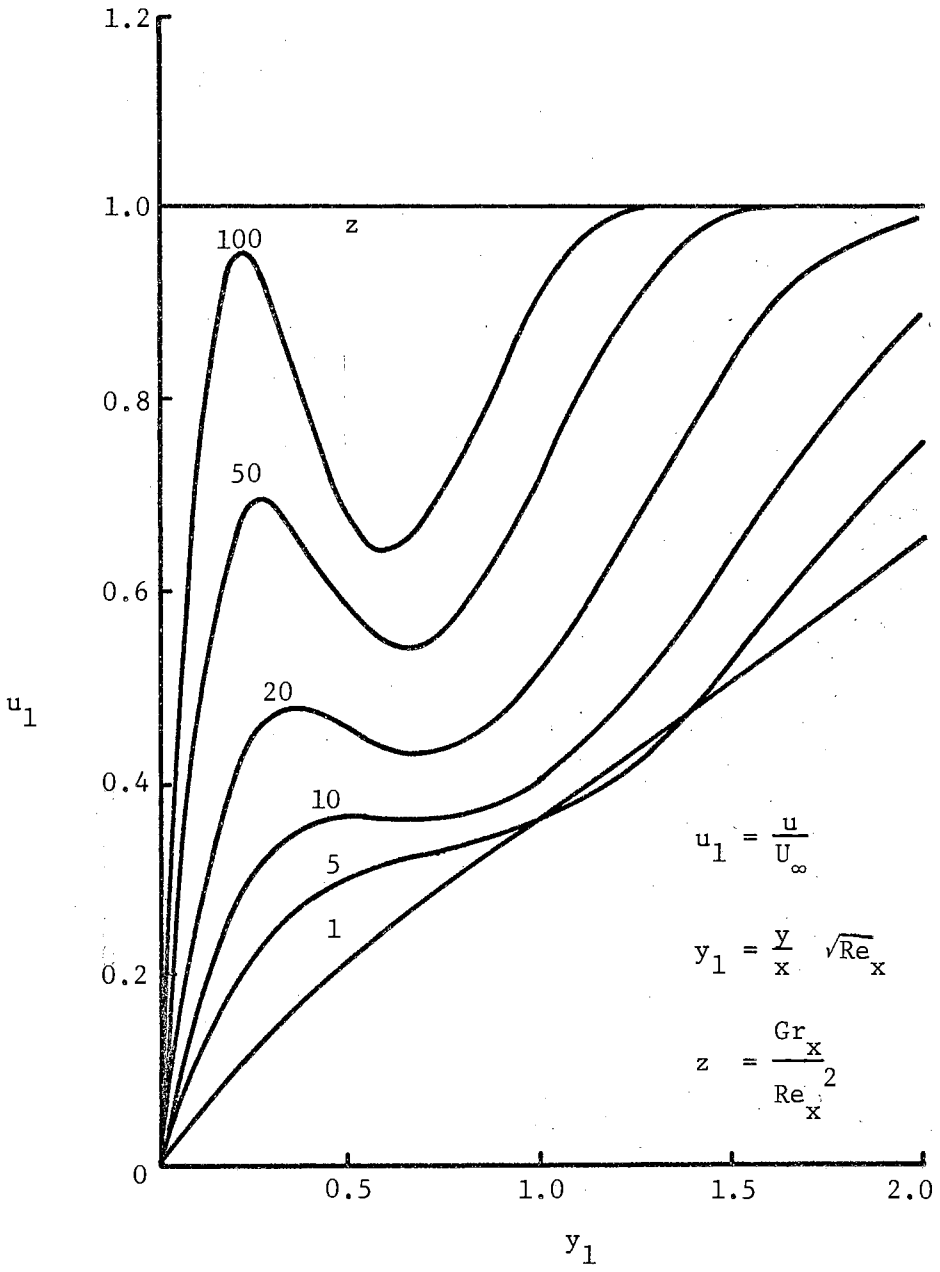

Figure 10. Velocity Profiles, Isothermal Flat Plate, Pr = 100.

n = 3, v = 0.95, w = 1.03

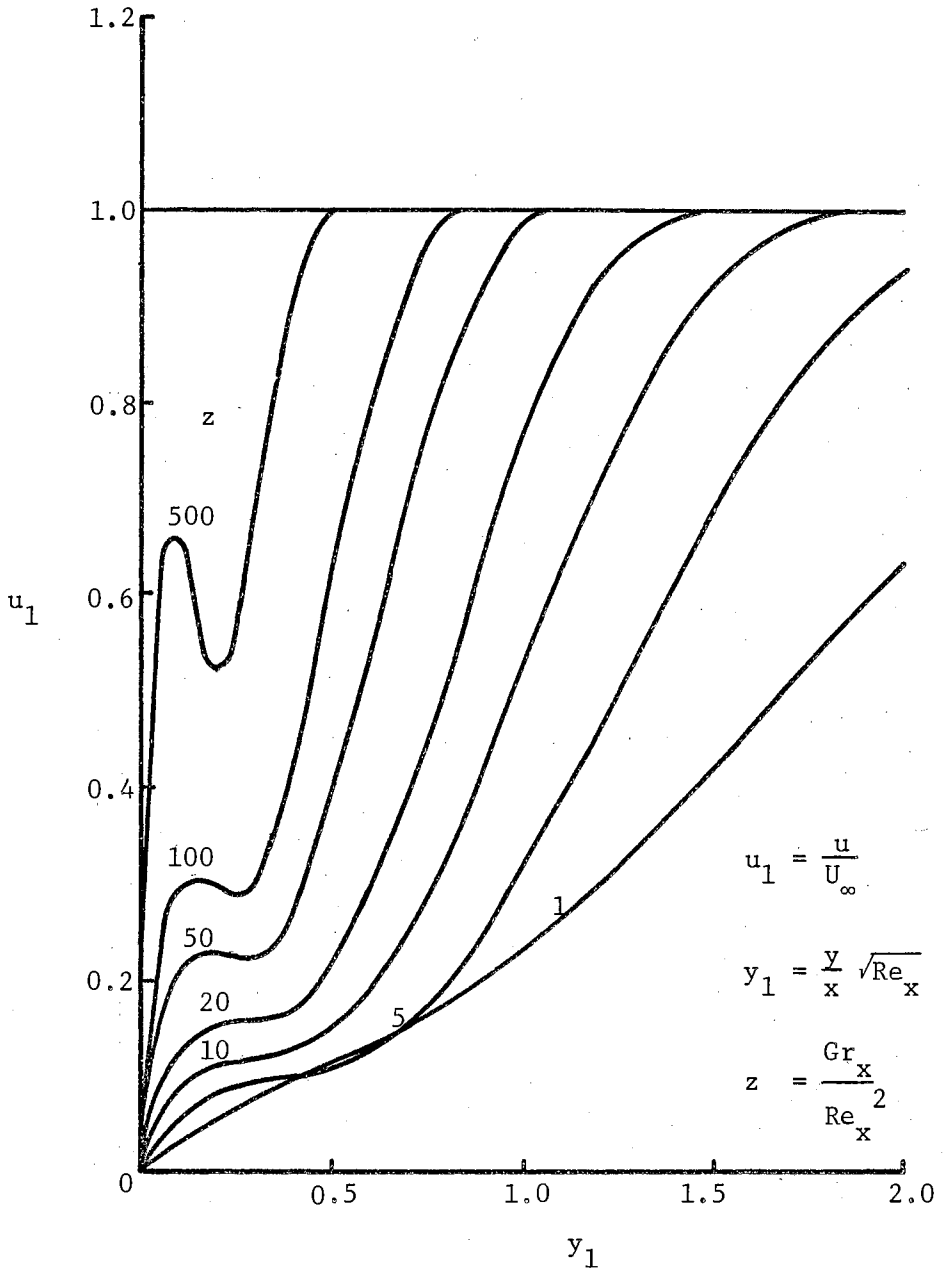

Figure 11. Velocity Profiles, Isothermal Flat Plate, Pr = 1000.

n = 3, v = 0.95, w = 1.03

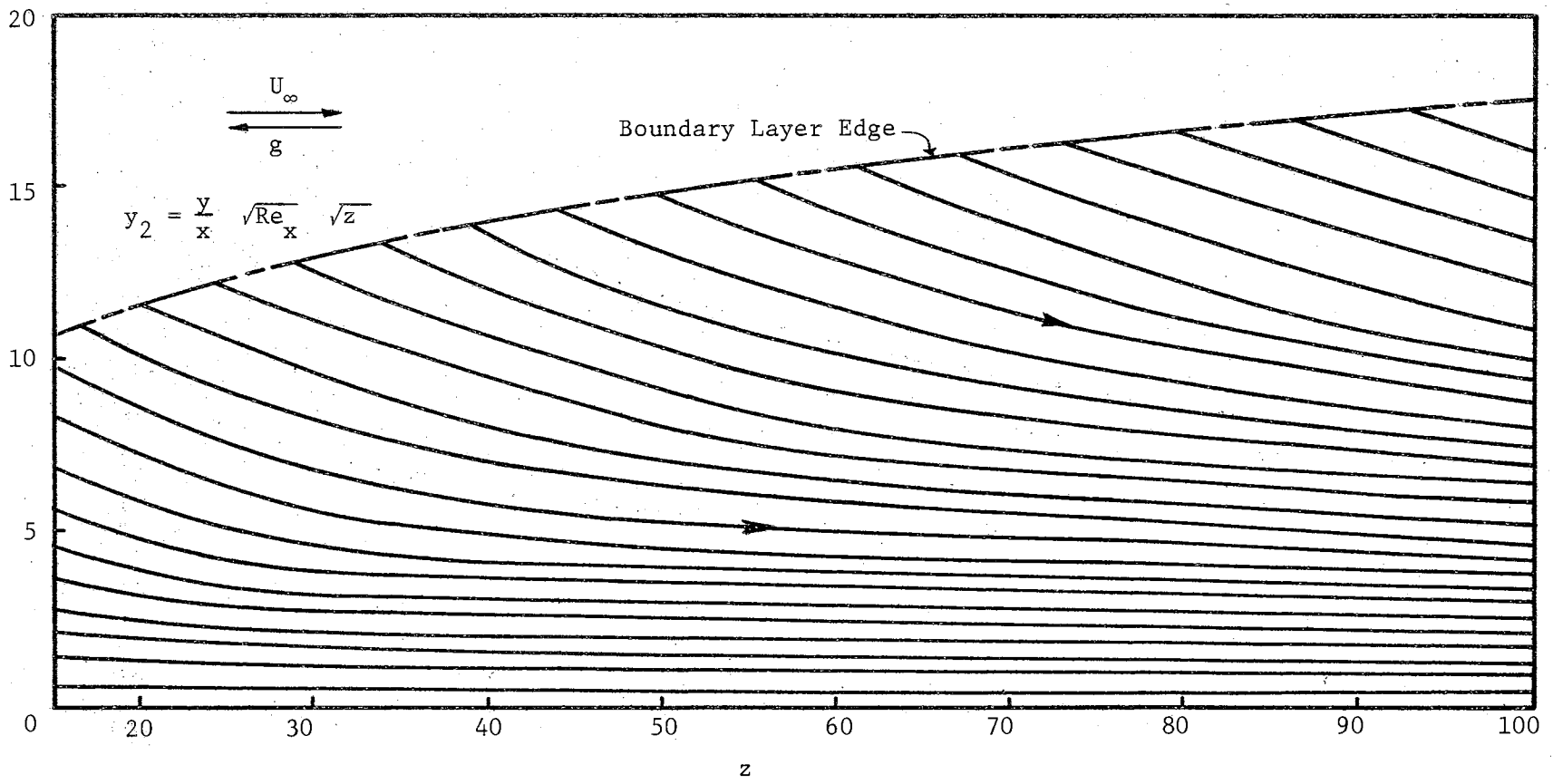

Figure 12. Streamlines, Aiding Flow, Isothermal Flat Plate, Pr = 0.73.

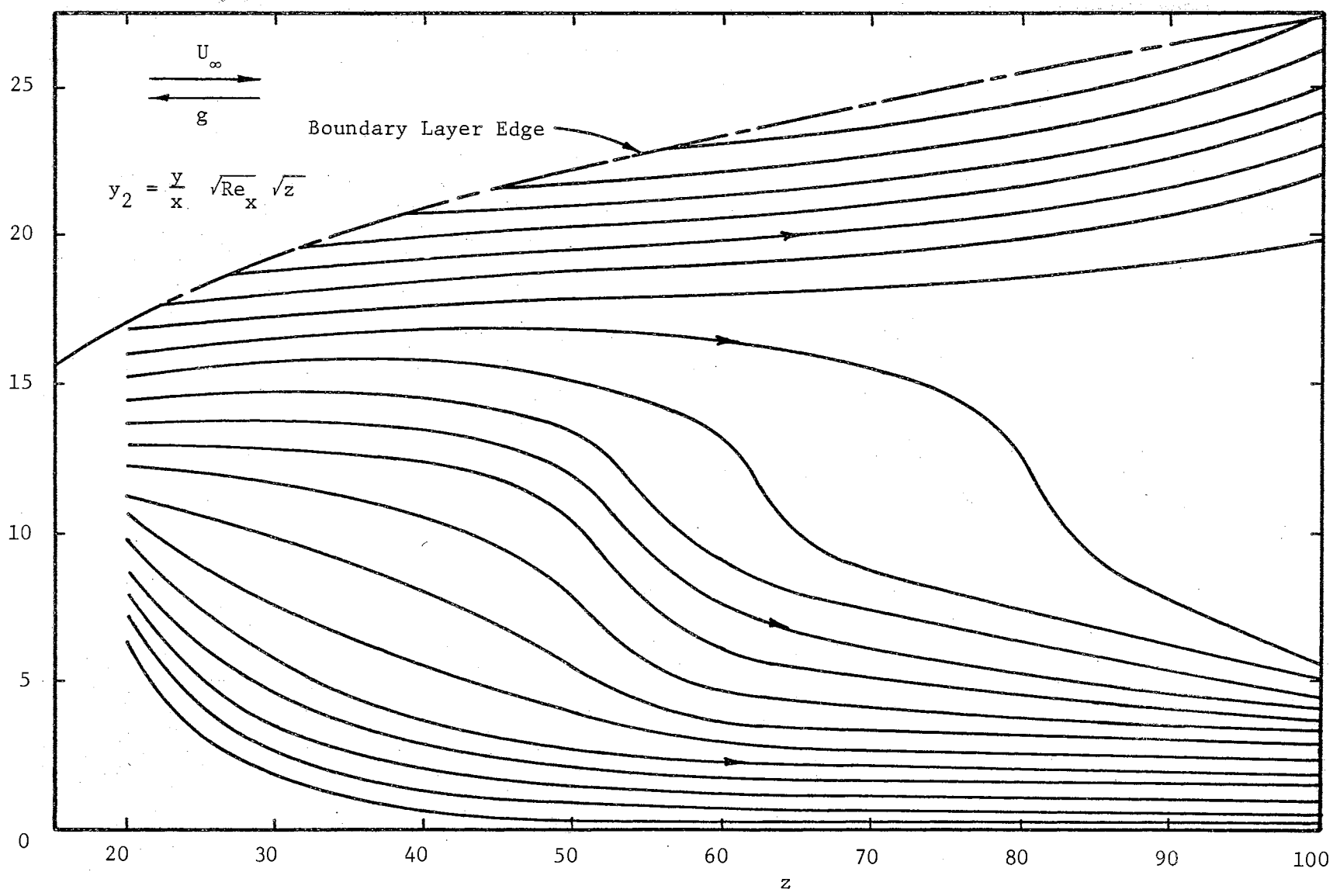

Figure 13. Streamlines, Aiding Flow, Isothermal Flat Plate, Pr = 10.

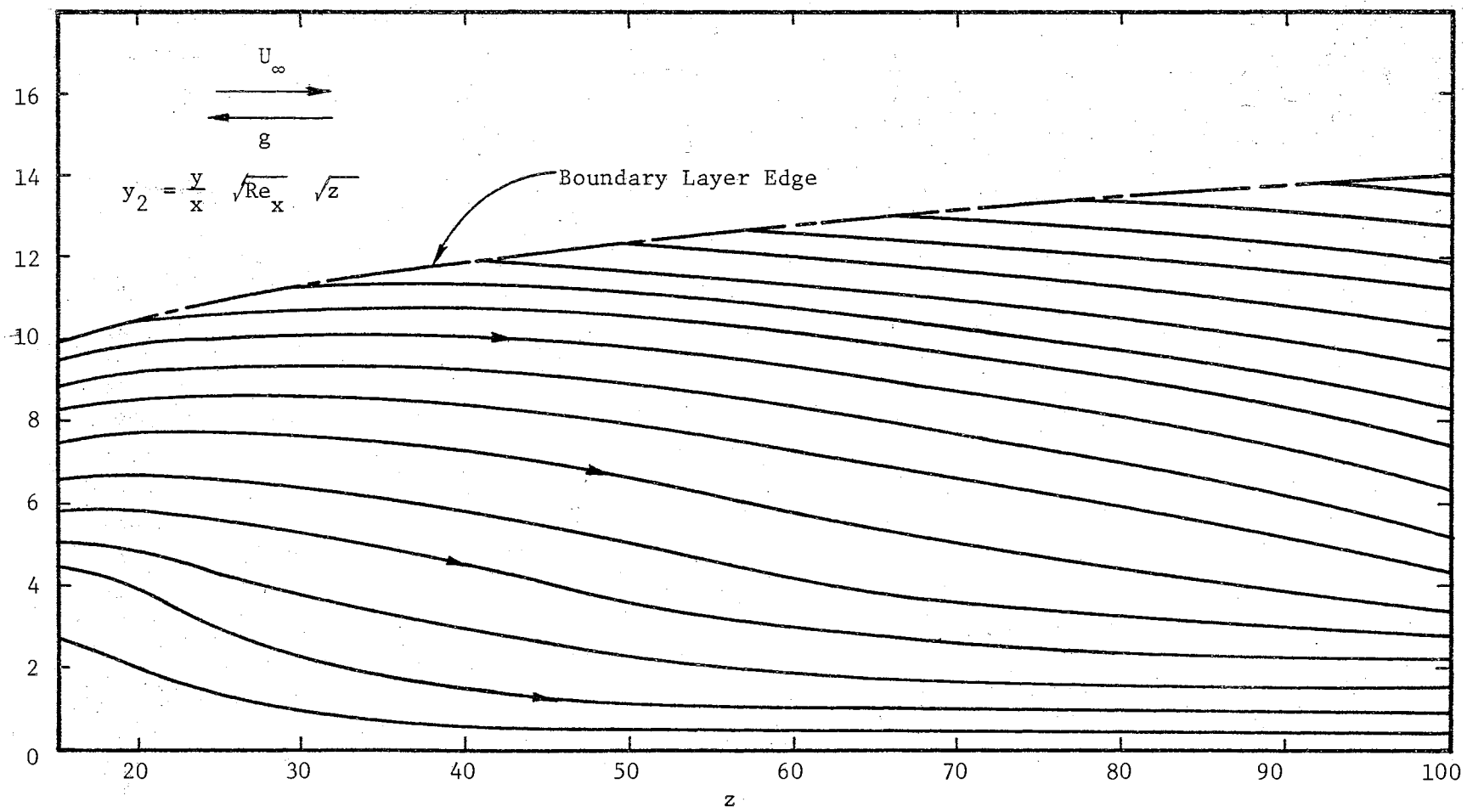

Figure 14. Streamlines, Aiding Flow, Isothermal Flat Plate, Pr = 100.

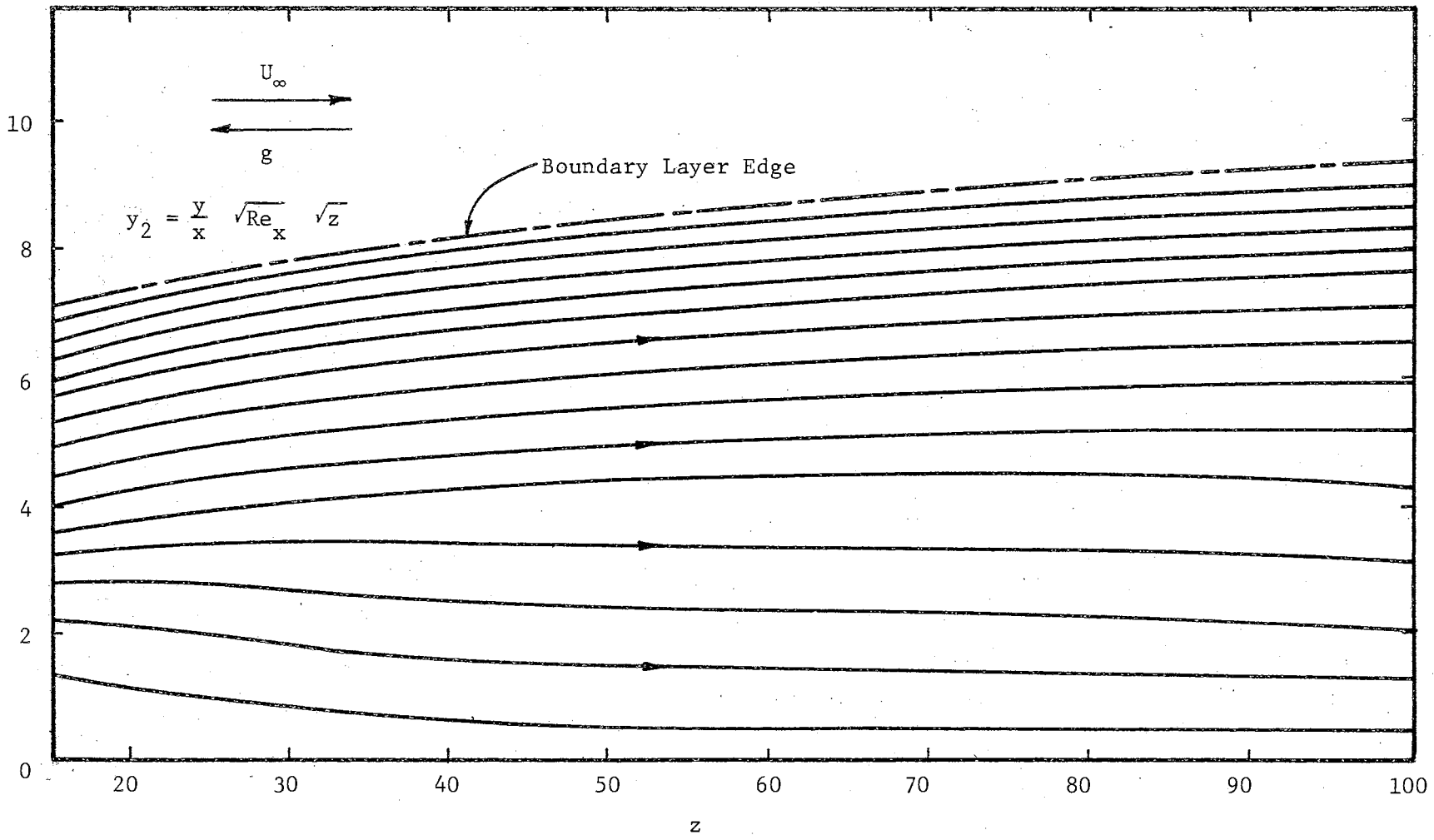

Figure 15. Streamlines Aiding Flow, Isothermal Flat Plate, Pr = 1000.

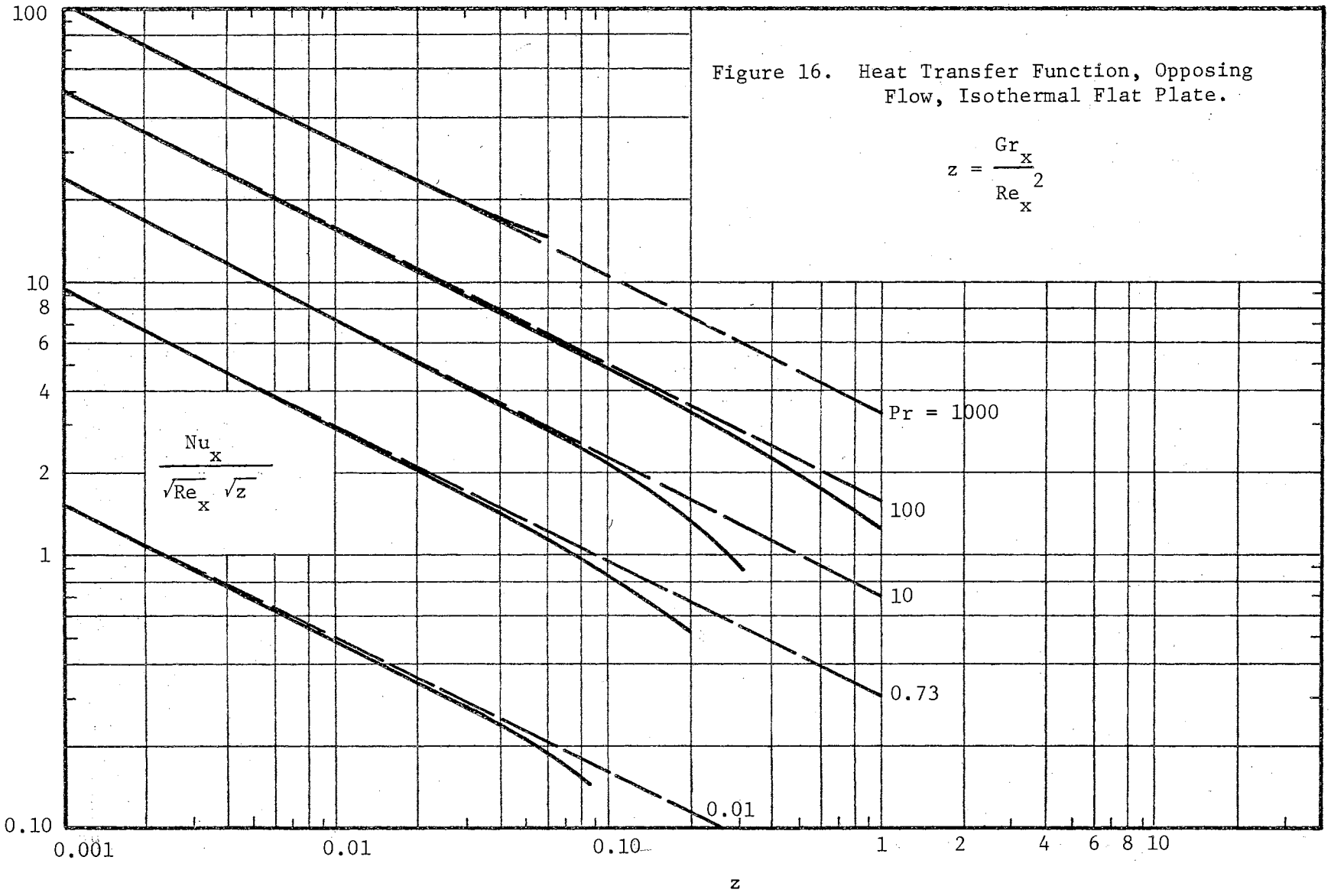

Figure 16. Heat Transfer Function, Opposing Flow, Isothermal Flat Plate.

$$z = \frac{Gr_x}{Re_x^2}$$

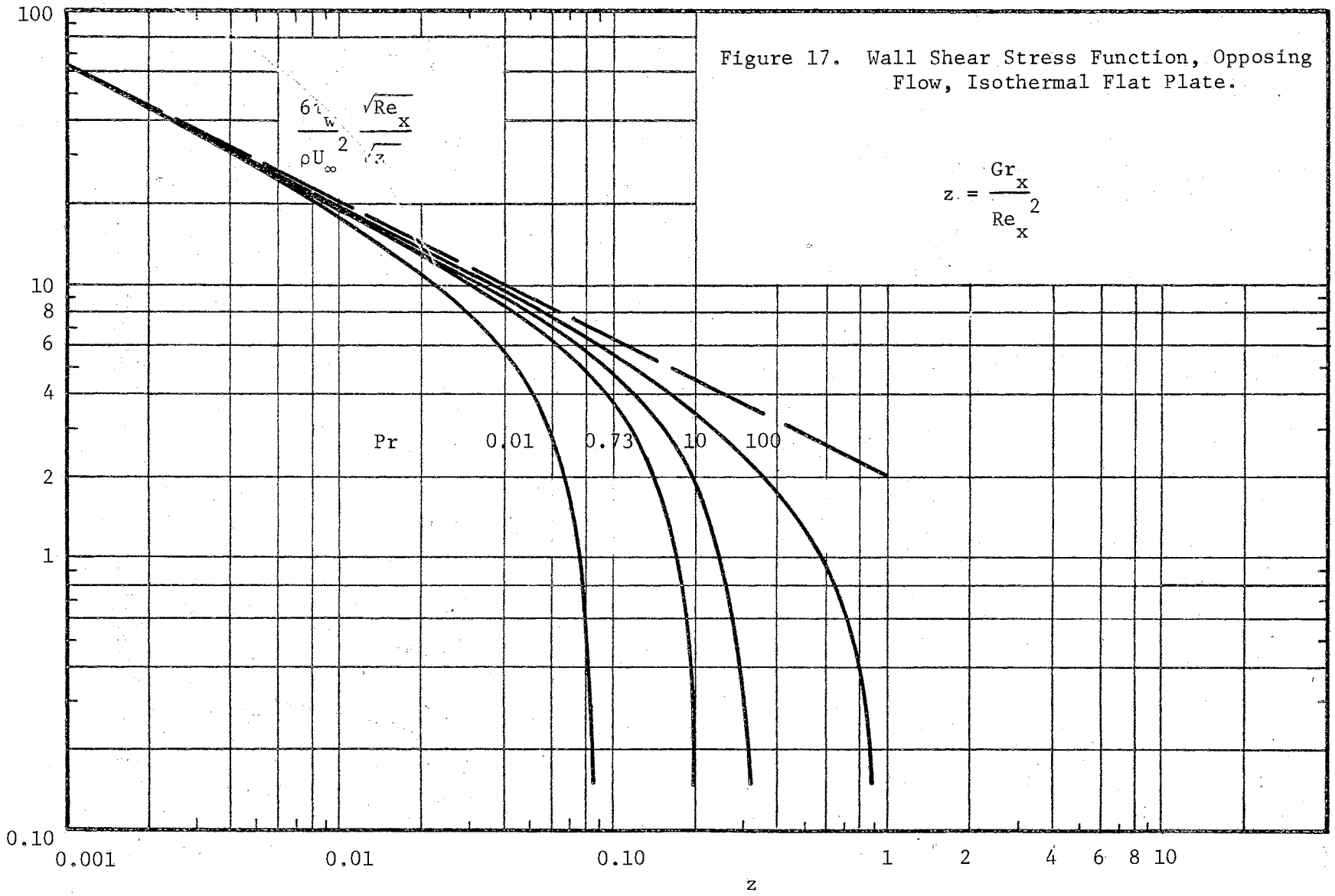

Figure 17. Wall Shear Stress Function, Opposing Flow, Isothermal Flat Plate.

$$z = \frac{Gr_x}{Re_x^2}$$

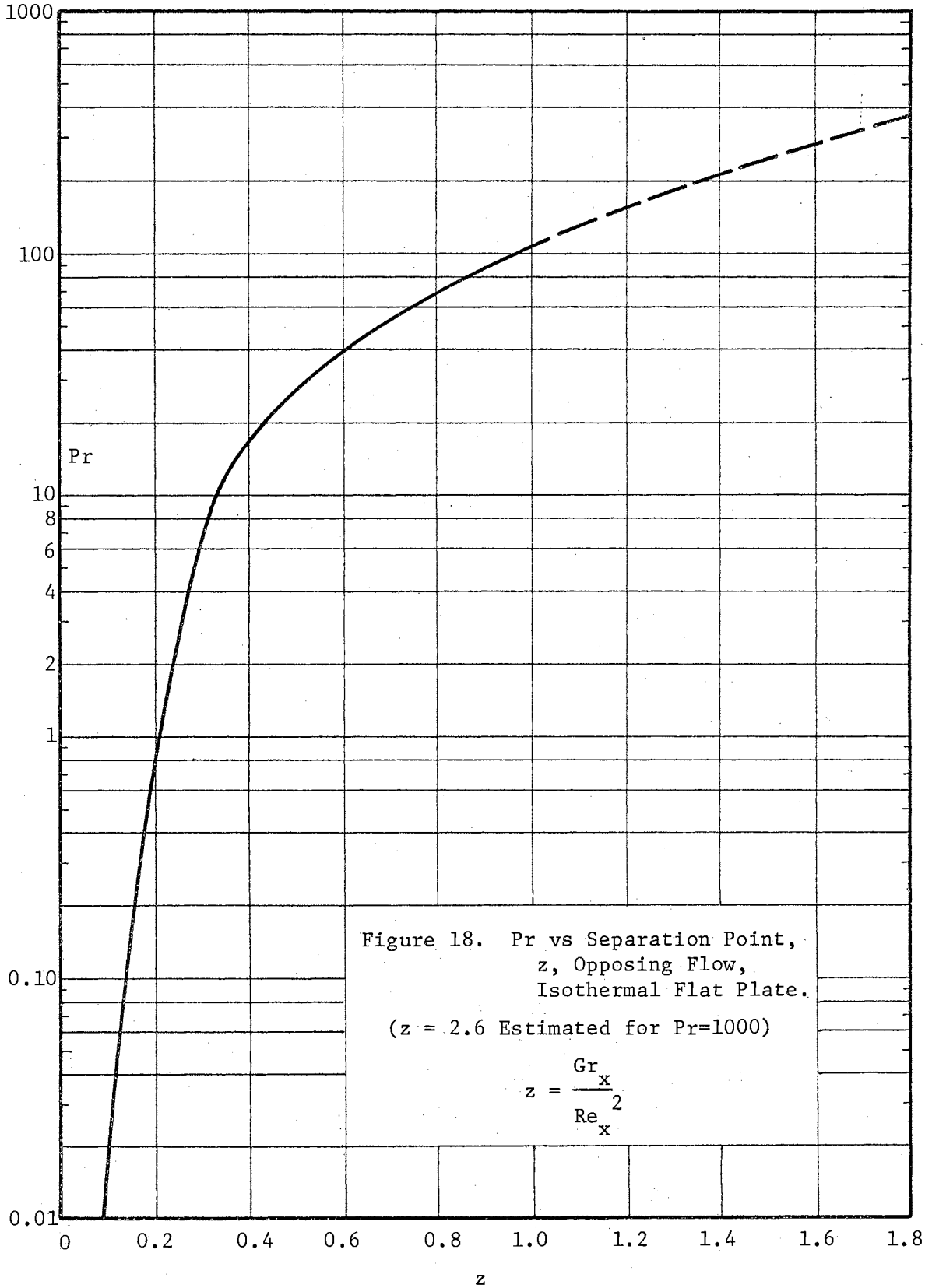

Figure 18. Pr vs Separation Point, z, Opposing Flow, Isothermal Flat Plate.

(z = 2.6 Estimated for Pr=1000)

$$z = \frac{Gr_x}{Re_x^2}$$

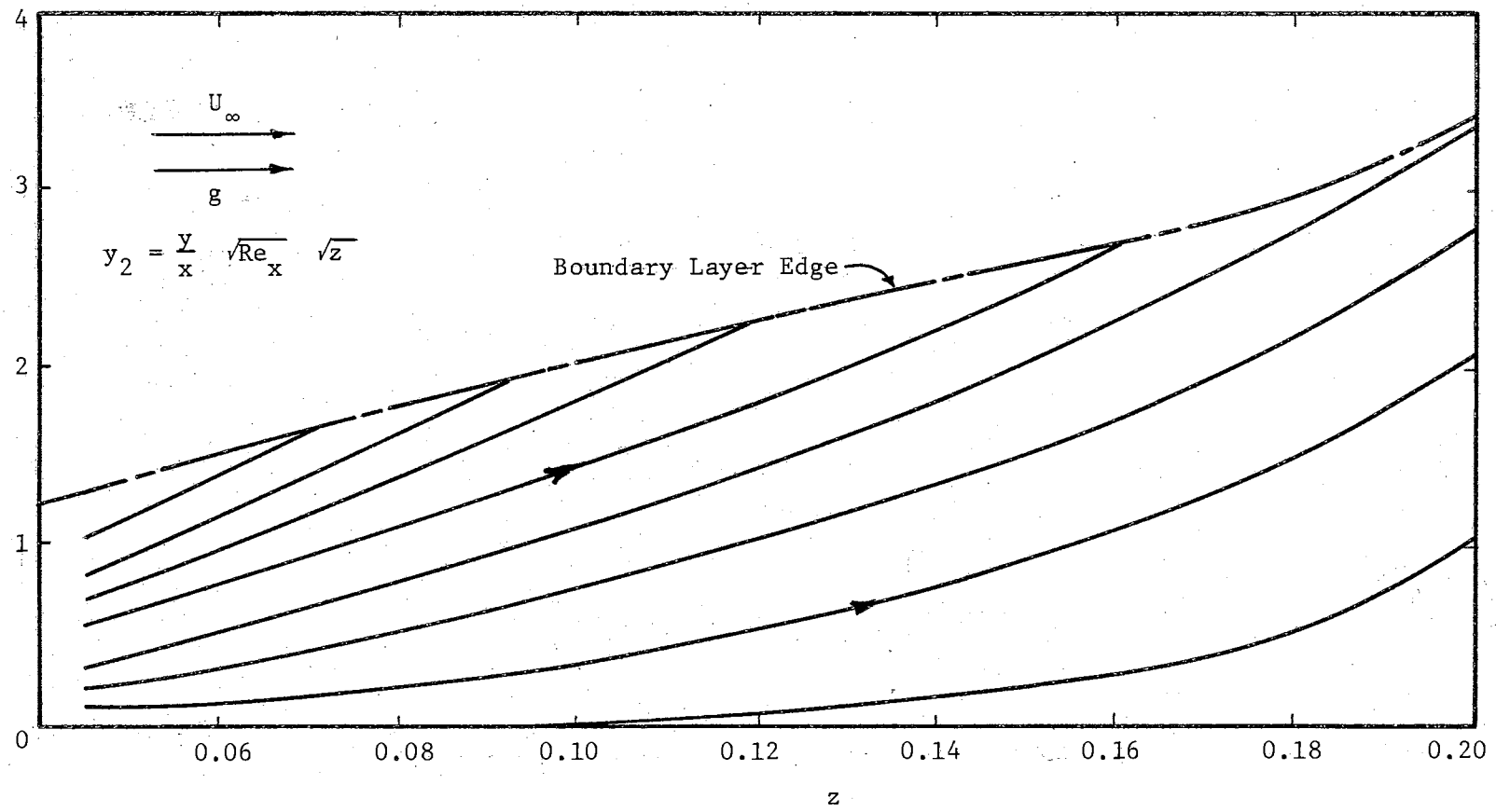

Figure 19. Streamlines, Opposing Flow, Isothermal Flat Plate, Pr = 0.73. Separation Point at z = 0.20.

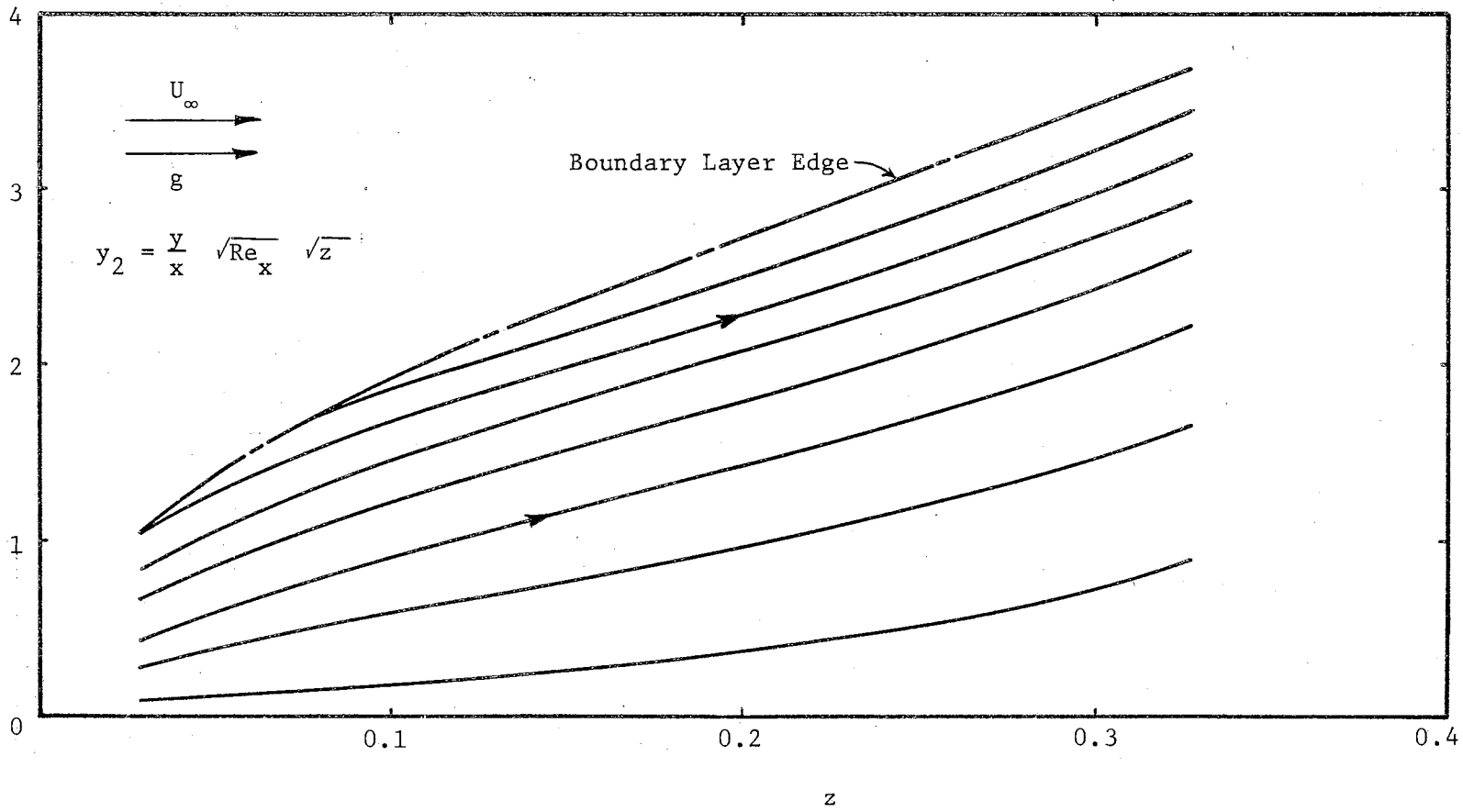

Figure 20. Streamlines, Opposing Flow, Isothermal Flat Plate, Pr = 10.
Separation Point at z = 0.33.

CHAPTER IV

MIXED CONVECTION FLOW OVER A VERTICAL WEDGE SURFACE

Sparrow, Eichhorn, and Gregg (1959) gave an exact solution for the mixed convection flow of a gas, Pr = 0.70, over a semi-infinite wedge. The wedge had a constant wall temperature, and the wedge angle was chosen so that the velocity distribution over its surface just outside of the boundary layer was $U = A_1 x^{\frac{1}{2}}$. These two choices allowed a similarity type solution. The purpose of this chapter is to compare the approximate integral method with the exact solution of Sparrow and his associates and to extend the approximate solution to Pr = 0.01 for comparison with the flat plate difficulties, Pr = 0.01, of Chapter III.

Development of Wedge Equations

Wedge flow being more complicated requires the use of the full momentum and energy integral equations of Chapter III.

Since

$$U_1 = \frac{U}{U_\infty} = \frac{A_1}{U_\infty} x^m$$

, for any wedge,

then $$U_1 \frac{dU_1}{dx} = m\left(\frac{A_1}{U_\infty}\right)^2 x^{2m-1}.$$

By following the transformation of Chapter II where $Z = x/L \cdot Gr_x/Re_x^2$ and L was replaced by x,

$$U_1 \frac{dU_1}{dZ} = m \frac{U_1^2}{Z}.$$

For $m = \frac{1}{2}$,

$$U_1 \frac{dU_1}{dZ} = \frac{U_1^2}{2Z} \tag{38}$$

The integral method can, of course, be applied to any wedge angle or value of the exponent m.

Three "asymptotic" boundary conditions were used in the wedge solution. At first, only two were tried but the resulting Nusselt number function was 35 percent higher than the exact solution, and the differential equations for δ_2 and Δ had a discontinuity at Z = 0.098.

T_∞ is the free stream temperature outside of the thermal boundary layer, along the wedge surface. Since the temperature boundary conditions are the same as those of the flat plate, the temperature profile in terms of η_T is also the same:

$$\Theta = 1 - 2\eta_T + 5\eta_T^4 - 6\eta_T^5 + 2\eta_T^6 .$$

With $m = \frac{1}{2}$, and since $m = \frac{\beta_1}{2-\beta_1}$, the wedge angle for this problem is $\beta_1 \pi = \frac{2}{3}\pi$ or 120°. Figure 21 shows the orientation of the vertical wedge surface.

Once again, $Z = Gr_x/Re_x^2$, but:

$$\frac{Gr_x}{Re_x^2} = \frac{|q_x| \cdot \beta \cdot |(T_W - T_\infty)| \cdot x}{U^2} = \frac{|q_x| \cdot \beta \cdot |(T_W - T_\infty)| \cdot x}{A_1^2 (x^{1/2})^2}$$

$$= \frac{|q_x| \cdot \beta \cdot |(T_W - T_\infty)|}{A_1^2} .$$

Therefore, for this wedge angle, necessary for a similarity trans-

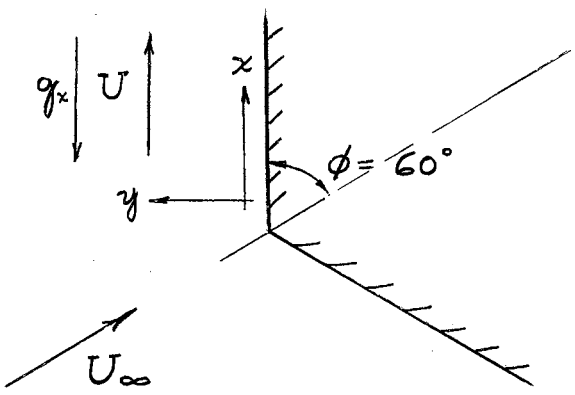

Fig. 21. Wedge Orientation, m = $\frac{1}{2}$

formation to apply in th exact solution, Z is independent of x. Z is constant all along the wedge for a given $(T_w - T_\infty)$ if β, the volumetric coefficient of expansion, is constant.

The same type and number of velocity boundary conditions are used as in the general case, Chapter II. If only aiding flow is considered, these are:

$$u_1\Big]_{\eta=1} = U_1$$

$$\frac{\partial u_1}{\partial y_2}\Big]_{\eta=1} = \frac{\partial^2 u_1}{\partial y_2^2}\Big]_{\eta=1} = \frac{\partial^3 u_1}{\partial y_2^3}\Big]_{\eta=1} = 0$$

$$\frac{\partial^2 u_1}{\partial y_2^2}\Big]_w = -\left(U_1 + \frac{dU_1}{dz}\right)$$

$$\frac{\partial^3 u_1}{\partial y_2^3}\Big]_w = -U_1 \frac{\partial \theta}{\partial y_2}\Big]_w = \frac{2U_1}{\delta_2 \Delta}$$

A sixth degree velocity profile, $f(\eta)$, is again used. An evaluation of the coefficients of η^m in $f(\eta)$ proceeds as before with much the same results. The only difference is that now,

$$b = -\frac{\delta_2^2}{2U_1}\left(U_1 + \frac{dU_1}{dz}\right) = -\frac{\delta_2^2}{2}\left(1 + \frac{1}{2z}\right)$$

Let j = (1+1/2Z); the velocity profile coefficients are then the same as equation (17);

$$a = 2 + 0.2\,\delta_2^2 j - \frac{1}{30}\,\frac{\delta_2^2}{\Delta}$$

$$b = -0.5\,\delta_2^2 j$$

$$c = \frac{1}{3}\,\frac{\delta_2^2}{\Delta}$$

$$d = -5 + \delta_2^2 j - \frac{2}{3}\,\frac{\delta_2^2}{\Delta}$$

$$e = 6 - \delta_2^2 j + 0.5\,\frac{\delta_2^2}{\Delta}$$

$$f = -2 + 0.3\,\delta_2^2 j - \frac{2}{15}\,\frac{\delta_2^2}{\Delta}$$

After evaluation of the momentum and energy integral equations of Chapter II, the two differential equations can again be written in the form of equations (29) and (31), Chapter III:

$$\frac{d\delta_2^2}{dz} = \frac{a_1 + b_1\frac{d\Delta}{dz}}{c_1} \tag{39}$$

and

$$\frac{d\Delta}{dz} = \frac{a_2 + b_2\frac{d\delta_2^2}{dz}}{c_2} \tag{40}$$

These two equations can also be written as explicit expressions as they were for the flat plate:

$$\frac{d\delta_2^2}{dz} = \frac{a_1 c_2 + a_2 b_1}{c_1 c_2 - b_1 b_2} \tag{41}$$

and

$$\frac{d\Delta}{dz} = \frac{a_2 c_1 + a_1 b_2}{c_1 c_2 - b_1 b_2} \tag{42}$$

However, the a_1, b_1, etc., terms are more complicated than they were for the flat plate. With recognition that $\frac{dj}{dz} = -\frac{1}{2z^2}$, they are:

$$a_1 = \frac{1}{z}\left(-0.57142857 z \delta_2^2 \Delta + 4z + 0.4 z \delta_2^2 j - 0.0666\ldots \frac{\delta_2^2 z}{\Delta} \right.$$
$$- 0.5043845 \delta_2^2 + 0.011632812 \delta_2^4 j + 0.00031080028 \delta_2^6 j^2$$
$$- 0.0032060532 \frac{\delta_2^4}{\Delta} - 0.000152810 17 \frac{\delta_2^6 j}{\Delta}$$
$$\left. + 0.000018993355 \frac{\delta_2^6}{\Delta^2} \right) + \frac{1}{2z^2}\left(-0.002109002 2 \delta_2^4 \right.$$
$$\left. - 0.000621600 54 \delta_2^6 j + 0.000152810 17 \frac{\delta_2^6}{\Delta} \right) ,$$

$$b_1 = 0.000825100 9 \frac{\delta_2^4}{\Delta^2} + 0.000152810 17 \frac{\delta_2^6 j}{\Delta^2}$$
$$+ 0.000037986 71 \frac{\delta_2^6}{\Delta^3} ,$$

$$c_1 = 0.109335 11 - 0.003163503 3 \delta_2^2 j - 0.000777000 68 \delta_2^4 j^2$$
$$+ 0.001237651 4 \frac{\delta_2^2}{\Delta} + 0.000382025 42 \frac{\delta_2^4 j}{\Delta}$$
$$- 0.000047483389 \frac{\delta_2^4}{\Delta^2} ,$$

$$a_2 = \frac{4}{\Delta P_r} + \frac{\delta_2^4 H_2}{z^2} - \frac{1}{z}\left(\delta_2^2 H_1 + \delta_2^4 j H_2 + \delta_2^4 H_3\right),$$

$$b_2 = -\left(H_1 + 3\delta_2^2 j H_2 + 3\delta_2^2 H_3\right)$$

and

$$c_2 = 2\delta_2^2 \frac{dH_1}{d\Delta} + 2\delta_2^4 j \frac{dH_2}{d\Delta} + 2\delta_2^4 \frac{dH_3}{d\Delta} .$$

For $Pr < 1$ or $\Delta > 1$, where

$$\int_0^{\delta_{T_2}} f\theta \, dy_2 = \int_0^{\delta_2} f\theta \, dy_2 + \int_{\delta_2}^{\delta_{T_2}} \theta \, dy_2 ,$$

$$H_1 = 0.285714 29 (\Delta - 1) + 0.119047 62 \frac{1}{\Delta} - 0.0202\ldots \frac{1}{\Delta^4}$$
$$+ 0.012987 04 \frac{1}{\Delta^5} - 0.002497 5023 \frac{1}{\Delta^6} ,$$

$$H_2 = 0.009523809\overline{6} - 0.005952380\overline{8}\,\frac{1}{\Delta} + 0.001443001\overline{4}\,\frac{1}{\Delta^4} - 0.000974025\overline{96}\,\frac{1}{\Delta^5} + 0.000194250\overline{19}\,\frac{1}{\Delta^6},$$

and

$$H_3 = -0.002380952\overline{3}\,\frac{1}{\Delta} + 0.001587301\overline{6}\,\frac{1}{\Delta^2} - 0.000420875\overline{42}\,\frac{1}{\Delta^5} + 0.000288600\overline{29}\,\frac{1}{\Delta^6} - 0.000058275\overline{058}\,\frac{1}{\Delta^7}.$$

The H_1, H_2, and H_3 expressions again are different for $Pr > 1$, $\Delta < 1$:

$$H_1 = 0.11904762\Delta^2 - 0.02020\cdots\Delta^5 + 0.012987013\Delta^6 - 0.0024975024\Delta^7,$$

$$H_2 = 0.0011904762\Delta^2 - 0.0099206345\Delta^3 + 0.004040\cdots\Delta^5 - 0.002164502\overline{2}\Delta^6 + 0.000374625\overline{36}\Delta^7,$$

and

$$H_3 = 0.001984127\Delta + 0.00277\cdots\Delta^3 - 0.002693602\overline{7}\Delta^4 + 0.001082251\overline{1}\Delta^5 - 0.000166500\overline{16}\Delta^6.$$

Since

$$\lim_{0} \delta_2^{2n} j = 0, \qquad n > 1 \text{ and integer},$$

$$\lim_{0} \delta_2^4 \frac{dj}{dz} = -\frac{1}{2}\left(\frac{d\delta_2^2}{dz}\right)^2\Bigg]_0,$$

$$\lim_{0} \delta_2^2 j = \frac{1}{2}\,\frac{d\delta_2^2}{dz}\Bigg]_0,$$

$$\lim_{0} \delta_2^4 j^2 = \frac{1}{4}\left(\frac{d\delta_2^2}{dz}\right)^2\Bigg]_0,$$

$$\lim_{0} \frac{\delta_2^2}{z} = \frac{d\delta_2^2}{dz}\Bigg]_0,$$

$$\lim_{0} \frac{\delta_2^4 f}{Z} = \frac{1}{2}\left(\frac{d\delta_2^2}{dZ}\right)\Big]_0$$

$$\lim_{0} \frac{\delta_2^6 f^2}{Z^2} = \frac{1}{4}\left(\frac{d\delta_2^2}{dZ}\right)^3\Big]_0$$

$$\lim_{0} \frac{\delta^4}{Z} = 0, \quad \lim_{0} \frac{\delta^6 f}{Z} = 0, \quad \lim_{0} \frac{\delta_2^6}{Z} = 0$$

and $$\lim_{0} \delta_2^6 f \frac{df}{dZ} = -\frac{1}{4}\left(\frac{d\delta_2^2}{dZ}\right)^3\Big]_0$$

the value of $\frac{d\delta_2^2}{dZ}$ as Z approaches zero is

$$\lim_{0} \frac{d\delta_2^2}{dZ} = \frac{d\delta_2^2}{dZ}\Big]_0 = 28.230347$$

In finding these limits it was assumed that as Z approaches zero, δ_2 approaches zero, since Z is a function of x^{1-2m}. For $m = \frac{1}{2}$, this is not true; but since it is true for any wedge with $m < \frac{1}{2}$, $m = \frac{1}{2}$ was considered a limiting case.

As Z approaches zero, the denominator of equation (40) also goes to zero. Therefore, to make $\frac{d\Delta}{dZ}$ a 0/0 indeterminate form, the numerator of equation (40) in the limit must equal zero; or

$$\frac{4}{\Delta_0 Pr} - 2H_1 \frac{d\delta_2^2}{dZ}\Big]_0 - H_2\left(\frac{d\delta_2^2}{dZ}\right)^2\Big]_0 = 0$$

For $Pr < 1$, $\Delta > 1$, this reduces to

$$8.0658135\Delta_0^7 - 4.2708016\Delta_0^6 + (0.9888732 - 2/Pr)\Delta_0^5 + 0.00469175\Delta_0^2 - 0.02149756\Delta_0 + 0.00689873 = 0 .$$

For $Pr > 1$, $\Delta < 1$,

$$2.8442085\Delta_0^8 - 0.99175932\Delta_0^7 + 2.07939\Delta_0^6 - 7.906287\Delta_0^4 + 16.209229\Delta_0^3 - 4/Pr = 0 .$$

These polynomials can be solved for Δ_o for any Prandtl number.

Although $\left.\frac{d\Delta}{dZ}\right]_o$ has been forced to a 0/0 form, successive applications of L'Hospital's Rule failed to produce a limiting value. Therefore, the integration for Pr = 0.70 was started at Z = 0.02 with starting values of δ_2 and Δ derived from the exact solution's heat transfer and shear stress values. The results were satisfactory. That is, there were no discontinuities in the differential equations; the integration was stable; and the results were in fair agreement with the exact solution. An integration is considered to be stable if, for a given error tolerance, the overall trend is to larger and larger intervals of integration as Z increases.

It was found later that integrations started from Z = 0 with arbitrary values of $\left.\frac{d\Delta}{dZ}\right]_o$ and starting intervals on the order of 10^{-9} were also satisfactory. For example, for Pr = 0.70, regardless of the choice of $\left.\frac{d\Delta}{dZ}\right]_o$ the values of δ_2 and Δ at $Z \geq 0.50$ were in close agreement with those obtained from starting at Z = 0.02. $\frac{d\Delta}{dZ}$ would oscillate at first; but as the interval automatically increased, $\frac{d\Delta}{dZ}$ would assume a stable value by a Z of about 10^{-4}.

An extension of the integration to the case of Pr = 0.01 was therefore feasible. The integration was successfully carried out to Z = 100. The results appeared satisfactory, but there was no exact solution available for comparison.

Wedge Results

The Nusselt number and friction factor functions used in this chapter are the same as those used by Sparrow, Eichhorn, and Gregg (1959) so as to facilitate comparison with the exact solution. Figure 22 shows

the Pr = 0.70 and 0.01 local heat transfer and shear stress results. The Pr = 0.70 curves follow the trend of the exact solution, but heat transfer predicted is a consistent 10 percent or so high, and shear stress is about 10 percent low at Z = 100.

Figure 23 depicts velocity profiles for Pr = 0.01, mixed convection wedge flow. The Pr = 0.01 profiles for a flat plate would be similar.

It is interesting that the liquid metal flat plate equations failed to integrate, but the liquid metal wedge equations integrated without trouble. It is possible that Z, explicit in the wedge differential equations, is a stabilizing influence at very low Prandtl numbers.

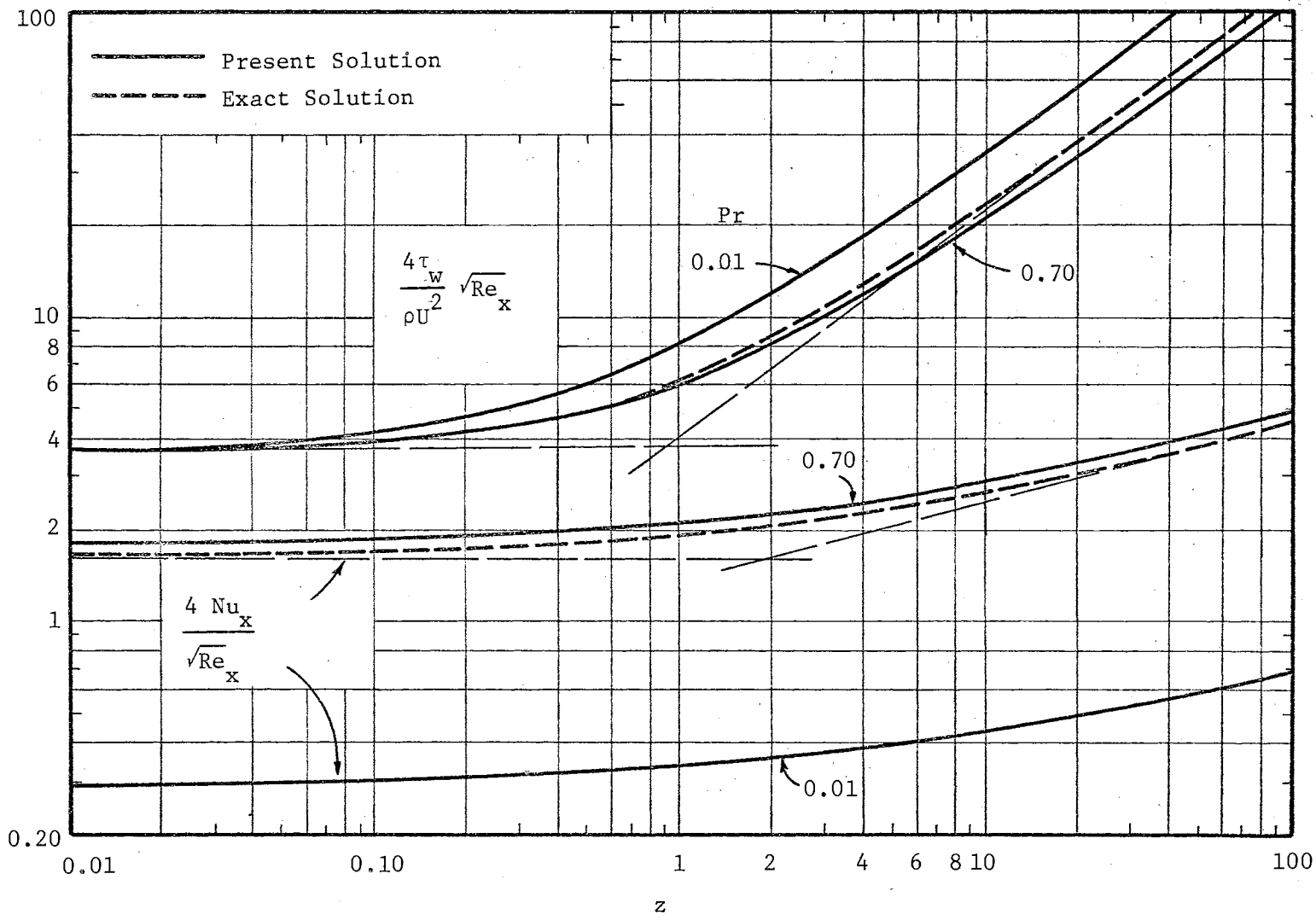

Figure 22. Heat Transfer and Wall Shear Stress Functions, Aiding Flow, 120° Isothermal Wedge.

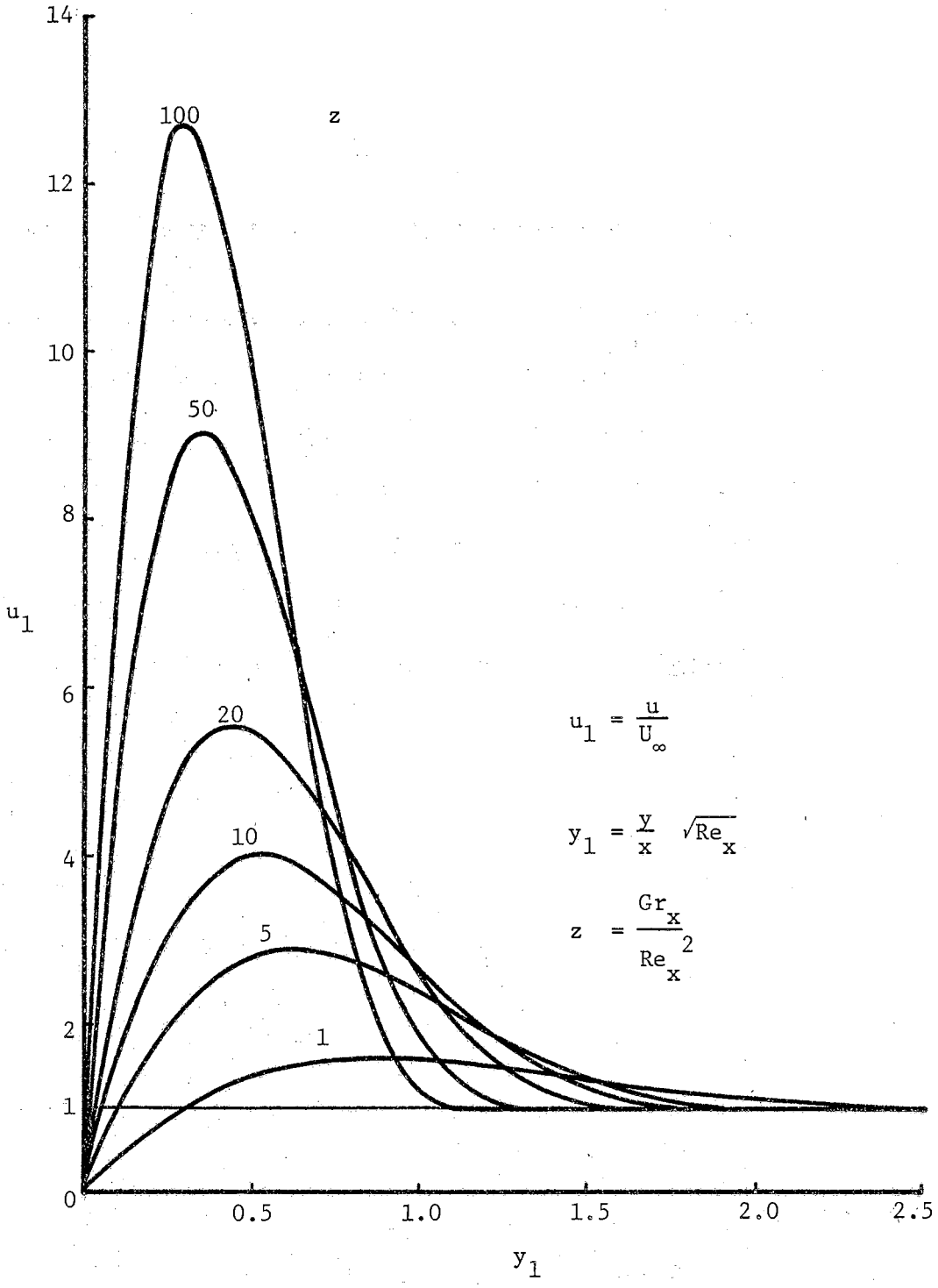

Figure 23. Velocity Profiles, 120° Isothermal Wedge, Pr = 0.01, n = 3.

CHAPTER V

THE NON-ISOTHERMAL VERTICAL FLAT PLATE; VARIABLE VISCOSITY

The preceding two chapters dealt with examples of the integral method as applied to mixed convection flow over isothermal surfaces. A more practical problem is mixed convection flow over a surface whose temperature is not constant. The two cases of non-isothermal surfaces which will be considered here are linearly varying surface temperature and uniform surface heat flux, both for a vertical flat plate. The case of variable viscosity is briefly considered for an isothermal surface in mixed convection.

Linearly Varying Wall Temperature

The temperature difference between the wall and the free stream is taken to be directly proportional to the distance along the plate,

$$(T_w - T_\infty) = \gamma x \tag{43}$$

From Appendix B, equation (B5) applied to a flat plate can be written as

$$u_1 \frac{\partial[(T_w - T_\infty)\theta]}{\partial x_1} + v_1 \frac{\partial[(T_w - T_\infty)\theta]}{\partial y_1} = \frac{1}{Pr} \frac{\partial^2[(T_w - T_\infty)\theta]}{\partial y_1^2} \tag{44}$$

Now, however,

$$\frac{\partial[(T_w-T_\infty)\theta]}{\partial x_1} = (T_w-T_\infty)\frac{\partial\theta}{\partial x_1} + \theta\frac{d(T_w-T_\infty)}{dx_1}$$
$$= (T_w-T_\infty)\frac{\partial\theta}{\partial x_1} + \theta\gamma L$$

where $x_1 = x/L$.

By again using the second set of transformations, equations (B4), Appendix B,

$$u_1\frac{\partial\theta}{\partial Z} + v_2\frac{\partial\theta}{\partial y_2} + \frac{u_1\theta\gamma L}{(T_w-T_\infty)}\frac{Re^2}{Gr} = \frac{1}{Pr}\frac{\partial^2\theta}{\partial y_2^2}$$

and then replacing L by x, so that $Z = Gr_x/Re_x^2 = \frac{|g|\cdot\beta\cdot|\gamma|x^2}{U_\infty^2}$,

the new boundary layer equation is:

$$u_1\frac{\partial\theta}{\partial Z} + v_2\frac{\partial\theta}{\partial y_2} + \frac{u_1\theta}{Z} = \frac{1}{Pr}\frac{\partial^2\theta}{\partial y_2^2} \tag{45}$$

The energy integral equation is, therefore,

$$\frac{d}{dZ}\left[\int_0^\infty u_1\theta\,dy_2\right] + \frac{1}{Z}\int_0^\infty u_1\theta\,dy_2 = -\frac{1}{Pr}\left(\frac{\partial\theta}{\partial y_2}\right)_w \tag{45a}$$

The boundary conditions on u_1 remain the same. Therefore, as in Chapter II, the coefficients of the velocity profile are, for aiding flow,

$$a = 2 + \frac{1}{5}\delta_2^2 - \frac{1}{10}c$$
$$b = -\frac{1}{2}\delta_2^2$$
$$d = -5 + \delta_2^2 - 2c \tag{46}$$
$$e = 6 - \delta_2^2 + \frac{3}{2}c$$

and

$$f = -2 + \frac{3}{10}\delta_2^2 - \frac{2}{5}c$$

where c is as yet undetermined.

Five of the boundary conditions on Θ are the same:

$$\left.\frac{\partial^m \Theta}{\partial y_2^m}\right]_{\eta_T = 1} = 0 \qquad m = 1, 2, 3$$

$$\left.\Theta\right]_{\eta_T = 1} = 0$$

$$\left.\frac{\partial^2 \Theta}{\partial y_2^2}\right]_w = 0$$

However, when equation (45) if differentiated with respect to y_2 and evaluated at the wall, the sixth boundary condition on Θ becomes

$$\left.\frac{\partial^3 \Theta}{\partial y_2^3}\right]_w = \left.\frac{Pr}{Z}\frac{\partial u_1}{\partial y_2}\right]_w . \tag{47}$$

From the first five boundary condition, the coefficients of Θ are

$$\begin{aligned} A &= -2 - \tfrac{1}{10} C , \\ B &= 0 , \\ D &= 5 - 2C , \\ E &= \tfrac{3}{2} C - 6 , \end{aligned} \tag{48}$$

and

$$F = -\tfrac{2}{5} C + 2 .$$

Equation (47) defines C;

$$\left.\frac{\partial^3 \Theta}{\partial y_2^3}\right]_w = \frac{6C}{\delta_{T_2}^3} ,$$

$$\left.\frac{Pr}{Z}\frac{\partial u_1}{\partial y_2}\right]_w = \frac{Pr}{Z}\frac{a}{\delta_2} ,$$

$$\therefore C = \frac{Pr\,\delta_2^2 \Delta^3}{6Z}\, a . \tag{49}$$

From $\left.\frac{\partial^3 u_1}{\partial y_2^3}\right]_w = -\left.\frac{\partial \theta}{\partial y_2}\right]_w$, the unused u_1 boundary condition,

$$\left.\frac{\partial^3 u_1}{\partial y_2^3}\right]_w = \frac{6c}{\delta_2^3}$$

and

$$-\left.\frac{\partial \theta}{\partial y_2}\right]_w = -\frac{A}{\delta_{T_2}}$$

therefore,

$$c = -\frac{1}{6}\frac{\delta_2^2}{\Delta}A = \frac{1}{6}\frac{\delta_2^2}{\Delta}\left(\frac{1}{10}C + 2\right)$$

$$= \frac{Pr}{360Z}\delta_2^4\Delta^2 a + \frac{1}{3}\frac{\delta_2^2}{\Delta}$$

Upon substitution of this expression for c into the one for a, equation (46),

$$a = \frac{2 + \frac{1}{5}\delta_2^2 - \frac{1}{30}\frac{\delta_2^2}{\Delta}}{1 + \frac{Pr}{3600Z}\delta_2^4\Delta^2} \quad . \tag{50}$$

Therefore,

$$c = 10\,Pr\,\delta_2^4\Delta^2\left(\frac{2 + \frac{1}{5}\delta_2^2 - \frac{1}{30}\frac{\delta_2^2}{\Delta}}{3600Z + Pr\,\delta_2^4\Delta^2}\right) + \frac{1}{3}\frac{\delta_2^2}{\Delta} \quad . \tag{51}$$

The velocity profile coefficients are now known in terms of δ_2, Δ, and Pr.

From equation (49),

$$C = 600\,Pr\,\delta_2^2\Delta^3\left[\frac{2 + \frac{1}{5}\delta_2^2 - \frac{1}{30}\frac{\delta_2^2}{\Delta}}{3600Z + Pr\,\delta_2^4\Delta^2}\right] \quad . \tag{52}$$

Thus the temperature profile coefficients are also determined.

But the use of equations (46), (48), (50), (51), and (52) to eval-

uate terms in the two integral equations such as

$$\frac{d}{dz}\int_0^\infty u_1\,\theta\,dy_z \quad \text{and} \quad \frac{d}{dz}\int_0^1 f(1-f)\,d\eta$$

represents a great amount of work before explicit equations for $\frac{d\delta_2^2}{dz}$ and $\frac{d\Delta}{dz}$ can be found.

A simpler approach can be employed to illustrate the use of the integral method. Acrivos (1958) applied an integral method to the mixed convection problem for an isothermal flat plate; the third derivatives of θ and u_1 evaluated at the wall were not considered; and only one "asymptotic" boundary condition on θ and two on u_1 were used. His results were satisfactory only for Pr = 0.73, but heat transfer and shear stress functions were practically identical to the present study for that Prandtl number. Therefore, it seems appropriate to try the flat plate, mixed convection flow case, Pr = 0.73, linearly varying wall temperature, with similar but simpler boundary conditions.

Two "asymptotic"boundary conditions were used on both θ and u_1, and the third derivatives at the wall were dropped. The details of the solution are similar to those previously given. The distinguishing difference, of course, is in the use of equation (45a) as the energy integral equation.

The velocity profile coefficients are

$$a = 2 + \frac{\delta_2^2}{6}$$

$$b = -\frac{\delta_2^2}{2}$$

$$c = -2 + \frac{\delta_2^2}{2}$$

$$d = 1 - \frac{\delta_2^2}{6}$$

and the temperature profile coefficients are A = -2, B = 0, C = 2, and D = -1.

The first differential equation is the same as Acrivos' with the exception of the last term in the numerator:

$$\frac{d\delta_2^2}{dz} = \frac{4 + \frac{1}{3}\delta_2^2 - \frac{3}{5}\delta_2^2\Delta}{0.11746032 - 0.00317460338_2^2 - 0.0000551146398_2^4} \quad (53)$$

The differential equation for $\frac{d\Delta}{dz}$ is different, however,

$$\frac{d\Delta}{dz} = \frac{\frac{4}{\Delta P_{z_2}} - \frac{2}{z}\left(\delta_2^2 H_1 + \delta_2^4 H_2\right) - \left(H_1 + 3\delta_2^2 H_2\right)\frac{d\delta_2^2}{dz}}{2\delta_2^2 \frac{dH_1}{d\Delta} + 2\delta_2^4 \frac{dH_2}{d\Delta}} \quad (54)$$

where $H_1 = 0.1333\ldots\Delta^2 - 0.02142857\Delta^4 + 0.00555\ldots\Delta^5$,

and $H_2 = 0.0111\ldots\Delta^2 - 0.011904762\Delta^3 + 0.005357142\Delta^4 - 0.00092592592\Delta^5$.

For Pr = 0.73, the starting conditions at Z = 0 are

$$\Delta_0 = 0.75737809$$

$$\frac{d\Delta}{dz} = -0.29223494$$

These are found by the limiting processes described in Chapter III.

Uniform Heat Flux

Free convection flow over a uniformly heated flat plate has been studied by Sparrow (1955) and Sparrow and Gregg (1956). The first paper was based on a simple integral method solution and the second on a similarity transformation. Chang, et al, (1964) reported on free con-

vection on a uniformly heated plate for low Prandtl number fluids; a perturbation method was utilized. The only mixed convection constant heat flux case analyzed has been one for a vertical wedge that made use of a similarity transformation to allow an exact solution, Sparrow, Eichhorn, and Gregg (1959).

This section is an analysis of the integral method applied to mixed convection flow over a flat plate with a constant heat flux. The plate-to-free-fluid temperature difference, $(T_w - T_\infty)$, is not specified initially but can be determined for a given heat flux, U_∞, and fluid properties from the two variables δ_2 and Δ.

If six boundary conditions are used on both u_1 and Θ, the same complexities occur that did for the linearly varying surface temperature case. The velocity and temperature profile coefficients are too lengthy and involved for convenient coefficient cross-multiplication and subsequent differentiation with respect to Z and separation of the derivatives, $\frac{d\delta_2}{dZ}$ and $\frac{d\Delta}{dZ}$, as explicit functions.

Becasue of these complexities, the constant heat flux case was solved in the same manner as was the case of linearly varying wall temperature. The third derivatives of u_1 and Θ at both the wall and at the edges of the boundary layer were not considered as boundary conditions, and the solution was accordingly restricted to a flat plate and a fluid of Pr = 0.73.

With reference to equation (44), since $(T_w - T_\infty)$ is a function of x, the thermal boundary layer equation after the first set of transformations (Appendix B) is

$$u_1 \frac{\partial \theta}{\partial x_1} + \frac{u_1 \theta}{(T_w - T_\infty)} \frac{d(T_w - T_\infty)}{dx_1} + v_1 \frac{\partial \theta}{\partial y_1} = \frac{1}{Pr} \frac{\partial^2 \theta}{\partial y_1^2}$$

Upon applying the second set of transformations, equations (B4), and replacing L by x,

$$u_1 \frac{\partial \theta}{\partial z} + v_2 \frac{\partial \theta}{\partial y_2} + u_1 \theta \frac{J'}{J} = \frac{1}{Pr} \frac{\partial^2 \theta}{\partial y_2^2} , \tag{55}$$

where $J = (T_w - T_\infty)$

and $J' = \frac{d(T_w - T_\infty)}{dz}$.

The energy integral equation is, therefore,

$$\frac{d}{dz}\left[\int_0^\infty u_1 \theta \, dy_2\right] + \frac{J'}{J}\int_0^\infty u_1 \theta \, dy_2 = \frac{1}{Pr}\left(\frac{\partial \theta}{\partial y_2}\right)_w . \tag{56}$$

An expression for J is found in the following way: let q" be the known constant heat flux from the plate (aiding flow), and therefore,

$$\frac{\partial T}{\partial y}\Big]_w = -\frac{q''}{k}$$

or

$$(T_w - T_\infty)\frac{\partial \theta}{\partial y}\Big]_w = -\frac{q''}{k} .$$

In terms of y_2, this is

$$\frac{\partial \theta}{\partial y_2}\Big]_w = -\frac{q''}{k(T_w - T_\infty)} \cdot \frac{x}{\sqrt{Re_x}\sqrt{z}} = -\frac{Q}{J^{3/2}} \tag{57}$$

where $Q = \frac{q''}{k}\left(\frac{\nu U_\infty}{|g| \cdot \beta}\right)^{1/2}$, a constant for a given situation.

The coefficients of the η and η_T terms in the velocity and temperature profile polynomials are the same as they were in the simpli-

fied linearly varying wall temperature case since the boundary conditions are identical. Therefore, since A = -2,

$$\left.\frac{\partial\theta}{\partial y_2}\right]_w = \frac{A}{\delta_2\Delta} = -\frac{2}{\delta_2\Delta} \quad . \tag{58}$$

Equations (57 and (58) are combined to give

$$J = \left(\frac{Q\,\delta_2\Delta}{2}\right)^{2/3} \tag{59}$$

which implies that

$$(T_w - T_\infty) = \left(\frac{q''}{2k}\,\delta_2\Delta\right)^{2/3}\left(\frac{\nu\,U_\infty}{|g|\cdot\beta}\right)^{1/3} . \tag{60}$$

The energy integral equation is, therefore,

$$\frac{d}{dz}\int_0^\infty u_1\theta\,dy_2 + \frac{2}{3}\left(\frac{1}{\Delta}\frac{d\Delta}{dz} + \frac{1}{2\delta_2^2}\frac{d\delta_2^2}{dz}\right)\int_0^\infty u_1\theta\,dy_2 = -\frac{1}{Pr}\left(\frac{\partial\theta}{\partial y_2}\right)_w . \tag{61}$$

The expression for $\frac{d\delta_2^2}{dz}$ is the same as equation (53), but

$$\frac{d\Delta}{dz} = \frac{\frac{4}{\Delta Pr} - \left[\frac{5}{3}H_1 + \frac{11}{3}\delta_2^2 H_2\right]\frac{d\delta_2^2}{dz}}{2\delta_2^2\frac{dH_1}{d\Delta} + 2\delta_2^4\frac{dH_2}{d\Delta} + \frac{4}{3}\frac{\delta_2^2}{\Delta}\left(H_1 + \delta_2^2 H_2\right)} \tag{62}$$

where H_1 and H_2 are the same as they were for equation (54).

With Pr = 0.73, the initial conditions at Z = 0 are found to be

$$\Delta_0 = 0.932101$$

and

$$\left.\frac{d\Delta}{dz}\right]_0 = 0.038176489 \quad .$$

Non-Isothermal Flat Plate Results

Figure 24 shows the heat transfer results from the integration of the differential equations for $\frac{d\delta_2^2}{dZ}$ and $\frac{d\Delta}{dZ}$ with Pr = 0.73. When the plate temperature varies linearly with x, the local Nusselt number function is predicted to be about 50 percent greater at a given value of Z than that for a constant temperature flat plate. A plate with a constant surface heat flux is seen to have a local Nusselt number function about 12 percent higher at a given Z than a constant temperature plate.

Variable Viscosity in Mixed Convection

The viscosity of liquids is quite temperature sensitive. For example, the Prandtl number for engine oil decreases by about a factor of 10 when the temperature of the oil is raised to 200° F from an initial value of 100° F. This behavior is primarily caused by the viscosity of the oil sharply decreasing with temperature; $\frac{d\mu}{dT}$ is a fairly large negative number. Most high Prandtl number fluids behave in this way: a viscosity very sensitive to temperature and a thermal conductivity practically independent of temperature. Therefore, it is of interest to study the effect variable viscosity has on the heat transfer between the immersed body and a liquid in the mixed convection range.

To illustrate the method of analysis, a constant temperature flat plate in aiding flow, $T_w > T_\infty$, is considered. The velocity boundary layer equation is written so as to take viscosity variation with temperature into effect:

$$-u_1 \frac{\partial u_1}{\partial z} + v_2 \frac{\partial u_1}{\partial y_2} = \theta + \frac{\partial}{\partial y_2}\left(\frac{\nu}{\nu_\infty} \frac{\partial u_1}{\partial y_2}\right) . \qquad (63)$$

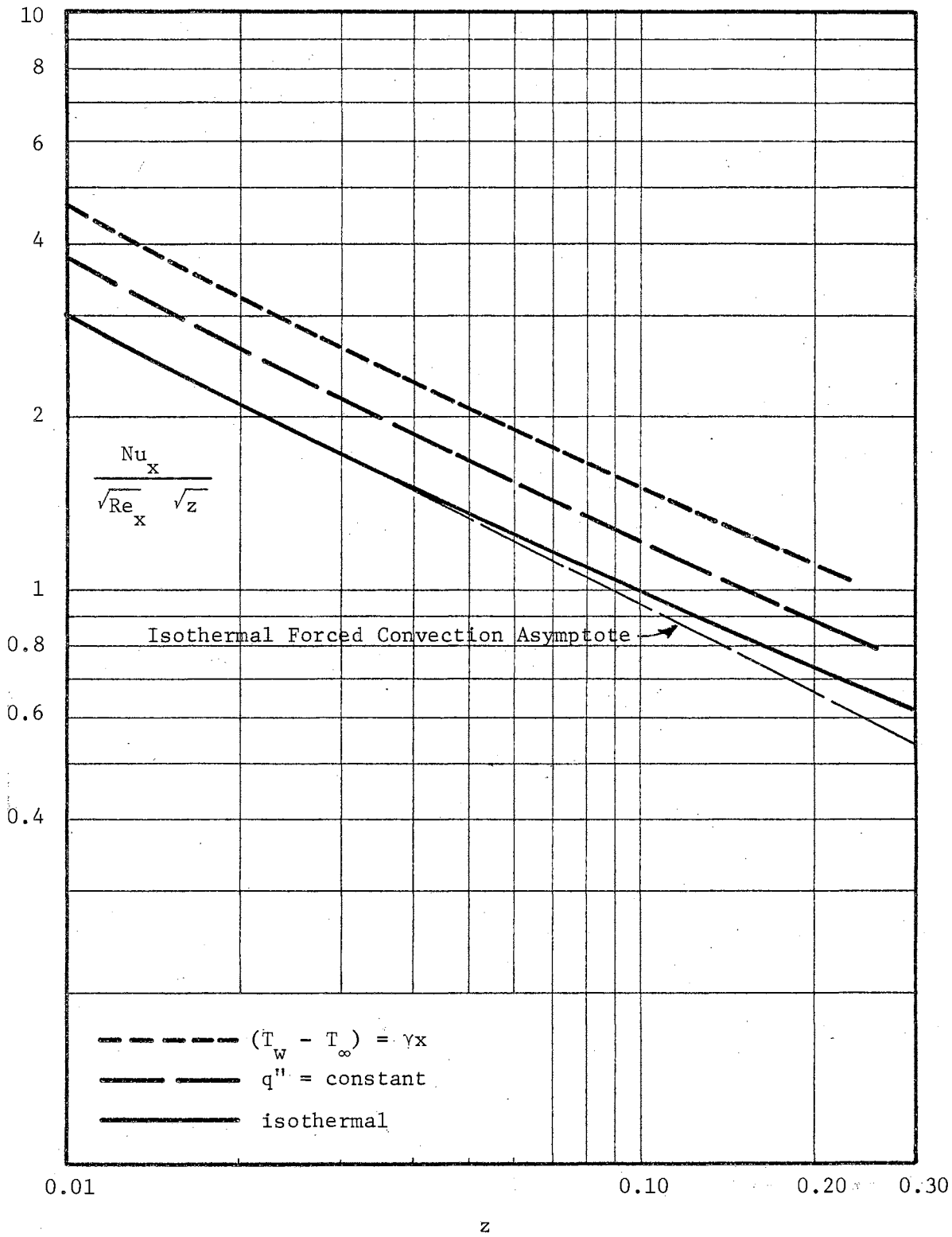

Figure 24. Comparison of Non-Isothermal Flat Plate Heat Transfer Functions With Isothermal Flat Plate, Pr = 0.73.

If Pr, Re_x, and Gr_x are based on ν_∞, the free stream viscosity, the thermal boundary layer equation and the continuity equation remain the same. The energy and momentum integral equations are the same as they were for the constant property case except for the last term in equation (64) below:

$$\frac{d}{dz}\left[\delta_2\int_0^1 f(1-f)\,d\eta\right] = -\delta_2\Delta\int_0^1 h\,d\eta_T + \frac{\nu_w}{\nu_\infty}\left(\frac{\partial u_1}{\partial y_2}\right)_w \tag{64}$$

$$\frac{d}{dz}\left[\int_0^\infty u_1\theta\,dy_2\right] = -\frac{1}{Pr}\left(\frac{\partial\theta}{\partial y_2}\right)_w . \tag{65}$$

The type of variation of viscosity with temperature has not yet been specified. In the development of equation (63) it has been assumed that fluid density is constant except in the buoyancy force term.

The simpler procedure of letting n = 1 in

$$\left.\frac{\partial^n\theta}{\partial y_2^n}\right]_{\eta_T=1} = \left.\frac{\partial^n u_1}{\partial y_2^n}\right]_{\eta=1} = 0$$

is used for illustration.

The θ boundary conditions are:

$$\left.\theta\right]_{\eta_T=1} = 0 ,$$

$$\left.\frac{\partial\theta}{\partial y_2}\right]_{\eta_T=1} = 0 ,$$

and

$$\left.\frac{\partial^2\theta}{\partial y_2^2}\right]_w = \left.\frac{\partial^3\theta}{\partial y_2^3}\right]_w = 0 ,$$

from which

$$\theta = 1 - \frac{4}{3}\eta_T + \frac{1}{3}\eta_T^4 . \tag{66}$$

The boundary conditions on u_1 are

$$u_1\Big]_{\eta=1} = 1 \,,$$

$$\frac{\partial u_1}{\partial y_2}\Big]_{\eta=1} = 0 \,,$$

$$\frac{\partial}{\partial y_2}\left(\frac{\nu}{\nu_\infty}\,\frac{\partial u_1}{\partial y_2}\right)\Big]_w = -1 \qquad (67)$$

and

$$\frac{\partial^2}{\partial y_2^2}\left(\frac{\nu}{\nu_\infty}\,\frac{\partial u_1}{\partial y_2}\right)\Big]_w = -\,\frac{\partial \theta}{\partial y_2}\Big]_w \,. \qquad (68)$$

An expansion of equation (67) gives

$$\frac{\partial}{\partial y_2}\left(\frac{\nu}{\nu_\infty}\,\frac{\partial u_1}{\partial y_2}\right)\Big]_w = \frac{\nu_w}{\nu_\infty}\,\frac{\partial^2 u_1}{\partial y_2^2}\Big]_w + \left(\frac{1}{\nu_\infty}\,\frac{d\nu}{d\theta}\,\frac{\partial \theta}{\partial y_2}\,\frac{\partial u_1}{\partial y_2}\right)\Big]_w = -1 \qquad (69)$$

A linear variation of ν with θ is now selected, in which ν increases as θ goes from 1 to 0,

$$\nu = (\nu_w - \nu_\infty)\,\theta + \nu_\infty \,.$$

Since $\frac{d\nu}{d\theta} = (\nu_w - \nu_\infty)$ and $\frac{\partial \theta}{\partial y_2}\Big]_w = -\frac{4}{3\delta_2 \Delta}$, and if we define $K = \frac{\nu_w}{\nu_\infty}$, equation (69) becomes

$$-\frac{4}{3}\,\frac{(K-1)}{\delta_2 \Delta}\,\frac{\partial u_1}{\partial y_2}\Big]_w + K\,\frac{\partial^2 u_1}{\partial y_2^2}\Big]_w + 1 = 0 \,. \qquad (70)$$

In a similar manner, equation (68) can be expanded and then simlified to

$$2(K-1)\frac{\partial^2 u_1}{\partial y_2^2}\Big]_w - \frac{3}{4}K\delta_2\Delta\frac{\partial^3 u_1}{\partial y_2^3}\Big]_w + 1 = 0 \quad . \tag{71}$$

If u_1 is written as

$$u_1 = a\eta + b\eta^2 + c\eta^3 + d\eta^4,$$

with the above boundary conditions, then

$$a = \frac{4}{3} - \frac{2}{3}b - \frac{1}{3}c$$

and

$$d = -\frac{1}{3} - \frac{1}{3}b - \frac{2}{3}c.$$

Since $\frac{\partial u_1}{\partial y_2}\Big]_w = \frac{a}{\delta_2}$, $\frac{\partial^2 u_1}{\partial y_2^2}\Big]_w = \frac{2b}{\delta_2^2}$ and $\frac{\partial^3 u_1}{\partial y_2^3}\Big]_w = \frac{6c}{\delta_2^3}$, equations (70) and (71) can be solved explicitly for the coefficients b and c in terms of δ_2, Δ, and K:

$$b = \frac{16K(K-1)\Delta - \frac{8}{9}(K-1)\delta_2^2 - 9K\Delta^2\delta_2^2}{8K(K-1)\Delta + \frac{32}{9}(K-1)^2 + 18K^2\Delta^2}$$

and

$$c = \frac{8}{9}\frac{(K-1)}{K\Delta}b + \frac{2}{9}\frac{\delta_2^2}{K\Delta}$$

For $K = 1$, these four coefficients, a, b, c, and d, reduce to the same form as those for the constant property case with n = 1.

The momentum and energy integral equations can then be evaluated to give $\frac{d\Delta}{dz}$ and $\frac{d\delta_2^2}{dz}$. The most tedious part of the solution would be the determination of Δ_0, $\frac{d\Delta}{dz}\Big]_0$, and $\frac{d\delta_2^2}{dz}\Big]_0$ by limiting processes. The differential equations for $\frac{d\Delta}{dz}$ and $\frac{d\delta_2^2}{dz}$ would be lengthy and would have to be assembled and solved on a digital computer. The computer program

given in Appendix A would apply with the statements for the new differential equations inserted between statement numbers 1000 and 100.

The solution of the variable viscosity mixed convection problem was not carried beyond this preliminary analysis. This section presents a method of solution by integral techniques and demonstrates the complexities that can arise from a slight change in the boundary layer equations. The assumption of a linear variation of viscosity with temperature would be accurate for moderate wall-to-free-stream temperature differences.

CHAPTER VI

DISCUSSION OF RESULTS

Summary and Conclusions

In Chapter I, the three major objectives of this thesis were set forth as 1) the determination of the effect of buoyancy forces on forced convection, 2) the exploration and improvement of the integral method, and 3) the investigation of the boundary layer velocity field when free and forced convection effects are competing.

A straightforward and rational approach to setting up the problem for an integral-type solution was used. That is, velocity and temperature profile expressions were both chosen as polynomials; and the polynomial coefficients were then determined strictly by the applications of the available boundary conditions. A minimum use was made of special functions and variables such as shape factors and special boundary layer thicknesses. The three prime variables, δ_2 , Δ , and Z were employed for all cases without modification of their definitions. Furthermore, only the integral equations derived directly from the boundary layer equations were employed. These simplifications make extension of the problem to other than a constant property fluid and a constant temperature flat plate somewhat easier and more understandable. By employment of the integral method in this manner to the mixed convection case of steady, laminar, vertical flow of constant property fluids over simple

vertical surfaces, new insights into boundary layer flow distributions and heat transfer phenomena for a wide range of Prandtl numbers were obtained. The main accomplishments of this study can be listed, not necessarily in order of importance, as:

(1) the determination of constant fluid property heat transfer coefficients and friction factors for Gr_x/Re_x^2 ranging from 0 to 100 for:

(a) aiding flow over a constant temperature vertical flat plate with fluid Prandtl numbers of 0.73, 10, 100, and 1000,

(b) opposing flow as in (a) for Prandtl numbers of 0.01, 0.73, 10, and 100 with the ascertainment of separation points,

and (c) aiding flow over a constant temperature vertical wedge surface with a potential flow of $U = A_1 x^{1/2}$ for fluid Prandtl numbers of 0.01 and 0.70,

(2) the development of the method of solution of the mixed convection problems of constant property fluids flowing over a vertical flat plate for:

(a) a constant plate heat flux,

and (b) a linearly varying plate temperature,

(3) the simplified solution and determination of heat transfer coefficients for the problems in (3) for a fluid of Pr = 0.73 in aiding flow over a vertical flat plate for small values of Gr_x/Re_x^2,

(4) the development of the method of solution of the mixed convection flow of high Prandtl number fluids with viscosity a linear function of temperature for an isothermal vertical flat plate,

(5) the determination of longitudinal velocity profiles for constant property fluids flowing over isothermal vertical surfaces for Prandtl numbers from 0.01 to 1000,

(6) the construction of streamline plots of the boundary layer velocity field for aiding and opposing flow of constant property fluids over a vertical isothermal plate for Prandtl numbers of 0.73, 10, 100, and 1000, and (7) the refinement of the integral method solution and ascertainment of its weaknesses and failures.

Acrivos (1958) and Kliegel (1959) have also investigated mixed convection flow and heat transfer by means of the integral method, the latperforming an experiment as well with air flowing over an isothermal flat plate. They considered only the flow of a constant property fluid over an isothermal vertical flat plate, with fluid Prandtl numbers ranging from 0.70 to 100.

Acrivos' approach was similar to the present one although he used only one "asymptotic" boundary condition on θ and two on u_1 at the boundary layer edges and did not consider the third derivatives of u_1 and θ at the wall as boundary conditions. He gave heat transfer coefficients and friction factors for Pr = 0.73, 10, and 100 in aiding and opposing flow situations. Only the results for the gas, Pr = 0.73, were satisfactory. Other Prandtl numbers resulted in discontinuous plots. He did not present velocity profiles or streamline plots.

Kliegel used the same boundary conditions as Acrivos except that he introduced a second "asymptotic" boundary condition on θ and an expression for u_1 as a polynomial in η and η_T to account for the coupling between the velocity and temperature fields in the mixed convection range. He gave heat transfer and shear stress results for fluids of Pr = 0.70, 6, and 100. His results for aiding flow for Pr = 0.70 and 100 agree with the present study although he, too, did not present velocity profile or streamline information. Kliegel's velocity profile was actu-

ally a superposition of a free convection profile upon a forced convection one and therefore could not represent the type of velocity profile found by the present method and shown in Figures 9 through 11.

Some general conclusions and observations can be made as a result of this study of mixed convection phenomena. The first is the conclusion that in the mixed convection, aiding flow regime both the heat transfer coefficient and the friction factor are greater than either free or forced convection considerations alone would predict. The mixed convection regime can be defined as the range of Gr_x/Re_x^2, or Z, over which the increases in heat transfer and friction are, say, 5 percent or more. For a gas this would be $0.15 < Z < 5$ based on heat transfer and $0.02 < Z < 20$ based on shear stress. A rule of thumb for any fluid would be to consider increasing the local heat transfer coefficient when Z is greater than 0.10 but less than 15. The heat transfer increase is greatest at the Z value where the heat transfer coefficients based on pure free and forced convection are equal, that is, at the intersection of the free and forced convection asymptotes. For fluids of $0.01 \leq Pr \leq 100$ this increase is about 25 percent but is considerably less for very high Prandtl numbers of around 1000. At this Z value the shear stress may be as much as 75 percent higher than the asymptotic values, but this fact is of less practical importance in free convection.

In opposing flow the buoyancy effect causes separation at very small values of Z; and the smaller the Prandtl number of the fluid is, the earlier the separation occurs. Prior to separation, the local shear stress and heat transfer are less than the pure forced convection values and, at separation, the local heat transfer coefficient will be about 30 percent low. This separation at low Z indicates instability and the on-

set of turbulence, and thus heating in downflow or cooling in upflow should be most effective for Z greater than one.

Figures 6 and 16 are plots of $\frac{Nu_x}{\sqrt{Re_x}\sqrt{Z}}$ versus Z. Since

$$Z = \frac{Gr_x}{Re_x^2} = \frac{|q_x| \cdot \beta \cdot |(T_w - T_\infty)|\, x}{U^2} .$$

Z is directly proportional to x for an isothermal flat plate. Also, since

$$Nu_x = \frac{hx}{k}$$

and

$$\frac{Nu_x}{\sqrt{Re_x}\sqrt{Z}} = \frac{h}{k}\left(\frac{\nu U}{|q_x| \cdot \beta \cdot |(T_w - T_\infty)|}\right)^{1/2}$$

it is seen that the local heat transfer coefficient is directly proportional to the ordinate, or heat transfer function, in these plots. Since k is large and ν is small for small Prandtl numbers, the fact that $\frac{Nu_x}{\sqrt{Re_x}\sqrt{Z}}$ is less for Pr = 0.01 than for Pr = 1000 should not be misinterpreted. For example, at Z = 0.20, a typical liquid metal with Pr = 0.01 will have a local heat transfer coefficient roughly 30 times that of an oil with a Prandtl number of 1000. The heat transfer ordinate in Figure 22 was used so that comparison could be made with the wedge results of Sparrow, Eichhorn, and Gregg (1959). It is $\frac{4Nu_x}{\sqrt{Re_x}}$, and since $U \sim x^{\frac{1}{2}}$, the local heat transfer coefficient in this plot is proportional to the ordinate divided by $x^{\frac{1}{4}}$. As noted in Chapter IV, this is also an unusual case since Z is independent of x, because again $U \sim x^{\frac{1}{2}}$ for this wedge.

In Figures 7 and 17 the ordinate, $\frac{6\tau_w}{\rho U_\infty^2}\frac{\sqrt{Re_x}}{\sqrt{Z}}$, is also directly proportional to the friction factor, $\frac{2\tau_w}{\rho U_\infty^2}$, for an isothermal flat plate. However,

$$\frac{6\tau_w}{\rho U_\infty^2}\frac{\sqrt{Re}}{\sqrt{Z}} = 3C_f\left(\frac{U_\infty^3}{2|g_x|\cdot\beta\cdot|(T_w-T_\infty)|}\right)^{1/2},$$

and therefore C_f for Pr = 0.01 is actually much less than C_f for Pr = 1000 because of the $\left(\frac{1}{2}\right)^{1/2}$ factor. Figure 7 also shows the correct relationship between wall shear stress and x in forced and free convection. As x increases in forced flow, τ_w decreases as the boundary layer thickness grows and the transverse velocity gradient, $\frac{\partial u}{\partial y}$, flattens out. Then, as x, or Z, goes into the free convection range, τ_w increases as the fluid near the wall accelerates and $\frac{\partial u}{\partial y}\Big]_w$ again becomes steeper.

Especially interesting aspects of this study are the unexpected velocity profiles and streamlines for high Prandtl number fluids in mixed convection. First of all, the velocity profiles for fluids of Pr = 0.01 and 0.73 are to be expected. The thermal boundary layer is equal to, or thicker than, the velocity boundary layer. Therefore, the buoyancy effects from heating result in a peak velocity near the wall from which the velocity decreases monotonically across the velocity boundary layer back to the free stream velocity. As Z increases, δ, the velocity boundary layer thickness, increases under the influence of the inertia and viscous forces of forced convection and the body forces of free convection until at some large value of Z the thermal and velocity boundary layer thicknesses are almost equal. Figure 8 shows that for Pr = 0.73 and Z = 5 on an isothermal vertical flat plate, u_1, or u/U_∞, is about 1.5 and at Z = 100, u_1 is about 5.75. In contrast, Figure 23 shows that for Pr = 0.01 and Z = 5 on an isothermal wedge surface, u_1 is about 2.75; and at Z = 100, u_1 has increased to almost 13. The highly

conductive and less viscous fluid responds more readily to free convection forces.

The behavior of fluids with $Pr > 1$ is very different. The forced convection thickness ratio, Δ_o, is less than 1.0 as shown in Figure 3; and the free convection thickness ratio, according to Ostrach (1953), is also considerably less than 1.0. Figures 9, 10, and 11 show mixed convection profiles for fluids of $Pr = 10$, 100, and 1000 flowing over an isothermal flat plate. For $Pr = 100$ and 1000 the velocities peak near the wall and then drop back to the forced convection profiles as y_2 increases; the free convection velocity components are not simply additive to the forced convection profiles as they appear to be in the case of $Pr < 1$. The streamlines for $Pr = 100$ show that fluid across the entire velocity boundary layer is pulled into the accelerated layer near the wall, while for $Pr = 1000$ where the free convection velocity peak is less pronounced part of the fluid is drawn towards the wall and the remainder continues about parallel to the boundary layer edge. The most extreme case is that of $Pr = 10$ where the velocity profiles show $u_1 > 1$ for $Z > 10$ with a slowing down of the fluid in the center of the boundary layer and, at $Z = 100$, the beginning of reverse flow. It is probable that if this is the true predicted situation in laminar flow, the flow would become turbulent before this point. The $Pr = 10$ streamlines show that as Z increases about half of the fluid is drawn towards the wall and the remainder is forced transversely out of the thickening boundary layer. It appears that for this Prandtl number the fluid is accelerated near the wall by buoyancy effects that do not influence the entire velocity boundary layer and the fluid is not viscous enough for all of the velocity boundary layer fluid to be drawn into the accelerated region

in an orderly manner.

There is nothing in the literature at present to verify or dispute the above phenomena. However, Morton (1959), in an exact Bessel function solution for laminar mixed convection flow in a vertical pipe with uniform wall heat flux, showed that in aiding flow a slow-up and flow reversal was possible at the center of the pipe at a Rayleigh number of 600.

The work in Chapter V on the non-isothermal flat plate concurs with previous investigators in that, for a uniform heat flux, the local Nusselt number function at a given Z is only about 12 percent higher than that for an isothermal flat plate. Although this solution was for Pr = 0.73 over a small range of Z, it may be true for all fluids for a wide range of Z. For the case of a linear increase of plate temperature with x, it was shown that the local Nusselt number function for a given Z is about 50 percent higher although the total heat transferred would be less than that for an isothermal plate of the same length and which terminated at the same Z.

With reference to the section on variable viscosity in Chapter V, it is necessary to know T_w and $(T_w - T_\infty)$ in order to select the value of $K = \frac{\nu_w}{\nu_\infty}$ for the liquid of interest. The effect of viscosity decreasing with temperature in mixed convection would be an accentuation of the velocity peaks near the wall and a decrease of the velocity boundary layer thickness. The result would be an increase in wall shear stress.

It was shown that the number of "asymptotic" boundary conditions, n, at the edges of the boundary layers had a significant effect at high Prandtl numbers; and the inclusion of the third derivative boundary con-

ditions at the wall was necessary for acceptable results. In addition, the wedge problem results were divergent with n = 2 but acceptable with n = 3. It is gratifying that the integral method worked as well as it did since integrations over Z covered two orders of magnitude or more and the equations contained a parameter, the Prandtl number, that ranged over five orders of magnitude.

Experimental Verification

Kliegel (1959) performed an experiment with a heated plate in a vertical wind tunnel and took heat transfer data for aiding flow for Z from 0.002 to 100 and for opposing flow from 0.002 to separation. Figure 25 shows the good agreement between theory and experiment for Pr = 0.70. Kliegel's theory predicted a separation point for air of Z = 0.26 and the experiment showed it to be at 0.17. The present theory predicts separation at Z = 0.20.

Experiments with viscous fluids would be more difficult because of more complicated equipment requirements; and, in order to interpret the results, the variable viscosity problem would first have to be solved. In order to achieve reasonably high Z values in laminar flow with a moderate $(T_w - T_\infty)$, the free stream velocity would have to be very low, on the order of 0.25 feet per second. As an example, ethylene glycol at $T_\infty = 68^\circ F$, $(T_w - T_\infty) = 36^\circ F$, $U_\infty = 0.25$ ft/sec, $\beta = 0.36 \times 10^{-3}$, and g = 32.2 ft/sec gives

$$Z = \frac{g\beta (T_w - T_\infty) x}{U_\infty^2} = 6.18x$$

A plate length, x, of 4 feet would give a maximum Z of about 25 which would be adequate to obtain velocity profiles that might show a

peak near the plate and then a decrease to below U_∞ as in Figure 10. However, over this $(T_w - T_\infty)$ range, Pr would vary from 94 at the wall to 204 at the edge of the thermal boundary layer, primarily because of viscosity change.

Suggestions for Extensions

Suggested extensions of the present investigation are listed below numerically:

(1) Non-Isothermal Vertical Flat Plate:

The two cases investigated briefly in this study, uniform wall heat flux and linearly varying wall temperature, might be solved with all available boundary conditions and w and v factors (if necessary) for a wide range of Pr and Z.

(2) Variable Viscosity:

A complete analytical study of the effects of viscosity as a function of temperature in the boundary layer for high Prandtl number liquids for a wide range of Gr_x/Re_x^2 should be made.

(3) Experimental Work:

After (2) above an experiment with liquids as mentioned in the preceding section would be worthwhile.

(4) Isothermal Flat Plate:

An analytical study could be made to determine if fourth derivative boundary conditions at the wall and at the boundary layer edge would contribute to the stability of the solution at high and low Prandtl numbers, and further numerical experimentation could be undertaken to study the effect of the v and w factors of Chapter III.

(5) Other Geometries:

The approximate solution for the wedge was about 10 percent off of the known exact similarity solution. If a way were found to match the integral solution to the exact solution, the method could be confidently extended to other geometries.

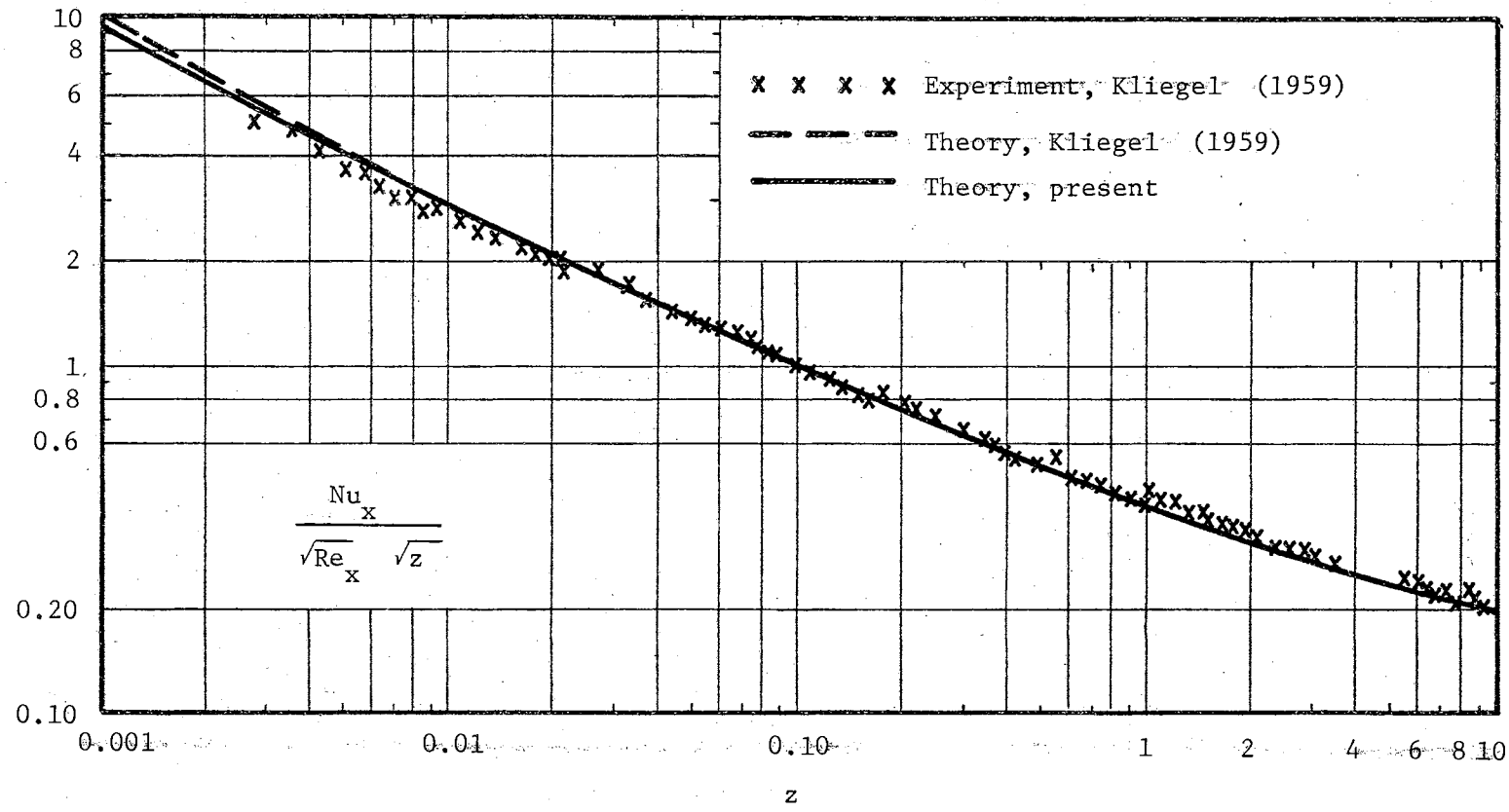

Figure 25. Heat Transfer Function, Isothermal Flat Plate, Comparison of Experiment With Theory, Pr = 0.73.

SELECTED BIBLIOGRAPHY

Acrivos, Andreas. "Combined Laminar Free- and Forced-Convection Heat Transfer in External Flows." American Institute of Chemical Engineering Journal, IV (September, 1958), 285-89.

Agrawal, H. C. "A Variational Method for Combined Free and Forced Convection in Channels." International Journal of Heat and Mass Transfer, V (1962), 439-44.

Brindley, J. "An Approximation Technique for Natural Convection in a Boundary Layer." International Journal of Heat and Mass Transfer, VI (1963), 1035-48.

Chang, K. S., R. G. Akins, L. Burris, Jr., and S. G. Bankoff. "Free Convection of a Low Prandtl Number Fluid in Contact with a Uniformly Heated Vertical Plate." Argonne National Laboratory Report 6835, January, 1964.

Eckert, E. R. G., and A. J. Diaguila. "Grashof and Reynolds Numbers for Mixed Convection Flow in a Vertical Tube." Transactions of the American Society of Mechanical Engineers, LXXVI (1954), 497-504.

_____, and Robert M. Drake, Jr. Heat and Mass Transfer. New York: McGraw-Hill Book Company, Inc., 1959.

Gebhart, Benjamin. Heat Transfer. New York: McGraw-Hill Book Company, Inc., 1961.

Gill, William N., and Eduardo Del Casal. "A Theoretical Investigation of Natural Convection Effects in Forced Horizontal Flows." American Institute of Chemical Engineering Journal, VIII (September, 1962), 513-18.

Hugelman, Rodney D. Letter to Dr. D. R. Haworth, Oklahoma State University, 23 September 1964.

Kliegel, James R. "Laminar Free and Forced Convective Heat Transfer from a Vertical Flat Plate." Ph. D. dissertation, University of California, 1959.

Mori, Yasuo. "Buoyancy Effects in Forced Laminar Convection Flow over a Horizontal Flat Plate." Journal of Heat Transfer, LXXXIII (November, 1961), 479-82.

Morton, B. R. "Laminar Convection in Uniformly Heated Pipes." Journal of Fluid Mechanics, VIII (May-August, 1960), 227-40.

Ostrach, Simon. "An Analysis of Laminar Free-Convection Flow and Heat Transfer about a Flat Plate Parallel to the Direction of the Generating Body Force." NACA Report 1111, 1953.

Ralston, Anthony, and Herbert S. Wilf. Mathematical Methods for Digital Computers. New York: John Wiley and Sons, Inc., 1960.

Rosen, Edward M., and Thomas J. Hanratty. "Use of Boundary-Layer Theory to Predict the Effect of Heat Transfer on the Laminar-Flow Field in a Vertical Tube with a Constant-Temperature Wall." American Institute of Chemical Engineering Journal, VII (March, 1961), 112-23.

Schlichting, Hermann. Boundary Layer Theory. Tr. J. Kestin. New York: McGraw-Hill Book Company, Inc., 1960.

Sparrow, E. M. "Laminar Free Convection on a Vertical Plate with Prescribed Nonuniform Wall Heat Flux or Prescribed Nonuniform Wall Temperature." NACA Technical Note 3508, 1955.

_____, R. Eichhorn, and J. L. Gregg. "Combined Forced and Free Convection in a Boundary Layer Flow." The Physics of Fluids, II (May-June, 1959), 319-28.

_____, and J. L. Gregg. "Laminar Free Convection from a Vertical Plate with Uniform Surface Heat Flux." Transactions of the American Society of Mechanical Engineers, LXXVIII (February, 1956), 435-40.

_____, and _____. "The Variable Fluid-Property Problem in Free Convection." Transactions of the American Society of Mechanical Engineers, LXXX (1958), 379-86.

_____, and _____. "Buoyancy Effects in Forced-Convection Flow and Heat Transfer." Transactions of the American Society of Mechanical Engineers, LXXXI, Series E (1959), 133.

APPENDIX A

COMPUTER PROGRAMS

The two differential equations in $\frac{d\delta_2^2}{dz}$ and $\frac{d\Delta}{dz}$ were solved explicitly for $\frac{d\delta_2^2}{dz}$ and $\frac{d\Delta}{dz}$ in terms of δ_2^2, Δ, Pr, and Z. These two simultaneous ordinary differential equations were then solved numerically on Oklahoma State University's IBM-1410 digital computer.

The final computer program evolved from one written for the Oklahoma State University IBM-1620. This first program used a simple Runge-Kutta method of integration. In order to speed up the caculations, the first program was rewritten in Fortran IV for the 1410. In its ultimate form the program employed a Runge-Kutta starter routine, a Milne predictor-corrector, four-point, step-by-step integration and an automatically varied increment in the independent variable.

The Milne predictor-corrector program with variable increment allowed a continual check on the relative error incurred at each step and was significantly faster, even without the variable increment feature, than the straight Runge-Kutta integration.

One version of the final integration program is included in this appendix. With variations this basic program was used for all of the different cases that were solved: $\Delta < 1$, $\Delta > 1$, aiding and opposing flow, etc. At Z = 0, $\frac{d\Delta}{dz}$ can be found only by a limiting process and must therefore be read in. The MON$$ statements signify monitor control peculiar to the 1410 PR-155 control system which directs the

computer to load the Fortran processor and compile the Fortran statements into machine language.

The basic forma of the predictor-corrector equations are

$$y_{i+1} = y_{i-3} + \frac{4h}{3}(2f_{i-2} - f_{i-1} + 2f_i) \qquad \text{(predictor)}$$

$$y_{i+1} = y_{i-1} + \frac{h}{3}(f_{i-1} + 4f_i + f_{i+1}) \qquad \text{(corrector)}$$

The value of y_{i+1} from the predictor equation is used to find a value of f_{i+1} which is then used in the corrector equation to give the final y_{i+1}, from which the final f_{i+1} is calculated. The corrector equation is Simpson's one-third rule. The relative error in y_{i+1} is proportional to the difference between the predicted and the corrected value.

With initial values of the two variables and the two derivatives given or calculated, the next three points are found by the Runge-Kutta method. These four consecutive values of the dependent variables are then used to find the fifth one by the Milne equations. The error term is checked after this calculation, and if it is within the preset limits the integration continues via the Milne equations. If the error term is too large, the integration sets back four increments in the independent variable, divides the present increment by two, and restarts with the Runge-Kutta equations.

The error term must be too small for four successive steps before the increment is doubled and the integration restarted. However, an error term too large will immediately cause the program to back up, decrease the increment, and restart. If the step preceding the one in which a too-large error is detected is a Milne computation, the program

goes back to that point to restart instead of going back four points as it does when the error is too large in the step immediately after a Runge-Kutta start or restart.

The maximum and minimum error tolerances used most frequently were 2×10^{-6} and 2×10^{-8}, respectively. The choice depends on the accuracy desired. These relatively stringent limits in some cases automatically allowed a step size or increment as large as 12.0. In other cases, with the same limits but more difficult equations, the step size was automatically restrained to 1×10^{-6} for a wide range of Z. The program stops when the step size becomes less than a preset lower limit.

The program also caculates and prints a Nusselt number function and a friction factor function (GNU and TAU) each time the values of δ_z^2 and $\triangle$ are printed. Asnwers are read out at each Nth calculation, N being a number preselected for a particular run. In addition, the values of the error terms, the integration increment, the two derivatives, the common denominator of the two explicit differential equations, and the numerator of each differential equation are printed with the answers. The latter items are useful in checking on the trend and stability of the integrations.

The data for the velocity profile and streamline plots were also obtained with the aid of the 1410. A sample program that caculates η, y_1, y_2, u_1, v_1, and v_2 for a given Prandtl number, Z, δ_z^2, and $\triangle$ is also included in this appendix.

Roots of the polynomials in $\triangle_o$ were found on the IBM-1620. General programming information was found in Ralston and Wilf (1960).

Major Fortran symbols that were employed are:

H = interval of integration

Y1, YY1 = δ_z^2

Y2, YY2 = Δ

P = Pr

D1, DD1 = $\frac{d\delta_z^2}{dz}$

D2, DD2 = $\frac{d\Delta}{dz}$

VBL = δ_z

DEL = Δ

TAU = $\frac{\tau_w}{\rho U_\infty^2}\sqrt{Re_x}\sqrt{\frac{Re_x^2}{Gr_x}}$

GNU = $\frac{Nu_x}{\sqrt{Re_x}}\sqrt{\frac{Re_x^2}{Gr_x}}$

Sample Integration Program

```
      MON$$     JOB  252740032 (INTEGRATION CASE IIIBPC/VH)
      MON$$     ASGN MJB,A2
      MON$$     ASGN MGO,A3
      MON$$     ASGN MW1,A4
      MON$$     ASGN MW2,A5
      MON$$     MODE GO,TEST
      MON$$     EXEQ FORTRAN,SOF,SIU,10,05,,,CASEIIIBPC
       DIMENSION D1(5),D2(5),Y2(5),Y1(5)
500    FORMAT (48X,36HMIXED CONVECTION PROBLEM CASE IIIBPC//)
501    FORMAT (38x,58HFLAT PLATE, CONSTANT PROPERTIES, CONSTANT WALL TEMP
     1ERATURE
502    FORMAT (54x,24HDONALD H ASIRE    MECHEN/)
503    FORMAT(I3,3E9.3,2E14.8)
504    FORMAT (2E14.8,F7.2,2E9.3,E14.8)
505    FORMAT (15X,26H    INITIAL CONDITIONS ARE/20X,2HZ=,F8.4,2X,3HY1=,E
     114.8,4X,3HY=2,E14.8,4X,3HD1=,E14.8,4X,3HD2=,E14.8)
506    FORMAT (15X,10HINTERVAL =,E14.8,5X,11HZ MAXIMUM =,E9.3)
507    FORMAT (15X,28HANSWERS ARE PRINTED AT EVERY,I5,14TH CALCULATION)
508    FORMAT (15X,16HPRANDTL NUMBER =,F7.2,10X,9HZ CHECK =,E14.8//)
509    FORMAT (5X,1HZ,8X,3HVBL,11X,3HDEL,10X,3HTAU,7X,3HGNU,9X,2HD1,13X,2
     1HD2,13X,5HDENOM,10X,4HNUM1,10X,4HNUM2/)
510    FORMAT(1X,E10.4,E14.7,E14.8,2E10.3,4E15.8,E14.7)
511    FORMAT (11X,6HERR1 =,E10.4,5X,6HERR2 =,E10.4,5X,3HH =,E10.4)
512    FORMAT (1X,16HDENOMINATOR ZERO)
513    FORMAT (1X,11HRESTART R-K)
514    FORMAT(1X,E10.4,E14.7,E14.8,2E10.3,5X,3HH =,E10.4)
       WRITE(3,500)
       WRITE(3,501)
       WRITE(3,502)
1      READ(1,503)N,H,ZMAX,Z,VBL,Y2(1)
       Y1(1)=VBL**2
```

```
      READ(1,504)D1(1),D2(1),P,ERMIN,ERMAX,ZCK
      WRITE(3,505)Z,Y1(1),Y2(1),D1(1),D2(1)
      WRITE(3,506)H,ZMAX
      WRITE(3,507)N
      WRITE(3,508)P,ZCK
      WRITE(3,509)
      B=SQRT(0.5)
      K=0
      M=0
5     K=K+4
      IF(H.LT..1E-09)GO TO 1
      DO 33 J=2,4
      L=1
      Y1(J)=Y1(J-1)+0.5*H*D1(J-1)
      Y2(J)=Y2(J-1)+0.5*H*D2(J-1)
      Q1=H*D1(J-1)
      Q2=H*D2(J-1)
      Z=Z+H/2.
      YY1=Y1(J)
      YY2=Y2(J)
      GO TO 1000
15    D1(J)=DD1
      D2(J)=DD2
      A=1.-B
      Y1(J)=Y1(J)+A*(H*D1(J)-Q1)
      Y2(J)=Y2(J)+A*(H*D2(J)-Q2)
      Q1=2.*A*H*D1(J)+(1.-3.*A)*Q1
      Q2=2.*A*H*D2(J)+(1.-3.*A)*Q2
      L=2
      YY1=Y1(J)
      YY2=Y2(J)
      GO TO 1000
20    D1(J)=DD1
      D2(J)=DD2
      A=1.+B
      Y1(J)=Y1(J)+A*(H*D1(J)-Q1)
      Y2(J)=Y2(J)+A*(H*D2(J)-Q2)
      Q1=2.*A*H*D1(J)+(1.-3.*A)*Q1
      Q2=2.*A*H*D2(J)+(1.-3.*A)*Q2
      Z=Z+H/2.
      L=3
      YY1=Y1(J)
      YY2=Y2(J)
      GO TO 1000
25    D1(J)=DD1
      D2(J)=DD2
      Y1(J)=Y1(J)+(1./6.)*(H*D1(J)-2.*Q1)
      Y2(J)=Y2(J)+(1./6.)*(H*D2(J)-2.*Q2)
      L=4
      YY1=Y1(J)
      YY2=Y2(J)
      GO TO 1000
30    D1(J)=DD1
```

```
      D2(J)=DD2
      VBL=SQRT(Y1(J))
      DEL=Y2(J)
      TAU=(2./VBL)+.2*VBL-(1./30.)*(VBL/DEL)
      GNU=2./(VBL*DEL)
      IF(J.EQ.2)WRITE(3,513)
      WRITE(3,514)Z,VBL,DEL,TAU,GNU,H
33    CONTINUE
      I=0
34    Z=Z+H
      L=5
      Y1(5)=Y1(1)+(4./3.)*H*(2.*D1(2)-D1(3)+2.*D1(4))
      Y2(5)=Y2(1)+(4./3.)*H*(2.*D2(2)-D2(3)+2.*D2(4))
      Y15A=Y1(5)
      Y25A=Y2(5)
      YY1=Y1(5)
      YY2=Y2(5)
      GO TO 1000
70    D1(5)=DD1
      D2(5)=DD2
      Y1(5)=Y1(3)+(H/3.)*(D1(3)+4.*D1(4)+D1(5))
      Y2(5)=Y2(3)+(H/3.)*(D2(3)+4.*D2(4)+D2(5))
      ERR1=(1./29.)*(Y15A-Y1(5))
      ERR2=(1./29.)*(Y25A-Y2(5))
      L=6
      YY1=Y1(5)
      YY2=Y2(5)
      GO TO 1000
72    D1(5)=DD1
      D2(5)=DD2
      ERRAB=ABS(ERR1)+ABS(ERR2)
      IF(Z.LT..01)GO TO 61
      IF(ABS(DD1)+ABS(DD2).GT.200.)GO TO 90
61    IF(Z.LT.ZCK)GO TO 71
      IF(ERRAB.GT.ERMAX)GO TO 100
71    IF(K.GE.N)GO TO 80
      K=K+1
75    DO 76 J=1,4
      Y1(J)=Y1(J+1)
      Y2(J)=Y2(J+1)
      D1(J)=D1(J+1)
76    D2(J)=D2(J+1)
      I=I+1
      IF(ERRAB.LT.ERMIN)GO TO 150
      M=0
      GO TO 34
80    VBL =SQRT(Y1(5))
      DEL=Y2(5)
      TAU =(2./VBL)+.2*VBL-(1./30.)*(VBL/DEL)
      GNU=2./(VBL*DEL)
      WRITE(3,510)Z,VBL,DEL,TAU,GNU,DD1,DD2,DENOM,UM1,UM2
      WRITE(3,511)ERR1,ERR2,H
      IF(Z.GE.ZMAX)GO TO 1
```

```
      IF(Z.LT..01)GO TO 85
      IF(ABS(DD1)+ABS(DD2).GT.200.)GO TO 1
85    K=1
      GO TO 75
90    WRITE(3,512)
      GO TO 80
1000  R1=YY2
      R2=YY2**2
      R3=YY2**3
      R4=YY2**4
      R5=YY2**5
      R6=YY2**6
      R7=YY2**7
      R8=YY2**8
      T1=YY1
      T2=YY1**2
      T3=YY2**3
      H1=-.28571429+.28571429*R1+.11904762/R1-.02020202/R4+.01298704/R5-
     1.0024975023/R6
      H2=.0095238096-.083333333/R1+.0015873016/R2+.0014430014/R4-.001394
     19014/R5+.00048285048/R6-.000058275058/R7
      DH1=.28571429-.11904762/R2+.080808081/R5-.0649352/R6+.014985014/R7
      DH2=.0083333333/R2-.0031746032/R3-.0057720056/R5+.006974507/R6-.00
     128971029/R7+.00040792541/R8
      A2=4./(R1*P)
      B2=-(H1+3.*T1*H2)
      C2=2.*T1*DH1+2.*T2*DH2
      A1=-.57142857*T1*R1+4.+.4*T1-.066666667*T1/R1
      B1=.0008251009*T2/R2+.00015281017*T3/R2-.000037986712*T3/R3
      C1=.10933511-.0031635034*T1-.00077700068*T2+.0012376514*T1/R1+.000
     138202542*T2/R1-.000047483389*T2/R2
      UM1=A1*C2+A2*B1
      UM2=A2*C1+A1*B2
      DENOM=C1*C2-B1*B2
      DD1=UM1/DENOM
      DD2=UM2/DENOM
      GO TO (15,20,25,30,70,72),L
100   IF(I.GE.1)GO TO 110
      IF(I.LT.1)GO TO 115
110   M=0
      Z=Z-H
      H=H/2.
      Y1(1)=Y1(4)
      Y2(1)=Y2(4)
      D1(1)=D1(4)
      D2(1)=D2(4)
      GO TO 5
115   M=0
      Z=Z-4.*H
      H=H/2.
      GO TO 5
150   M=M+1
      IF(M.GE.4)GO TO 155
```

```
      GO TO 34
155   M=0
      H=2.*H
      Y1(1)=Y1(4)
      Y2(1)=Y2(4)
      D1(1)=D1(4)
      D2(1)=D2(4)
      GO TO 5
      END
     MON$$      EXEQ LINKLOAD
                PHASEENTIREPGM
                CALL CASEIIIBPC
     MON$$      EXEQ ENTIREPGM,MJB
```

Sample Velocity Program

```
     MON$$      JOB  252740032 (VELOCITY PROFILES CASE III)
     MON$$      ASGN MJB,A2
     MON$$      ASGN MGO,A3
     MON$$      ASGN MW1,A4
     MON$$      ASGN MW2,A5
     MON$$      MODE GO,TEST
     MON$$      EXEQ FORTRAN,SOF,SIU,,,,,VELPROIII
C     D H ASIRE  MECHEN      VELOCITY PROFILES CASE III
C     ETA = Y/DELTA
C     YSUB1 = (Y/X)*SQRT(REX)
C     YSUB2=YSUB1*SQRT(Z)
C     USUB1=(U/U INFINITY)
C     VSUB1=(V/U INFINITY)*SQRT(REX)
C     VSUB2=(VSUB1)/SQRT(Z)
C     PLOT USUB1 VS YSUB1
C     PLOT VSUB1 VS YSUB1
C     SEE SCHLICHTING PG 120
500   FORMAT(53X,27HVELOCITY PROFILES, CASE III)
501   FORMAT(4E14.8,2F7.2)
502   FORMAT(54X,23HDONALD H ASIRE   MECHEN//)
503   FORMAT(1HL,9X,20HINPUT CONDITIONS ARE)
504   FORMAT (12X,4HVBL=,E14.8,5X,3HY2=,E14.8)
505   FORMAT (13X,3HD1=,E14.8,5X,3HD2=,E14.8)
506   FORMAT (13X,3HPR=,F8.2,6X,2HZ=,F10.4)
507   FORMAT(10X,F5.2,5E20.8)
508   FORMAT(11X,3HETA,10X,7HY-SUB-1,13X,7HY-SUB-2,13X,7HU-SUB-1,13X,7HV
     1-SUB-1,13X,7HV-SUB-2)
      WRITE(3,500)
      WRITE(3,502)
1     READ(1,501)VBL,Y2,D1,D2,P,Z
      WRITE(3,503)
      WRITE(3,504)VBL,Y2
      WRITE(3,505)D1,D2
      WRITE(3,506)P,Z
      WRITE(3,508)
```

```
      Y1=VBL**2
      QUOD=(Y2*D1-Y1*D2)/(Y2**2)
      AA=.2*D1-(1./30.)*QUOD
      BB=-.5*D1
      CC=(1./3.)*QUOD
      DD=D1-(2./3.)*QUOD
      EE=-D1+.5*QUOD
      FF=.3*D1-.13333333*QUOD
      DELTA=Y2
      A=2.+0.2*(VBL**2)-0.0333333*(VBL**2)/(DELTA)
      B=-0.5*(VBL**2)
      C=0.333333*(VBL**2)/(DELTA)
      D=-5.+(VBL**2)-0.666667*(VBL**2)/(DELTA)
      E=6.-(VBL**2)+0.5*(VBL**2)/(DELTA)
      F=-2.+0.3*(VBL**2)-0.133333*(VBL**2)/(DELTA)
      ETA=0.0
      YSUB1=0.0
      YSUB2=0.0
      U=0.0
      VSUB1=0.0
      VSUB2=0.0
      WRITE(3,507)ETA,YSUB1,YSUB2,U,VSUB1,VSUB2
10    ETA=ETA+0.02
      YSUB2=ETA*VBL
      YSUB1=YSUB2/(SQRT(Z))
      VA=(AA/2.)*(ETA**2)+(BB/3.)*(ETA**3)+(CC/4.)*(ETA**4)
      VB=(DD/5.)*(ETA**5)+(EE/6.)*(ETA**6)+(FF/7.)*(ETA**7)
      VC=(A/2.)*(ETA**2)+(2./3.)*B*(ETA**3)+.75*C*(ETA**4)+.8*D*(ETA**5)
     1+(5./6.)*E*(ETA**6)+(6./7.)*F*(ETA**7)
      VSUB2=-VBL*(VA+VB)+(.5/VBL)*D1*VC
      VSUB1=SQRT(Z)*VSUB2
      U1=A*ETA+B*(ETA**2)+C*(ETA**3)+D*(ETA**4)
      U2=E*(ETA**5)+F*(ETA**6)
      U=U1+U2
      WRITE(3,507)ETA,YSUB1,YSUB2,U,VSUB1,VSUB2
      IF(ETA.LT.1.)GO TO 10
      IF(ETA.GE.1.)GO TO 1
      END
     MON$$      EXEQ LINKLOAD
                PHASEENTIREPGM
                CALL VELPROIII
     MON$$      EXEQ ENTIREPGM,MJB
```

APPENDIX B

TRANSFORMATION OF THE BOUNDARY LAYER EQUATIONS

The constant property, steady state, two-dimensional, boundary layer equations for incompressible flow are:

$$u\frac{\partial u}{\partial x} + v\frac{\partial u}{\partial y} = g_x\beta(T-T_\infty) + U\frac{dU}{dx} + \nu\frac{\partial^2 u}{\partial y^2}$$

$$u\frac{\partial T}{\partial x} + v\frac{\partial T}{\partial y} = \frac{k}{\rho g c_p}\frac{\partial^2 T}{\partial y^2}$$

$$\frac{\partial u}{\partial x} + \frac{\partial v}{\partial y} = 0$$

The following two sets of transformations are those used by Acrivos (1958). The first set is:

$$\begin{aligned}
u_1 &= \frac{u}{U_\infty} && \Rightarrow && u = u_1 \cdot U_\infty \\
v_1 &= \frac{v}{U_\infty}\sqrt{Re} && \Rightarrow && v = \frac{v_1 U_\infty}{\sqrt{Re}} \\
x_1 &= \frac{x}{L} && \Rightarrow && x = x_1 \cdot L \\
y_1 &= \frac{y}{L}\sqrt{Re} && \Rightarrow && y = \frac{y_1 L}{\sqrt{Re}} \\
U_1 &= \frac{U}{U_\infty} && \Rightarrow && U = U_1 U_\infty \\
\Theta &= \frac{T-T_\infty}{T_w-T_\infty} && \Rightarrow && T = \Theta(T_w-T_\infty)+T_\infty
\end{aligned} \qquad \text{(B1)}$$

Re is the Reynolds number based on the local free stream velocity,

$$Re = \frac{UL}{\nu}$$

Substitution of these transforming equations into the boundary layer equation yields

$$u_1 U_\infty \frac{\partial(u_1 U_\infty)}{\partial(x_1 L)} + \frac{\nu_1 U_\infty}{\sqrt{Re}} \frac{\partial(u_1 U_\infty)}{\partial\left(\frac{y_1 L}{\sqrt{Re}}\right)}$$

$$= g_x \beta (T_w - T_\infty)\theta + U_1 U_\infty \frac{d(U_1 U_\infty)}{dx_1 L} + \nu \frac{\partial^2(u_1 U_\infty)}{\partial\left(\frac{y_1 L}{\sqrt{Re}}\right)^2}$$

or

$$\frac{U_\infty^2}{L}\left(u_1 \frac{\partial u_1}{\partial x_1} + \nu_1 \frac{\partial u_1}{\partial y_1}\right) = g_x \beta (T_w - T_\infty)\theta$$

$$+ \frac{U_\infty^2}{L} U_1 \frac{dU_1}{dx_1} + \frac{Re}{L^2} U_\infty \cdot \nu \frac{\partial^2 u_1}{\partial y_1^2}$$

This further reduces to

$$u_1 \frac{\partial u_1}{\partial x_1} + \nu_1 \frac{\partial u_1}{\partial y_1} = g_x \beta (T_w - T_\infty) \frac{L}{U_\infty^2} \cdot \frac{U^2}{U^2}\theta$$

$$+ U_1 \frac{dU_1}{dx_1} + Re \frac{\nu}{U_\infty L} \cdot \frac{U}{U} \cdot \frac{\partial^2 u_1}{\partial y_1^2}$$

or

$$u_1 \frac{\partial u_1}{\partial x_1} + \nu_1 \frac{\partial u_1}{\partial y_1} = \frac{g_x \beta (T_w - T_\infty) L}{U^2} U_1^2 \theta$$

$$+ U_1 \frac{dU_1}{dx_1} + U_1 \frac{\partial^2 u_1}{\partial y_1^2} \qquad \text{(B2)}$$

The Grashof number is

$$Gr = \frac{|g_x| \cdot \beta \cdot |(T_w - T_\infty)| \, L^3}{\nu^2}$$

If the Grashof number is divided by the square of the Reynolds number, the result is $\frac{Gr}{Re^2} = \frac{|g_x| \cdot \beta \cdot |(T_w - T_\infty)| \, L^3 \nu^2}{\nu^2 U^2 L^2}$

or $$\frac{Gr}{Re^2} = \frac{|g_x| \cdot \beta \cdot |(T_w - T_\infty) L}{U^2} .$$

The boundary layer equation was written so that a positive pressure gradient or a gravity force or acceleration vector in the opposite direction to fluid flow would produce body forces opposing the flow. Since the Grashof number with its absolute value signs is always positive, a ± pair of signs must precede the Gr/Re^2 term when it is placed in the momentum equation as the coefficient of the $U_1^2\theta$ term. Thus a minus sign indicates either that $T_\infty > T_w$ or g_x acts with the flow. Either situation is called "opposing" flow. The boundary layer equation with this substitution becomes

$$u_1 \frac{\partial u_1}{\partial x_1} + v_1 \frac{\partial u_1}{\partial y_1} = \pm \frac{Gr}{Re^2} U_1^2 \theta + U_1 \frac{dU_1}{dx_1} + \nu \frac{\partial^2 u_1}{\partial y_1^2} . \qquad (B3)$$

A second set of transformations takes this equation into the form that will be used in this thesis:

$$Z = x_1 \frac{Gr}{Re^2} \quad \Rightarrow \quad x_1 = Z \frac{Re^2}{Gr}$$

$$y_2 = y_1 \sqrt{\frac{Gr}{Re^2}} \quad \Rightarrow \quad y_1 = y_2 \sqrt{\frac{Re^2}{Gr}} \qquad (B4)$$

$$v_2 = v_1 \sqrt{\frac{Re^2}{Gr}} \quad \Rightarrow \quad v_1 = v_2 \sqrt{\frac{Gr}{Re^2}}$$

Substitution of these equations for v_1, y_1, and x_1 gives:

$$u_1 \frac{\partial u_1}{\partial\left(z \cdot \frac{Re^2}{G\nu}\right)} + v_2 \sqrt{\frac{G\nu}{Re^2}} \frac{\partial u_1}{\partial\left(y_2 \sqrt{\frac{Re^2}{G\nu}}\right)} = \pm \frac{G\nu}{Re^2} U_1^2 \theta$$

$$+ U_1 \frac{dU_1}{d\left(z \frac{Re^2}{G\nu}\right)} + U_1 \frac{\partial^2 u_1}{\partial\left(y_2 \sqrt{\frac{Re^2}{G\nu}}\right)^2}$$

or

$$u_1 \frac{\partial u_1}{\partial z} + v_2 \frac{\partial u_1}{\partial y_2} = \pm U_1^2 \theta + U_1 \frac{dU}{dz} + U_1 \frac{\partial^2 u_1}{\partial y_2^2} \tag{1}$$

The thermal boundary layer equation, after the first set of substitutions for T, u, v, x, and y, is

$$u_1 U_\infty \frac{\partial\left[(T_w - T_\infty)\theta + T_\infty\right]}{\partial(x_1 L)} + \frac{v_1 U_\infty}{\sqrt{Re}} \frac{\partial\left[(T_w - T_\infty)\theta + T_\infty\right]}{\partial\left(\frac{y_1 L}{\sqrt{Re}}\right)}$$

$$= \alpha \frac{\partial^2\left[(T_w - T_\infty)\theta + T_\infty\right]}{\partial\left(\frac{y_1 L}{\sqrt{Re}}\right)^2}, \tag{B5}$$

where $\alpha = \frac{k}{\rho g c_p}$.

If T_w is constant, this reduces to

$$\frac{U_\infty}{L}\left(u_1 \frac{\partial\theta}{\partial x_1} + v_1 \frac{\partial\theta}{\partial y_1}\right) = \frac{\alpha Re}{L^2} \frac{\partial^2\theta}{\partial y_1^2}$$

$$= \frac{\alpha U}{\nu L} \frac{\partial^2\theta}{\partial y_1^2}.$$

Since $\frac{\nu}{\alpha}$ = Pr, the Prandtl number, the final equation is

$$u_1 \frac{\partial\theta}{\partial x_1} + v_1 \frac{\partial\theta}{\partial y_1} = \frac{U_1}{Pr} \frac{\partial^2\theta}{\partial y_1^2} \tag{B6}$$

The second set of substitutions for x_1, y_1, and v_1 gives

$$\frac{G\nu}{Re^2} u_1 \frac{\partial\theta}{\partial z} + \frac{G\nu}{Re^2} v_2 \frac{\partial\theta}{\partial y_2} = \frac{U_1}{Pr} \frac{\partial^2\theta}{\partial y_2^2} \frac{G\nu}{Re^2},$$

or

$$u_1 \frac{\partial \theta}{\partial z} + v_2 \frac{\partial \theta}{\partial y_2} = \frac{U_1}{Pr} \frac{\partial^2 \theta}{\partial y_2^2} \qquad (2)$$

The continuity equation after two sets of transformation substitutions is unchanged in form but has new variables:

$$\frac{\partial u_1}{\partial z} + \frac{\partial v_2}{\partial y_2} = 0 \; . \qquad (3)$$

It is convenient to replace L by x in all of the previous definitions and equations so that parameters can be based on local coordinates. Then Gr becomes Gr_x and Re becomes Re_x:

$$Gr_x = \frac{|q_x| \cdot \beta \cdot |(T_w - T_\infty)| \, x^3}{\nu^2}$$

$$Re_x = \frac{U x}{\nu}$$

$$\frac{Gr_x}{Re_x^2} = \frac{|q_x| \cdot \beta \cdot |(T_w - T_\infty)| \, x}{U^2}$$

The last expression shows that for a flat plate, for which $U = U_\infty$, Gr_x/Re_x^2 is directly proportional to x.

Since

$$Z = x_1 \frac{Gr}{Re^2}$$

and now

$$x_1 = \frac{x}{L} = 1 \; ,$$

then

$$Z = \frac{Gr_x}{Re_x^2} \; .$$

With this replacement of L by x, it is also noteworthy that

$$v_2 = v_1 \sqrt{\frac{Re_x^2}{Gr_x}} = \frac{\nu}{U_\infty} \sqrt{Re_x} \sqrt{\frac{Re_x^2}{Gr_x}}$$

$$v_2 = \left(\frac{U^3}{2 |q_x| \cdot \beta \cdot |(T_w - T_\infty)|} \right)^{1/2} \frac{\nu}{U_\infty} \quad . \tag{B7}$$

Thus v_2 is directly proportional to v for a flat plate.

Also,

$$y_2 = y \sqrt{\frac{Gr_x}{Re_x^2}} = \frac{y}{x} \sqrt{Re_x} \sqrt{\frac{Gr_x}{Re_x^2}} \quad .$$

Therefore, for a flat plate, y_2 is directly proportional to y:

$$y_2 = \left(\frac{|q_x| \cdot \beta \cdot |(T_w - T_\infty)|}{2U} \right)^{1/2} y \quad . \tag{B8}$$

APPENDIX C

DERIVATION OF THE DIFFERENTIAL-INTEGRAL EQUATIONS

If equation (1) is integrated with respect to the transverse distance, y_2, from the surface to infinity, the result is:

$$\int_0^\infty \left(u_1 \frac{\partial u_1}{\partial z} + v_2 \frac{\partial u_1}{\partial y_2}\right) dy_2 = \int_0^\infty \left(\pm U_1^2 \theta + U_1 \frac{dU_1}{dz} + U_1 \frac{\partial^2 u_1}{\partial y_2^2}\right) dy_2 \qquad (C1)$$

From the continuity equation, (2),

$$v_2 = -\int_0^{y_2} \frac{\partial u_1}{\partial z}\, dy_2 .$$

This latter expression applied to the first equation, with an integration by parts, yields:

$$\int_0^\infty \left(u_1 \frac{\partial u_1}{\partial z} - U_1 \frac{\partial u_1}{\partial z} + u_1 \frac{\partial u_1}{\partial z}\right) dy_2 = \pm U_1^2 \int_0^\infty \theta\, dy_2 + \int_0^\infty U_1 \frac{dU_1}{dz}\, dy_2 - U_1 \left(\frac{\partial u_1}{\partial y_2}\right)_w$$

$$\int_0^\infty \left(\frac{\partial u_1^2}{\partial z} - U_1 \frac{\partial u_1}{\partial z} - U_1 \frac{dU_1}{dz}\right) dy_2 = \pm U_1^2 \int_0^\infty \theta\, dy_2 - U_1 \left(\frac{\partial u_1}{\partial y_2}\right)_w$$

$$\int_0^\infty \left[\frac{\partial (u_1 U_1 - u_1^2)}{\partial z} + \frac{dU_1}{dz}(U_1 - u_1)\right] dy_2 = \mp U_1^2 \int_0^\infty \theta\, dy_2 + U_1 \left(\frac{\partial u_1}{\partial y_2}\right)_w \qquad (C2)$$

Let $\frac{u_1}{U_1} = f(\eta)$, or $u_1 = U_1 \cdot f(\eta)$, and $\theta = h(\eta_T)$,

where

$$\eta = \frac{y}{\delta} = \frac{y_1}{\delta_1} = \frac{y_2}{\delta_2}$$

and

$$\eta_T = \frac{y}{\delta_T} = \frac{y_1}{\delta_{T_1}} = \frac{y_2}{\delta_{T_2}} .$$

Since

$$dy_2 = \delta_{T_2} \cdot d\eta_T = \delta_2 \cdot d\eta ,$$

$$f = 1 , \eta \geq 1 \quad , \text{when } y_2 \geq \delta_2 ,$$

and $$\theta = 0 , \eta_T \geq 1 \quad , \text{when } y_2 \geq \delta_{T_2} ,$$

the first integral equation in its most general form is:

$$\frac{d}{dz}\left[U_1^2 \cdot \delta_2 \int_0^1 f(1-f)\,d\eta\right] + \frac{dU_1}{dz} U_1 \cdot \delta_2 \int_0^1 (1-f)\,d\eta = \mp U_1^2 \cdot \delta_{T_2} \int_0^1 h\,d\eta_T + U_1 \left(\frac{\partial u_1}{\partial y_2}\right)_w . \tag{4}$$

In a similar manner, starting with the energy equation, (2), the second integral equation is found to be:

$$\frac{d}{dz}\left[\int_0^\infty u_1 \theta\, dy_2\right] = -\frac{U_1}{Pr}\left(\frac{\partial \theta}{\partial y_2}\right)_w . \tag{5}$$

Equation (4) is one form of the momentum integral equation. Equation (5) is called the energy integral equation in this study, since it is derived by a partial integration of the transformed thermal boundary layer equation, (2).

VITA

Donald Henry Asire

Candidate for the Degree of

Doctor of Philosophy

Thesis: APPLICATIONS OF THE INTEGRAL METHOD TO STEADY STATE LAMINAR MIXED CONVECTION HEAT TRANSFER

Major Field: Mechanical Engineering

Biographical:

Personal Data: Born in Chicago, Illinois, July 8, 1923, the son of Ida C. Asire and the late Harry F. Asire. Married to the former Ardyce J. Reisner.

Education: Graduated from Farragut High School, Chicago, Illinois, in 1941; received the Bachelor of Science degree from the Illinois Institute of Technology, with a major in Mechanical Engineering, in June, 1947; received the Master of Science degree from the Air Force Institute of Technology, with a major in Nuclear Engineering, in March, 1958; completed requirements for the Doctor of Philosophy degree in May, 1965.

Professional Experience: Entered the United States Army Air Corps in 1943 and served until 1945 as a fighter pilot; served as a pilot in the California Air National Guard from 1947 until 1950; in October, 1950, was recalled to active duty in the United States Air Force and flew a fighter-bomber combat tour during the Korean War; has had continuous service since that time and now holds the rank of Major. As a civilian, from 1947 until 1950, worked as a design engineer with C. F. Braun and Company of Alhambra, California. From 1958 to 1962 worked with the United States Atomic Energy Commission as a project officer; presently assigned to Headquarters, Air Force Systems Command.

Organizations: Tau Beta Pi, Pi Tau Sigma, Tau Omega; registered Professional Engineer in the State of Ohio.